LOAN DOCUMENT

PHOTOGRAPH THIS SHEET

DTIC FILE COPY

AD-A224 412

DTIC ACCESSION NUMBER

LEVEL

1

INVENTORY

AFOSR TR 90 0785

DOCUMENT IDENTIFICATION

MAY 1985

DISTRIBUTION STATEMENT A

Approved for public release;
Distribution Unlimited

DISTRIBUTION STATEMENT

HANDLE WITH CARE

ACCESSION FOR

NTIS GRA&I

DTIC TRAC

UNANNOUNCED

JUSTIFICATION

BY

DISTRIBUTION/

AVAILABILITY CODES

DISTRIBUTION	AVAILABILITY AND/OR SPECIAL	
A-1		

DISTRIBUTION STAMP

DTIC COPY INSPECTED

DTIC ELECTE JUL 3 0 1990 S D E

DATE ACCESSIONED

DATE RETURNED

90 07 25 080

DATE RECEIVED IN DTIC

REGISTERED OR CERTIFIED NUMBER

PHOTOGRAPH THIS SHEET AND RETURN TO DTIC-FDAC

DTIC FORM 70A JUN 90

DOCUMENT PROCESSING SHEET

PREVIOUS EDITIONS MAY BE USED UNTIL STOCK IS EXHAUSTED.

LOAN DOCUMENT

AFOSR-TR- 90- 0785

HIGHER ORDER ACOUSTIC RAYLEIGH MODES FOR SENSOR APPLICATIONS

Prepared for

Air Force Office of Scientific Research
Bolling Air Force Base
Washington, D.C. 20332
Attention: Dr. Howard Schlossberg

Prepared by:

Dr. Edward J. Staples
Amerasia Technology Inc.
2239 Townsgate Road, Suite 208
Westlake Village, California 91361

and

Professor David M. Barnett
Materials Science and Engineering
Stanford University
Palo Alto, California 94305

May 1985

Submitted by:

Francis Chang
Vice-President
Operations and Finance

The views and conclusions contained in this document are those of the authors and should not be interpreted as necessarily representing the official policies or endorsements, either expressed or implied, of the Air Force Office of Scientific Research or the U.S. Government.

REPORT DOCUMENTATION PAGE

Form Approved
OMB No. 0704-0188

1. AGENCY USE ONLY (Leave blank)	2. REPORT DATE	3. REPORT TYPE AND DATES COVERED
	May 1985	

4. TITLE AND SUBTITLE

Higher Order acoustic rayleigh models for sensor applications.

5. FUNDING NUMBERS

6. AUTHOR(S)

Dr. Edward J. Staples

7. PERFORMING ORGANIZATION NAME(S) AND ADDRESS(ES)

Amerasia technology Inc.
2239 Townsgate Road, Suite 208
Westlake Village, Ca 91361

8. PERFORMING ORGANIZATION REPORT NUMBER

AFOSR-TR- 90 0785

9. SPONSORING/MONITORING AGENCY NAME(S) AND ADDRESS(ES)

US Air Force.

10. SPONSORING/MONITORING AGENCY REPORT NUMBER

11. SUPPLEMENTARY NOTES

12a. DISTRIBUTION/AVAILABILITY STATEMENT

Approved for public release; distribution unlimited.

12b. DISTRIBUTION CODE

13. ABSTRACT (Maximum 200 words)

14. SUBJECT TERMS

15. NUMBER OF PAGES

16. PRICE CODE

17. SECURITY CLASSIFICATION OF REPORT	18. SECURITY CLASSIFICATION OF THIS PAGE	19. SECURITY CLASSIFICATION OF ABSTRACT	20. LIMITATION OF ABSTRACT
Unclassified	Unclassified	Unclassified	Unclassified

TABLE OF CONTENTS

	PAGE
SUMMARY	1
1.Ø INTRODUCTION	
1.1 Surface Acoustic Wave Accelerometers	2
1.2 Present SAW technology Limitations	4
2.Ø OBJECTIVES	
2.1 Work statement	6
3.Ø TECHNICAL APPROACH	
3.1 Surface Acoustic Waves	9
3.2 Surface Acoustic Waves in Layered Media	13
3.3 Interfacial Waves	19
3.4 Multi-Layered Resonators	21
4.Ø TECHNICAL RESULTS	
4.1 Layered Substrate Analyses	24
4.1.1 Analysis of MgO/ST-Quartz	25
4.1.2 Analysis of Y_2O_3/ST-Quartz	31
4.1.3 Analysis of SiO_x/ST-Quartz	36
4.1.4 Analysis of AlN/ST-Quartz	41
4.1.5 Analysis of TiO_2/ST-Quartz	48
4.1.6 Analysis of Al_2O_3/ST-Quartz	53
4.2 Interfacial Wave Analyses	58
4.2.1 Analysis of Copper	59
4.2.2 Analysis of Quartz	6Ø
4.3 Stoneley Interface-Wave Accelerometer	66
4.4 Comparison With Experimental Results	69
5.Ø CONCLUSIONS AND RECOMMENDATIONS	73
6.Ø REFERENCES	75
7.Ø APPENDICES	
7.1 Appendix I- Material Constants	76
7.2 Appendix II- Technical Background	79

LIST OF FIGURES

Page

1. Typical Rayleigh wave resonator structure showing reflective gratings (acoustic mirrors) and input/output interdigital transducer 3

2. Cantilever beam-type Rayleigh wave accelermeter where the output is the difference frequency between the opposing top and bottom resonant cavities 4

3. Diagram showing coordinate system orientation for theoretical analysis of wave propagation..... 1Ø

4. Rayleigh wave displacements and potential on ST-Quartz when the surface is shorted and unshorted..... 14

5. Diagram showing coordinate system orientation for theoretical analysis of wave propagation in layered media..... 15

6. Four possible transducer electrode configurations when both layer and substrate are piezoelectric..... 18

7. Diagram showing coordinate system orientation for analysis of wave propagation along the interface between two anisotropic materials..... 19

8. Coordinate system for two-layered resonator geometry.. 21

9. Velocity dispersion (a) and wave coupling (b) as a function of layer thickness for MgO/ST-Quartz..... 26

1Ø. Layered velocity solution for MgO/ST-Quartz when the top layer and interface are unshorted. Layer thickness is 1Ø% of a wavelength..... 27

11. Layered velocity solution for MgO/ST-Quartz when the top layer surface is shorted. Layer thickness is 1Ø% of a wavelength..... 28

12. Layered velocity solution for MgO/ST-Quartz when the top layer and interface are shorted. Layer thickness is 1Ø% of a wavelength..... 29

13. Layered velocity solution for MgO/ST-Quartz when the top layer and interface are unshorted. Layer thickness is Ø.1% of a wavelength..... 3Ø

Page

14. Velocity dispersion and wave coupling as a function of layer thickness for Y_2O_3/ST-Quartz..... 32

15. Layered velocity solution for Y_2O_3/ST-Quartz when top layer and interface are unshorted..... 33

16. Layered velocity solution for Y_2O_3/ST-Quartz when top layer surface is shorted..... 34

17. Layered velocity solution for Y_2O_3/ST-Quartz when top and interface surfaces are shorted..... 35

18. Velocity dispersion and wave coupling as a function of layer thickness for SiO_x/ST-Quartz..... 37

19. Layered velocity solution for SiO_x/ST-Quartz when top layer and interface are unshorted..... 38

20. Layered velocity solution for SiO_x/ST-Quartz when top layer surface is shorted..... 39

21. Layered velocity solution for SiO_x/ST-Quartz when top and interface surfaces are shorted..... 40

22. Velocity dispersion and wave coupling as a function of layer thickness for AlN on ST-Quartz with electrodes either at the interface or top surface..... 42

23. Velocity dispersion and wave coupling as a function of layer thickness for AlN on ST-Quartz with interdigital electrodes and an opposing ground plane..... 43

24. Layered velocity solution for AlN/ST-Quartz when top and interface surfaces are unshorted..... 44

25. Layered velocity solution for AlN/ST-Quartz when top surface is shorted and interface is unshorted..... 45

26. Layered velocity solution for AlN/ST-Quartz when top surface is unshorted and interface is shorted..... 46

27. Layered velocity solution for AlN/ST-Quartz when top and interface surfaces are shorted..... 47

28. Velocity dispersion and wave coupling as a function of layer thickness for TiO_2/ST-Quartz..... 49

29. Layered velocity solution for TiO_2/ST-Quartz when top and interface surfaces are unshorted..... 50

30. Layered velocity solution for TiO_2/ST-Quartz when top surface is shorted and interface is unshorted..... 51

Page

31. Layered velocity solution for TiO_2/ST-Quartz when top surface is unshorted and interface is shorted..... 52

32. Velocity dispersion and wave coupling as a function of layer thickness for Al_2O_3/ST-Quartz..... 54

33. Layered velocity solution for Al_2O_3/ST-Quartz when top and interface surfaces are unshorted..... 55

34. Layered velocity solution for Al_2O_3/ST-Quartz when top surface is shorted and interface is unshorted..... 56

35. Layered velocity solution for Al_2O_3/ST-Quartz when top and interface surfaces are shorted..... 57

36. Coordinate system relative to the interface plane for Stoneley wave analysis..... 58

37. Stoneley wave velocity vs material rotation angle in single crystal copper (ØØ1) plane..... 59

38. Stoneley wave solution on Copper for a rotation angle $\pm$ 1Ø° and $\pm$ 2Ø°..... 61

39. Stoneley wave solution for modified copper compared to normal copper..... 62

4Ø. Stoneley wave velocity solution for XZ Quartz when the interface is unshorted..... 63

41. Stoneley wave velocity solution for XZ Quartz when the interface is shorted..... 64

42. Expanded plot of displacements and potential for Stoneley waves on XZ Quartz..... 65

43. Stoneley interface wave resonator configuration..... 66

44. Proposed baseline interface wave accelerometer in guidance system..... 68

45. Experimentally measured frequency, resistance, and Q for SAW resonators on ST-Quartz with sputtered films of MgO and SiO_x..... 7Ø

46. Experimentally measured frequency, resistance, and Q for SAW resonators on ST-Quratz with sputtered films of Y_2O_3 and AlN..... 71

SUMMARY

The objective of this project was to establish the theoretical foundations for applying higher order Rayleigh and interface modes to resonators for high stability sensors. Existing crystal resonators, because of their surface sensitivity and thermal characteristics, are not able to meet the stability requirements of Air Force tactical systems.

Theoretical studies of the characteristics of Rayleigh waves in single and multi-layer structures were carried out for ST-cut Quartz substrates. Specified materials for this study were MgO, Y_2O_3, AlN, SiO_x, Al_2O_3, and TiO_2. Velocity dispersion and coupling to bulk modes were predicted and confirmed by comparison with experimental results for sputtered films.

Stoneley (interfacial) waves were investigated as possible candidates for resonator structures because of their inherently stable and low cost geometry without any type of hermetic enclosure or package. A successful search technique was developed which accurately predicts the existence of Stoneley waves in general anisotropic (and piezoelectric) materials. Using this technique, Stoneley waves were for the first time predicted in single crystal quartz. Several useful orientations where Stoneley waves are well bound and piezoelectrically active were found to exist.

Future plans are to design, fabricate and test interface wave resonators. The end goal is to utilize interface wave resonators and sensors in Air Force tactical systems.

1.Ø INTRODUCTION

The purpose of the work reported was to perform analyses of the propagation characteristics of higher order acoustic Rayleigh waves in multiple layered, anisotropic materials. The objective was to establish theoretical foundations for predicting the performance of higher order acoustic waves and to apply this knowledge to the design of acoustic resonators as strain sensors for cantilever beam-type accelerometers. These higher order Rayleigh waves differ from the normal surface waves because their energy is distributed between the layers and the substrate, but not entirely at the top surface of the layers. This has the advantage that the propagation characteristics are less sensitive to contamination or other undesireable effects at the surface of the crystal. The reflective grooves in the resonator structure can be passivated by the layers, thus reducing the possibility of false sensor readings. These conditions all contribute to making a more stable sensor.

1.1 Surface Acoustic Wave Accelerometer

A Rayleigh acoustic wave is an elastic wave which propagates along the surface of an elastic solid. Since its energy is conconfined near the surface, it can be generated, reflected, and detected on the surface. Rayleigh wave devices constitute what is called a planar technology and hence can be fabricated by photolithographic techniques. Thus, these sensors can be produced at costs comparable to those of silicon integrated circuits.

The Rayleigh wave resonator, introduced by Dr. Staples in 1974, consists of a pair of reflective gratings on a surface as mirrors in a Fabry-Perot resonator structure. These waves can be generated and detected by an interdigital transducer on a piezoelectric substrate. The output of the acoustically resonant cavity, shown in Figure. 1, is connected to a feedback amplifier to maintian a high Q, standing wave in the cavity formed by the two grating reflectors.

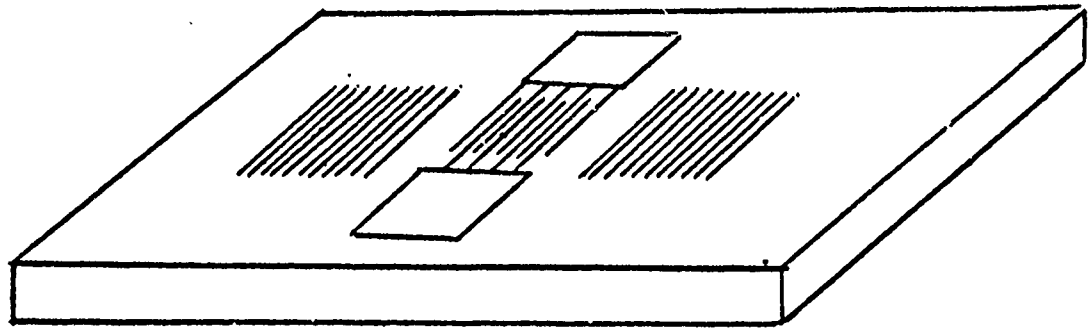

Figure 1- Typical Rayleigh wave resonator structure showing reflective gratings (acoustic mirrors) and the input/output interdigital transducer.

Since Rayleigh waves are confined to the surface, the sensor can be configured as a cantilever beam, as shown in Figure 2. In this "push-pull" open loop configuration, thermal effects are reduced by using two resonators (top and bottom) and the output is then the difference frequency of the two resonator frequencies.

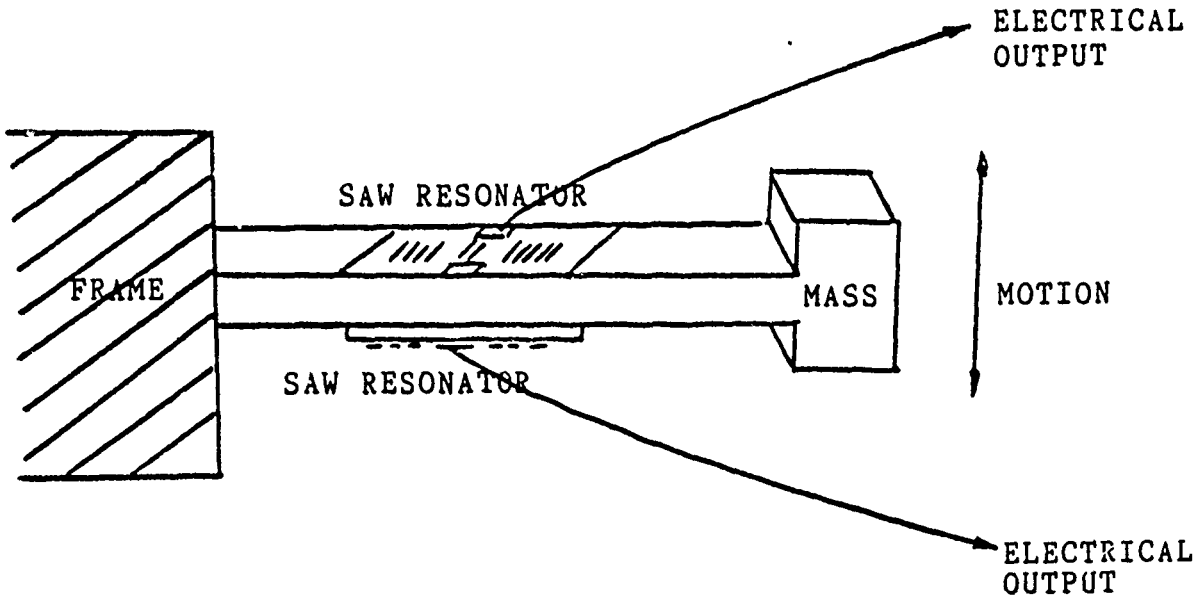

Figure 2- Cantilever beam-type rayleigh Wave Accelerometer where the output is the difference frequency between the opposing top and bottom resanant cavities.

1.2 Present SAW Technology Limitations

At the present time, short-term frequency stability of Rayleigh wave resonators is comparable to that of bulk-wave crystal oscillators. Long-term stability of fundamental mode Rayleigh resonators[1] is not as good as that of bulk wave crystal oscillators. Rayleigh wave resonators typically have short-term (seconds to minutes) frequency stability with a root Allan variance of 10^{-10} parts/part of the resonant freuqency, and long-term aging rates in the range of 10^{-8} part/part/day.

Short-term stabilty for tactical missile applications (flight time typically is less tan 20 minutes) is not a significant problem. A variation of 10^{-10} of 500 MHz would equal 0.05 Hz. With an assumed quantization of 0.1 fps/bit and input acceleration of 200 g, this would equal 100 micro-g acceleration error.

Long-term frequency stability is a more serious problem since it controls the bias stability of Rayleigh wave sensors. The dual Rayleigh wave sensor aging rate under "ovenized" conditions is about 10-8 per year.[2] For a Rayleigh wave accelerometer with 500 MHz frequency and 0.1 fps/bit, this gives a bias stability error of 0.016 g/year. This stability is adequate for "moderately accurate" inertial grade accelerometer applications. Without oven control of the temperature, the oscillator stability is typically 10^{-6}/year and the resulting bias stability 0.02 g/year which exceeds current tactical missile specifications. Temperature control is a definite limitation of current Rayleigh wave technology.

An important limitation of Rayleigh mode resonators is that 90% of its energy is on the surface, hence it is very sensitive to surface conditions. Changes of 1 part per billion have been observed in the resonator frequency in a period of one hour.[2] This can be traced to molecular surface chemistry, dust particles, or other surface effects on the substrate. After the SAW pattern is defined it would be highly desireable to cover or passivate the surface so as to protect the wave from surface contaimination. This would negate the need for costly packaging and sealing of the sensors. This last limitation is addressed by the current study where higher order acoustic solutions are sought which do not possess the high degree of surface sensitivity.

2.Ø OBJECTIVES

The objective of the phase I research was to establish the theoretical foundations for using higher order Rayleigh and interfacial wave resonators as strain sensors in cantilever-type accelerometers. Existing crystals, because of their surface sensitivity and thermal characteristics, are not able to meet the technical specifications of inertial grade accelerometers for Air Force tactical systems.

The overall research objective is to obtain resonator structures with improved aging characteristics, so that these sensors can meet the performance requirmenets for "moderate accuracy" accelerometers of Air Force tactical inertial navigation systems, including missiles and aircraft.

2.1 Work statement

The research conducted under Phase I was defined by the following work statement:

Task 1. Perform theoretical studies of Rayleigh waves at single layer surfaces on quartz substrates, to determine the thickness limitations and effects of the layer. Selected materials for this study will include layered acoustic wave resonators of MgO, Y_2O_3, AlN, SiO_x, Al_2O_3, and TiO_2.

Task 2. Correlate the theoretical analysis with any existing published experimental results in either technical journals or DoD reports.

Task 3. Expand the analysis of single layers to three anisotropic layers. Studies will be made in characterizing various combination of "loading and stiffening" layers on quartz.

Task 4. Design and develop a high stability Rayleigh wave sensor using the theoretical reults of the above studies.

Task 5. Investigate theoretically and numerically Stoneley waves in joined piezoelectric half-spaces.

3.Ø TECHNICAL APPROACH

Higner order Rayleigh waves differ from the normal surface waves because their energy is distributed between the layer and the substrate. This has the advantage that the wave characteristics such as velocity and impedance are less sensitive to changes in the surface acoustic and/or electrical conditions. Also, the reflective grooves and electrode materials in a resonator structure are passivated by the layer and the effects of contamination are reduced. These conditions all contribute to the making of a more stable resonator.

Lord Rayleigh in 1887[3] predicted the propagation of seismic waves along the surface of the earth. Ewing, Jardetzky and Press[4] extended Rayleigh's work to layered isotropic media. Since most crystals are anisotropic, Lim and Musgrave in 1970[5] studied interface wave propagation at boundaries between two similar anisotropic media and they extended the work of Stoneley[6] to include anisotropic media.

Farnell and Adler in 1972[7] studied Rayleigh wave propagation in layered anisotropic media. They concentrated their studies on special cases where the thickness of the layers was small compared to a wavelength. The results showed the existence of single-mode Rayleigh waves at the boundary of half spaces with a single layer of dissimilar material.

Recently the advantages of layered wave behavior has been demonstrated by Yamonouchi[8] for SiO_x on $LiTaO_3$ and $LiNbO_3$. In addition to the advantages of surface passivation, these layered substrates show temperature compensation due to the dissimilar

thermal expansion and elastic constants with temperature.

In order to study propagation of waves in layered acoustic media two approaches were taken. The first followed the analysis of Farnell[9] to describe and predict wave behavior for Rayleigh wave propagation in layered media. This analysis was used to evaluate several layer materials deposited on ST-cut quartz. The theoretical predictions were then compared with previously published experimental results.

The second approach was undertaken jointly with Professor D. Barnett of Stanford University. Professor Barnett specifically analyzed search methods for interfacial wave propagation in general anisotropic media. These search methods were derived from the theory published by Barnett and Lothe.[10] A reprint of this paper is included with this report as Appendix II. Theory of interfacial wave propagation is described in section 3, and numerical results for prescribed materials are presented in section 4. The importance of this work is that a method was developed which predicts the existence of interface waves. Unlike surface waves, interface waves do not exist for all material combinations. Until now an exhausting search was always required to determine the existence of such waves. Using new search techniques, Stoneley wave behavior has been predicted without completely solving wave equations. For the first time Stoneley waves have been found in quartz. By properly selecting the cuts of quartz used, it was found that Stoneley waves with good piezoelectric coupling and fast decay with distance from the interface do exist.

3.1 Surface Acoustic Waves

In a piezoelectric material the three displacement components u_j along the Cartesian axes x_j, and the electrostatic potential are related by the equations of motion and electrostatics,

$$\rho \frac{\partial^2 u_i}{\partial t^2} - c_{ijkl} \frac{\partial^2 u_k}{\partial x_j \partial x_l} - e_{kij} \frac{\partial^2 \varphi}{\partial x_j \partial x_k} = 0$$
$$e_{ikl} \frac{\partial^2 u_k}{\partial x_i \partial x_l} - \epsilon_{ik} \frac{\partial^2 \varphi}{\partial x_i \partial x_k} = 0 \qquad (1)$$

in which ρ is the density of the material and c_{ijkl}, e_{kij} and ϵ_{ik} are respectively, the tensors for the elastic stiffness measured at constant electric field, for the piezoelectric coupling and for dielectric permittivity measured at constant strain. The subscripts i,j,k, and l range over the values 1,2, and 3 and the summation convention on repeated subscripts is employed. The contracted matrix notation and the full tensor notation will be used interchangeably in this report. Particular elastic, piezoelectric, and dielectric constants for materials studied in this report are given in Appendix I.

All solutions considered are straight crested in that the planes of constant phase are perpendicular to the direction of propagation and there is no variation of the amplitude in the direction perpendicular to the sagittal plane. The coordinate system used throughout this report is as shown in Figure 3 with the x_1 direction taken as parallel to the propagation vector and the x_3 direction taken as perpendicular to the surface (also interface in later sections).

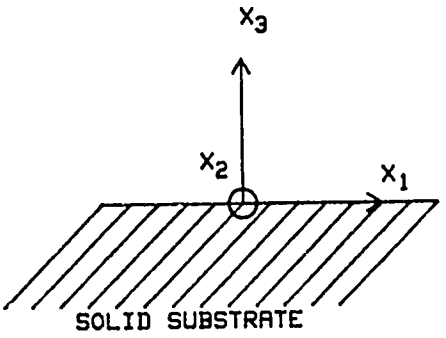

Figure 3- Diagram showing coordinate system orientation for theoretical analysis of wave propagation.

For a single material surface, Rayleigh wave solutions will be of the form

$$u_i = \alpha_i \exp(ikbx_3) \exp[ik(x_1 - vt)] \qquad (2)$$
$$\varphi = \alpha_4 \exp(ikbx_3) \exp[ik(x_1 - vt)].$$

Substituting (2) into the equations of motion (1) results in a secular matrix of the form

$$\begin{bmatrix} (\Gamma_{11} - \rho v^2) & \Gamma_{12} & \Gamma_{13} & \Gamma_{14} \\ \Gamma_{12} & (\Gamma_{22} - \rho v^2) & \Gamma_{23} & \Gamma_{24} \\ \Gamma_{13} & \Gamma_{23} & (\Gamma_{33} - \rho v^2) & \Gamma_{34} \\ \Gamma_{14} & \Gamma_{24} & \Gamma_{34} & \Gamma_{44} \end{bmatrix} \begin{bmatrix} \alpha_1 \\ \alpha_2 \\ \alpha_3 \\ \alpha_4 \end{bmatrix} = 0. \qquad (3)$$

where the terms of the matrix are related to the material constants by the following quadratic coefficients:

$$
\begin{aligned}
\Gamma_{11} &= c_{1313}b^2 + 2c_{1113}b + c_{1111} \\
\Gamma_{22} &= c_{2323}b^2 + 2c_{1223}b + c_{1212} \\
\Gamma_{33} &= c_{3333}b^2 + 2c_{1333}b + c_{1313} \\
\Gamma_{12} &= c_{1323}b^2 + (c_{1123} + c_{1312})b + c_{1112} \\
\Gamma_{13} &= c_{1333}b^2 + (c_{1133} + c_{1313})b + c_{1113} \\
\Gamma_{23} &= c_{2333}b^2 + (c_{1233} + c_{2313})b + c_{1213}, \\
\Gamma_{14} &= e_{331}b^2 + (e_{131} + e_{311})b + e_{111} \\
\Gamma_{24} &= e_{332}b^2 + (e_{132} + e_{312})b + e_{112} \\
\Gamma_{34} &= e_{333}b^2 + (e_{133} + e_{313})b + e_{113}, \\
\Gamma_{44} &= -(\epsilon_{33}b^2 + 2\epsilon_{13}b + \epsilon_{11}).
\end{aligned}
\tag{4}
$$

The above homogeneous equations have a nontrivial solution only if the determinant of the square Γ matrix is zero. A computer program was written to expand the above matrix assuming a known velocity, v, as a polynomial (8th order for piezoelectric materials) in the decay constant b. The program evaluated the complex roots b_i which occured as conjugate pairs. In the substrate the solutions of interest decay with depth away from the surface, hence only roots in the lower half of the complex plane are retained.

In order to now satisfy the free surface boundary conditions a wave solution composed of sums of terms given by eq.(2) where each term satisfies the wave equation (1) is used. Each term is considered an eigenfunction, $\alpha^{(n)}$, with an associated eigenvalue or decay constant $b^{(n)}$. The total solution is then given by

$$u_i = \sum C_n \alpha_i^{(n)} \exp(ikb^{(n)} x_3) \exp[ik(x_1 - vt)]$$
$$\varphi = \sum C_n \alpha_4^{(n)} \exp(ikb^{(n)} x_3) \exp[ik(x_1 - vt)] \qquad (5)$$

where summation over all the root numbers (4 for piezoelectrics).

The complete solution is obtained by satisfying the mechanical and electrical boundary conditions. Mechanically the normal stress compoents T_{13}, T_{23}, and T_{33} must be zero at the surface. Electrically there must be continutity of electric potential and the normal componentf displacement current D_3.

Substitution of eqs.(5) results in a different set of four homogeneous equations in the four weighting functions C_n, and for nontrivial solutions the determinant of the coefficients of C_n must vanish.

$$\begin{vmatrix} (c_{33i1} + c_{3313}b^n)\alpha_i^n + (e_{133} + e_{333}b^n)\alpha_4^n \\ (c_{31i1} + c_{3113}b^n)\alpha_i^n + (e_{131} + e_{331}b^n)\alpha_4^n \\ (c_{32i1} + c_{3213}b^n)\alpha_i^n + (e_{132} + e_{332}b^n)\alpha_4^n \\ -(\hat{e}_{3i1} + \hat{e}_{3i3}b^n)\alpha_i^n + (\hat{\epsilon}_{31} + \hat{\epsilon}_{33}b^n - i\epsilon_{11})\alpha_4^n \end{vmatrix} \begin{vmatrix} \\ \\ C_n \\ \\ \end{vmatrix} = 0 \qquad (6)$$

An objective of this study was to determine the behavior of Rayleigh waves on ST-cut quartz. Equations 1-6 were solved numerically using an iterative search on velocity until equation (6) was satisfied. A plot of the displacement components and potential are shown in Figure 4a. When the surface is shorted the last row of eq.(6) is replaced by the the eigenvectors which forces the potential to zero at the surface. A plot of the displacements and potential for this case is shown in Figure 4b.

3.2 Surface Acoustic Waves in Layered Media

When the surface of a crystal is covered with a layer of dissimilar material as shown in Figure 5, the behavior of the Rayleigh wave is modified to take into account (1) the elastic properties of the layer and (2) the electric boundary conditions of the layer surface and the interface region.

Solutions to the layered problem can be obtained by solving equations 1-3 in the layer and substrate separately using the appropriate material constants. The individual solutions in the layer and infinite substrate are still assumed to be the same form as equation 5 where the appropriate layer or substrate roots apply.

The complete solution is obtained by satisfying the appropriate boundary conditions. In the case of layered media the boundary condition determinant is more complex. The surface of the layer is stress free and electrically open or shorted. However, the interface region must also be satisfied by matching the normal stresses, the displacements, and electrical potential and/or displacement currents.

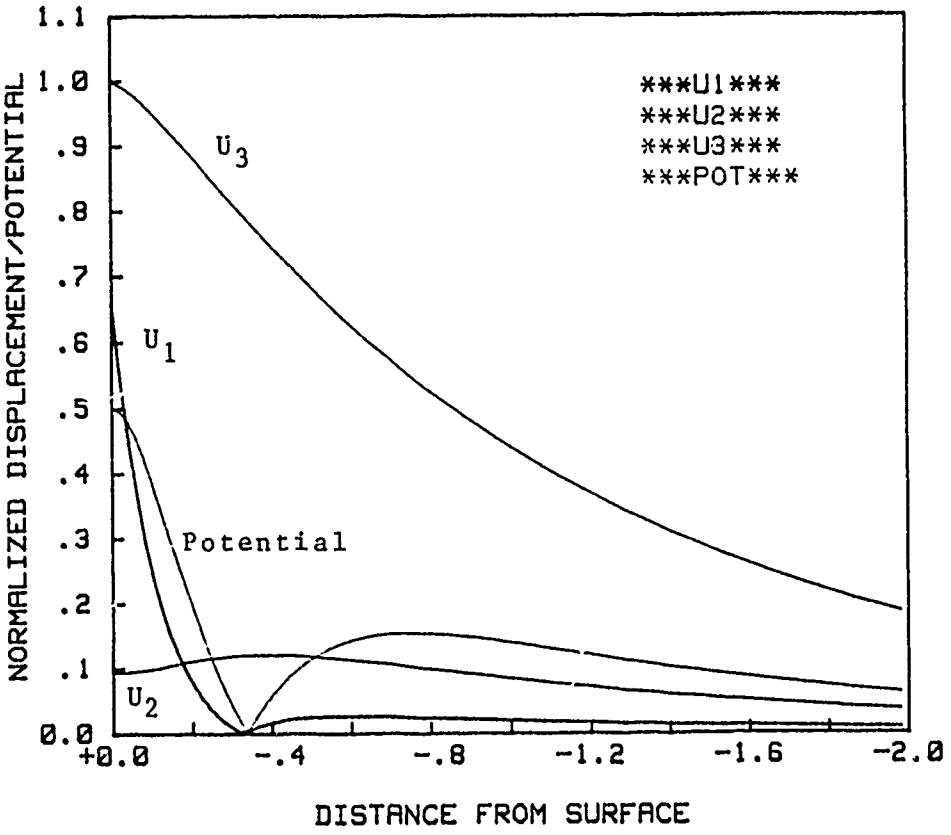

(A)

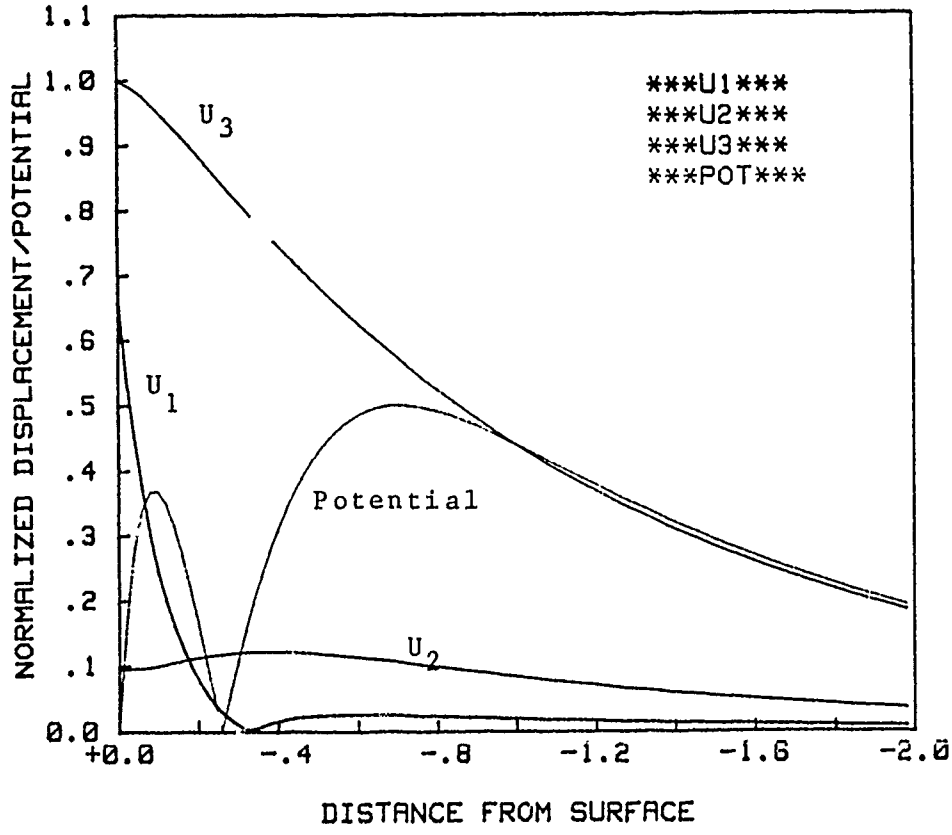

(B)

Figure 4- Rayleigh wave displacements and potential on ST-Quartz when the surface is (A) unshorted and (B) shorted.

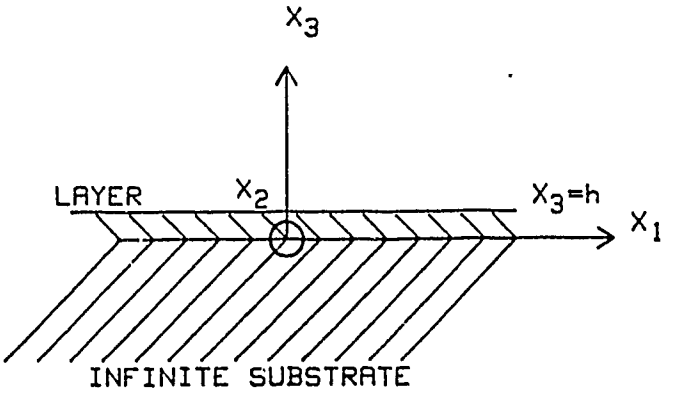

Figure 5 - Diagram showing coordinate system orientation for theoretical analysis of wave propagation in layered media.

In this report three distinct types of materials were analyzed. The first situation involved a piezoelectric substrate (YX-Quartz) and a non-piezoelectric isotropic layer such as fused quartz, hereafter designated PN53 after the notation of Farnell.[9] In this case the transverse displacement component is uncoupled and there are 7 boundary conditions which must be satisfied. The boundary condition equations for a unshorted interface are

$$\left[\begin{array}{c|c} T_3^L(X_3=0) & -T_3^S(X_3=0) \\ T_5^L(X_3=0) & -T_5^S(X_3=0) \\ T_3^L(X_3=h) & 0 \\ T_5^L(X_3=h) & 0 \\ u_1^L(X_3=0) & -u_1^S(X_3=0) \\ u_3^L(X_3=0) & -u_3^S(X_3=0) \\ \hline D_3^L(X_3=0) & 0 \end{array}\right] \left[C_n\right] = 0 \qquad (7)$$

and for a shorted interface are

$$\left[\begin{array}{c|c} T_3^L(X_3=0) & -T_3^S(X_3=0) \\ T_5^L(X_3=0) & -T_5^S(X_3=0) \\ T_3^L(X_3=h) & 0 \\ T_5^L(X_3=h) & 0 \\ u_1^L(X_3=0) & -u_1^S(X_3=0) \\ u_3^L(X_3=0) & -u_3^S(X_3=0) \\ \hline \phi^L(X_3=0) & 0 \end{array}\right]\left[C_n\right]=0 \qquad (8)$$

The displacement vectors of equations 7 and 8 are modified to account for the dielectric constant of the layer and the free space above the layer. When the substrate crystal solution contains transverse displacements these must be accounted for in the boundary conditions. This applies whether the layer material is isotropic (no coupled transverse displacements) or anisotropic. This case is represented by ST-Quartz substrates and layer materials such as fused quartz, Rutile, Sapphire, and Yittrium Oxide. In these cases the unshorted boundary conditions are

$$\left[\begin{array}{c|c} T_3^L(X_3=0) & -T_3^S(X_3=0) \\ T_5^L(X_3=0) & -T_5^S(X_3=0) \\ T_4^L(X_3=0) & -T_4^X(X_3=0) \\ T_3^L(X_3=h) & 0 \\ T_5^L(X_3=h) & 0 \\ T_4^L(X_3=h) & 0 \\ u_1^L(X_3=0) & -u_1^S(X_3=0) \\ u_2^L(X_3=0) & -u_2^S(X_3=0) \\ u_3^L(X_3=0) & -u_3^S(X_3=0) \\ \hline D_3^L(X_3=0) & 0 \end{array}\right]\left[C_n\right]=0 \qquad (9)$$

and for shorted electrical conditions are

$$\left[\begin{array}{c|c} T_3^L(X_3=0) & -T_3^S(X_3=0) \\ T_5^L(X_3=0) & -T_5^S(X_3=0) \\ T_4^L(X_3=0) & -T_4^X(X_3=0) \\ T_3^L(X_3=h) & 0 \\ T_5^L(X_3=h) & 0 \\ T_4^L(X_3=h) & 0 \\ u_1^L(X_3=0) & -u_1^S(X_3=0) \\ u_2^L(X_3=0) & -u_2^S(X_3=0) \\ u_3^L(X_3=0) & -u_3^S(X_3=0) \\ \hline \phi^L(X_3=0) & 0 \end{array}\right] \left[C_n\right] = 0 \qquad (10)$$

The boundary conditions are further complicated when the layer material is itself piezoelectric and with coupled transverse displacements. This case was analyzed for the substrate material ST-Quartz and layer Aluminum Nitride. The boundary condition determinant in this case contains twelve equations. The form for unshorted surface and interface is

$$\left[\begin{array}{c|c} T_3^L(X_3=0) & -T_3^S(X_3=0) \\ T_5^L(X_3=0) & -T_5^S(X_3=0) \\ T_4^L(X_3=0) & -T_4^X(X_3=0) \\ T_3^L(X_3=h) & 0 \\ T_5^L(X_3=h) & 0 \\ T_4^L(X_3=h) & 0 \\ u_1^L(X_3=0) & -u_1^S(X_3=0) \\ u_2^L(X_3=0) & -u_2^S(X_3=0) \\ u_3^L(X_3=0) & -u_3^S(X_3=0) \\ \hline D_3^L(X_3=h) & 0 \\ \phi^L(X_3=0) & -\phi^S(X_3=0) \\ D_3^L(X_3=0) & -D_3^S(X_3=0) \end{array}\right] \left[C_n\right] = 0 \qquad (11)$$

When the top surface and interface regions are shorted electrically the new for of the boundary matrix is

$$\left[\begin{array}{c|c} T_3^L(X_3=0) & -T_3^S(X_3=0) \\ T_5^L(X_3=0) & -T_5^S(X_3=0) \\ T_4^L(X_3=0) & -T_4^X(X_3=0) \\ T_3^L(X_3=h) & 0 \\ T_5^L(X_3=h) & 0 \\ T_4^L(X_3=h) & 0 \\ u_1^L(X_3=0) & -u_1^S(X_3=0) \\ u_2^L(X_3=0) & -u_2^S(X_3=0) \\ u_3^L(X_3=0) & -u_3^S(X_3=0) \\ \hline \phi_3^L(X_3=h) & 0 \\ \phi^L(X_3=0) & 0 \\ 0 & \phi_3^S(X_3=0) \end{array}\right] \left[C_n\right] = 0 \qquad (12)$$

In the general case there will be a solution which satisfies the wave equations in the layer and substrate and simultaneously satisfies all 12 of the above boundary conditions. Electrical coupling is estimated by comparing the shorted and unshorted wave velocities. For a piezoelectric layer on a piezoelectric substrate there will be four possible combinations of boundary conditions corresponding to four possible transducer electrode configurations shown in Figure 6.

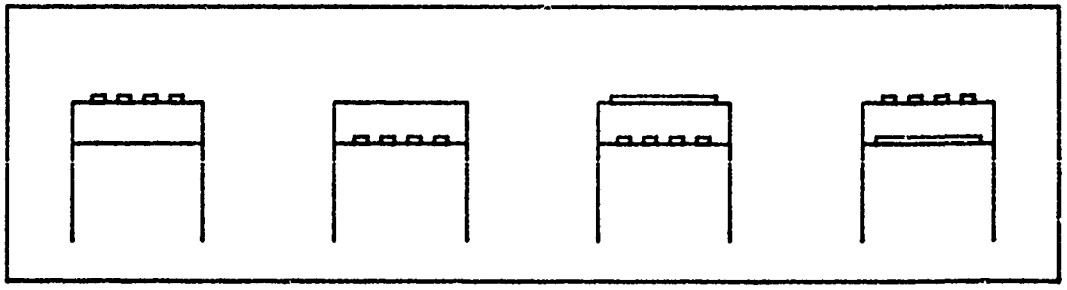

Figure 6- Four possible transducer electrode configurations when both layer and substrate are piezoelectric.

3.3 Interfacial Waves

Interfacial waves, commonly called Stoneley Waves, occur at the boundary of two infinite dissimilar materials as shown in Figure 7. Unlike surface acoustic waves, Stoneley waves only exist under special circumstances. The exact nature of these special circumstances is not well understood and an objective of this study was to develop methods of searching for Stoneley waves in general anisotropic media.

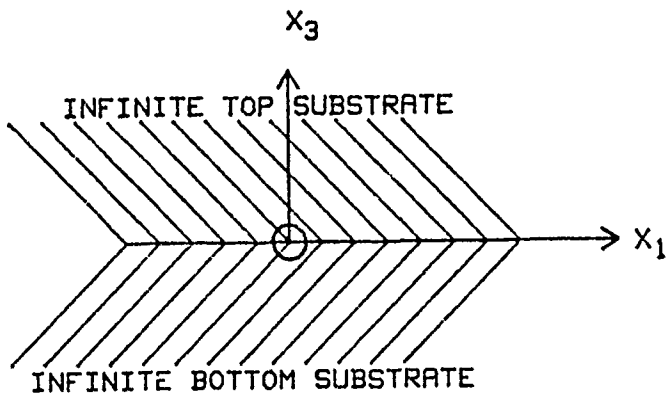

Figure 7- Diagram showing coordinate system orientation for analysis of wave propagation along the interface between two anisotropic materials.

The analysis of interfacial waves is similar to analyzing layered surface acoustic waves. The equations of motion are solved independently in each material and then summation solutions are used to satisfy the boundary conditions. For interface waves the unshorted boundary condition matrix is

$$\left[\begin{array}{c|c} T_3^t(X_3=0) & -T_3^b(X_3=0) \\ T_5^t(X_3=0) & -T_5^b(X_3=0) \\ T_4^t(X_3=0) & -T_4^b(X_3=0) \\ u_1^t(X_3=0) & -u_1^b(X_3=0) \\ u_2^t(X_3=0) & -u_2^b(X_3=0) \\ u_3^t(X_3=0) & -u_3^b(X_3=0) \\ \hline \phi^t(X_3=0) & -\phi^b(X_3=0) \\ D_3^t(X_3=0) & -D_3^b(X_3=0) \end{array}\right]\left[\begin{array}{c} \\ \\ \\ \\ \\ \\ \\ \\ \end{array} C_n \right] = 0 \qquad (13)$$

The above notation refers to the top (t) and bottom (b) materials and their respective material constants. When the interface is shorted by a conducting plane the boundary condition matrix takes the form

$$\left[\begin{array}{c|c} T_3^t(X_3=0) & -T_3^b(X_3=0) \\ T_5^t(X_3=0) & -T_5^b(X_3=0) \\ T_4^t(X_3=0) & -T_4^b(X_3=0) \\ u_1^t(X_3=0) & -u_1^b(X_3=0) \\ u_2^t(X_3=0) & -u_2^b(X_3=0) \\ u_3^t(X_3=0) & -u_3^b(X_3=0) \\ \hline \phi^t(X_3=0) & 0 \\ 0 & -\phi^b(X_3=0) \end{array}\right]\left[\begin{array}{c} \\ \\ \\ \\ \\ \\ \\ \\ \end{array} C_n \right] = 0 \qquad (14)$$

3.4 Multi-Layered Resonators

Multi-layered resonators are photo etched on crystals containing multiple layers of dissimilar materials on a piezoelectric substrate. The layers may be piezoelectrically active also and shorting planes may exist at any interface as depicted in figure 8 for a two layer system.

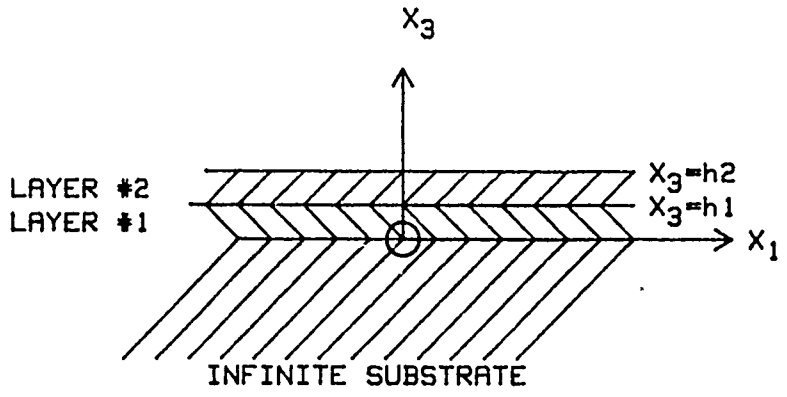

Figure 8- Coordinate system for a two-layered resonator geometry.

Analysis reveals the solution contains both Rayleigh and Stoneley wave like solutions. Because of this, the behavior of Rayleigh and Stoneley waves in the individual material sub-sets was studied before solutions in multi-layered media were undertaken.

The analysis follows a familiar trend. The equations of motion are solved independently in each material and summation solutions are used to satisfy the boundary conditions. For waves in unshorted multi-layered resonators the boundary condition matrix is as follows:

$$
\left[\begin{array}{c|c|c}
T_3^s(X_3=0) & -T_3^n(X_3=0) & 0 \\
T_5^s(X_3=0) & -T_5^n(X_3=0) & 0 \\
T_4^s(X_3=0) & -T_4^n(X_3=0) & 0 \\
u_1^s(X_3=0) & -u_1^n(X_3=0) & 0 \\
u_2^s(X_3=0) & -u_2^n(X_3=0) & 0 \\
u_3^s(X_3=0) & -u_3^n(X_3=0) & 0 \\
0 & T_3^n(X_3=h1) & -T_3^m(X_3=h1) \\
0 & T_5^n(X_3=h1) & -T_5^m(X_3=h1) \\
0 & T_4^n(X_3=h1) & -T_4^m(X_3=h1) \\
0 & u_1^n(X_3=h1) & -u_1^m(X_3=h1) \\
0 & u_2^n(X_3=h1) & -u_2^m(X_3=h1) \\
0 & u_3^n(X_3=h1) & -u_3^m(X_3=h1) \\
0 & 0 & T_3^m(X_3=h2) \\
0 & 0 & T_5^m(X_3=h2) \\
0 & 0 & T_4^m(X_3=h2) \\
\hline
\phi^s(X_3=0) & -\phi^n(X_3=0) & 0 \\
D_3^s(X_3=0) & -D_3^n(X_3=0) & 0 \\
0 & \phi^n(X_3=h1) & -\phi^m(X_3=h1) \\
0 & D_3^n(X_3=h1) & -D_3^m(X_3=h1) \\
0 & 0 & D_3^m(X_3=h2)
\end{array}\right]
\left[\begin{array}{c} \\ \\ \\ \\ \\ \\ \\ \\ \\ \\ \\ \\ \\ \\ \\ \\ \\ \\ \\ \end{array}\right]
C_n = 0 \qquad (15)
$$

The above notation refers to the top layer(m), intermediate layer(n) and substrate(s). When the two interfaces and top layer are shorted the boundary condition matrix takes the form:

$$
\left[\begin{array}{c|c|c}
T_3^s(X_3=0) & -T_3^n(X_3=0) & 0 \\
T_5^s(X_3=0) & -T_5^n(X_3=0) & 0 \\
T_4^s(X_3=0) & -T_4^n(X_3=0) & 0 \\
u_1^s(X_3=0) & -u_1^n(X_3=0) & 0 \\
u_2^s(X_3=0) & -u_2^n(X_3=0) & 0 \\
u_3^s(X_3=0) & -u_3^n(X_3=0) & 0 \\
0 & T_3^n(X_3=h1) & -T_3^m(X_3=h1) \\
0 & T_5^n(X_3=h1) & -T_5^m(X_3=h1) \\
0 & T_4^n(X_3=h1) & -T_4^m(X_3=h1) \\
0 & u_1^n(X_3=h1) & -u_1^m(X_3=h1) \\
0 & u_2^n(X_3=h1) & -u_2^m(X_3=h1) \\
0 & u_3^n(X_3=h1) & -u_3^m(X_3=h1) \\
0 & 0 & T_3^m(X_3=h2) \\
0 & 0 & T_5^m(X_3=h2) \\
0 & 0 & T_4^m(X_3=h2) \\
\hline
\phi^s(X_3=0) & 0 & 0 \\
0 & \phi^n(X_3=0) & 0 \\
0 & \phi^n(X_3=h1) & 0 \\
0 & 0 & \phi^m(X_3=h1) \\
0 & 0 & \phi^m(X_3=h2)
\end{array}\right]
\left[\begin{array}{c} \\ \end{array}\right]
\left[\begin{array}{c} \\ \end{array}\right]
C_n = 0 \qquad (16)
$$

Clearly intuitive methods of solution determination would be difficult in this case due to 20 equations in 20 unknowns. However recognizing certain groupings as natural Rayleigh and/or Stoneley wave solution sub-sets may be used as a search method in these multi-layered structures.

4.Ø TECHNICAL RESULTS

In this section the technical results of research conducted under Phase I (Section 2.1) is presented. In Section 4.1 the results of layered media surface wave velocity studies are presented for six different layer materials. In Section 4.2 the results of studies on interfacial waves are presented. The discovery of interface waves (Stoneley) in quartz for the first time is an important result of the phase I study and may lead to a new class of acoustic resonators. Using these results, a SAW sensor design is discussed in section 4.3 and in Section 4.4 theoretical results are compared to published experimental results for layered SAW resonators.

4.1 Layered Substrate Analyses

In this section six different materials are considered as candidates for passivation of SAW resonators. The materials considered are magnesium oxide (MgO), yittrium oxide (Y_2O_3), silicon dioxide (SiO_2), aluminum nitride (AlN), rutile or titanium dioxide (TiO_2), and sapphire (Al_2O_3). The theoretical approach for analyzing layered SAW velocity was discussed in Section 3.2. Results are presented as dispersion diagrams, surface wave coupling ($\Delta V/Vo$) and displacement/potential vectors vs distance from the top of the layered surface. For completeness tables of numerical solutions are included with displacement diagrams.

4.1.1 Analysis of MgO/ST-Quartz

Layers of MgO deposited on ST cut Quartz substrates were analyzed. Elastic and dielectric constant data for single crystal MgO (Appendix I) were used with the crystal c-axis perpendicular to the surface and the X-axis parallel to the Quartz X-axis.

Surface wave velocity vs normalized layer thickness is shown in Figure 9a. Because MgO is a faster (higher velocity) material the velocity increases with layer thickness until reaching the slow-shear wave velocity (dotted line) of ST-Quartz. Surface wave coupling is proportional to $\Delta V/Vo$ and this parameter is plotted in Figure 9b for two transducer configurations. Coupling drops quickly for layers greater than 1% of a wavelength.

Selected numerical solutions for MgO layers are shown in Figures 10,11,12, and 13. Figures 10-12 show the effect of shorting the electric field when the layer is 10% of the wavelength. The displacements/potential show penetration increasing with layer thickness. In Figure 13 displacements and potential are shown for a layer only 0.1% of the wavelength. The increased penetration with increasing layer thickness is due to the nearness of the bulk shear wave in the Quartz substrate.

Numerically MgO/ST-Quartz is governed by equations 9 and 10 of section 3.2 which contain 10 sub-solutions. These are presented in the Tables of Figures 10-13. Displacement/potential vectors associated with each sub-solution root (decay constant) are shown together with the 10 complex weighting factors for the complete summation solution per equation 5 of Section 3.1.

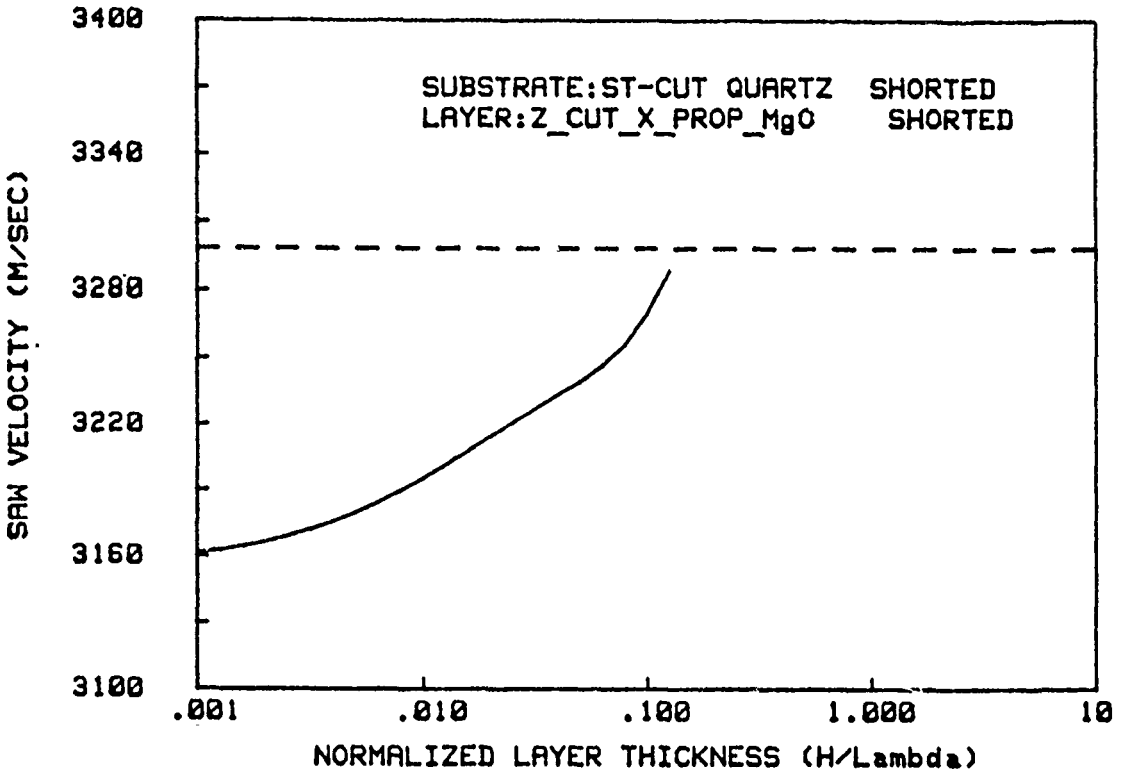

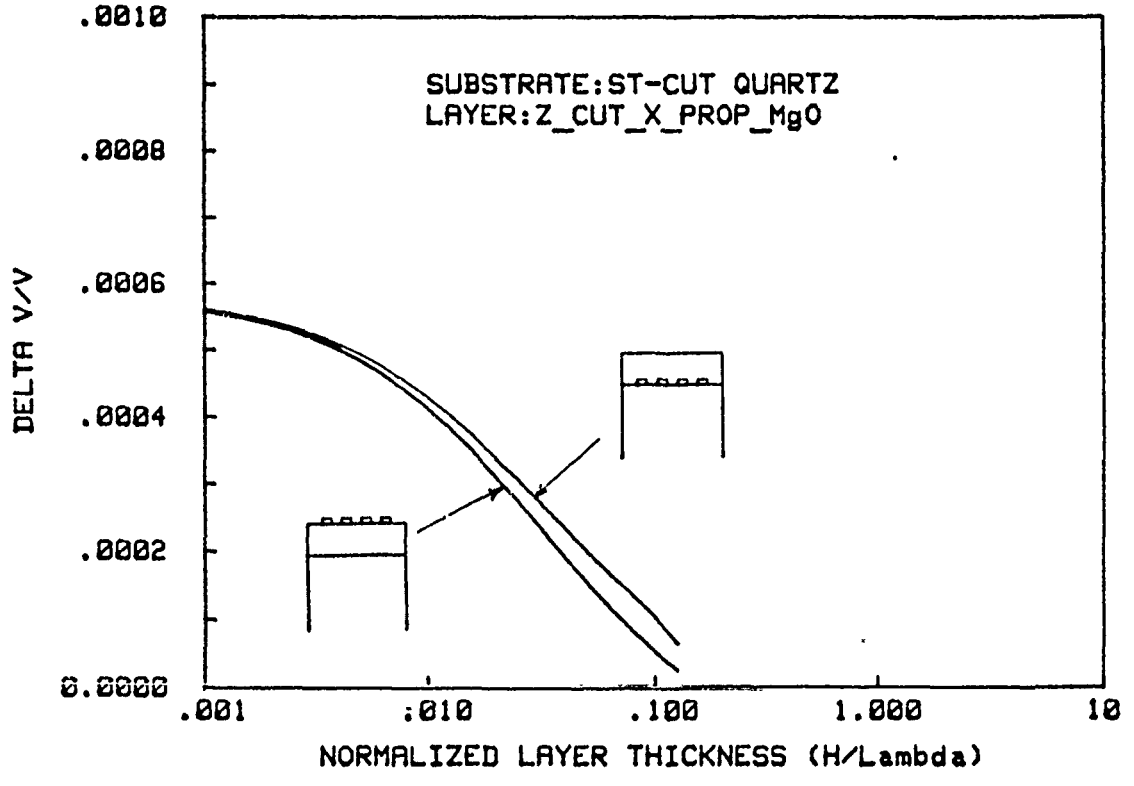

Figure 9- Velocity dispersion (a) and wave coupling (b) as a function of layer thickness for MgO/ST-Quartz.

```
THE VELOCITY IS W=3270.3999
BC DETERMINANT=+3.463E-18,-4.941E-09

ROOT#  1      +0.0000,-1.2366          U1=  +0.000,  +5.838  SUB
                                        U2=  -2.461,  +0.000  SUB
                                        U3=  +1.000,  +0.000  SUB
                                       U4=+0.000E+00,-5.987E+10  SUB
ROOT#  2      +0.0000,-1.0598          U1=  +0.000,  +2.978  SUB
                                        U2= -18.525,  +0.000  SUB
                                        U3=  +1.000,  +0.000  SUB
                                       U4=+0.000E+00,+4.770E+11  SUB
ROOT#  3      +0.0000,-1.0161          U1=  +0.000,  +3.195  SUB
                                        U2=  -3.731,  +0.000  SUB
                                        U3=  +1.000,  +0.000  SUB
                                       U4=+0.000E+00,-1.289E+11  SUB
ROOT#  4      +0.0000, -.0627          U1=  +0.000,   +.020  SUB
                                        U2=   +.196,  +0.000  SUB
                                        U3=  +1.000,  +0.000  SUB
                                       U4=+0.000E+00,+4.764E+08  SUB
ROOT#  5       +.4827, -.7599          U1=   -.849,   +.458 LAYER
                                        U2=  +0.000,  +0.000  LAYER
                                        U3=  +1.000,  +0.000  LAYER
ROOT#  6       -.4827, -.7599          U1=   +.849,   +.458 LAYER
                                        U2=  +0.000,  +0.000  LAYER
                                        U3=  +1.000,  +0.000  LAYER
ROOT#  7       +.4827, +.7599          U1=   -.849,   -.458 LAYER
                                        U2=  +0.000,  +0.000  LAYER
                                        U3=  +1.000,  +0.000  LAYER
ROOT#  8       -.4827, +.7599          U1=   +.849,   -.458 LAYER
                                        U2=  +0.000,  +0.000  LAYER
                                        U3=  +1.000,  +0.000  LAYER
ROOT#  9      +0.0000, -.8685          U1=  +0.000,  +0.000 LAYER
                                        U2=  +1.000,  +0.000  LAYER
                                        U3=  +0.000,  +0.000  LAYER
ROOT# 10      +0.0000, +.8685          U1=  +0.000,  +0.000 LAYER
                                        U2=  +1.000,  +0.000  LAYER
                                        U3=  +0.000,  +0.000  LAYER

WEIGHTING FACTORS
F(1)=-1.757E-01,-6.217E-15      F(2)=+5.962E-02,+1.108E-15
F(3)=+4.909E-01,+6.947E-15      F(4)=+1.962E+01,-2.490E-14
F(5)=+5.213E+00,+4.063E+00      F(6)=+5.213E+00,-4.063E+00
F(7)=+4.784E+00,-4.489E+00      F(8)=+4.784E+00,+4.489E+00
F(9)=+3.357E-01,+0.000E+00      F(10)+1.000E+00,+0.000E+00
```

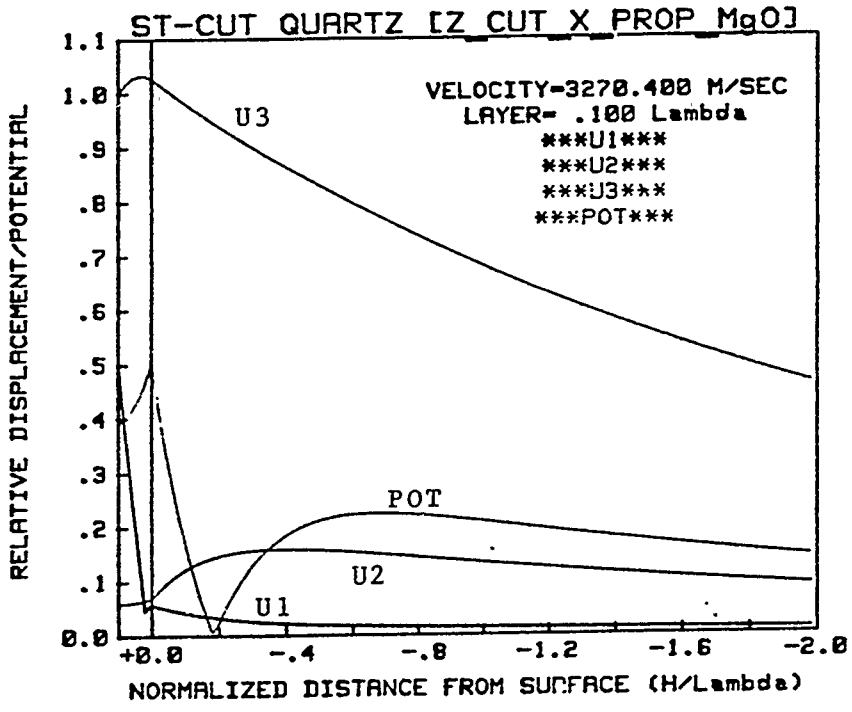

Figure 10- Layered velocity solution for MgO/ST-Quartz when the top layer and interface are unshorted. Layer thickness is 10% of a wavelength.

```
THE VELOCITY IS W=3270.2243
BC DETERMINANT=+1.135E-17,-1.780E-12

ROOT#  1     +0.0000,-1.2367        U1=  +0.000,  +5.838  SUB
                                    U2=  -2.461,  +0.000  SUB
                                    U3=  +1.000,  +0.000  SUB
                                   U4=+0.000E+00,-5.986E+10  SUB
ROOT#  2     +0.0000,-1.0598        U1=  +0.000,  +2.979  SUB
                                    U2= -18.488,  +0.000  SUB
                                    U3=  +1.000,  +0.000  SUB
                                   U4=+0.000E+00,+4.755E+11  SUB
ROOT#  3     +0.0000,-1.0161        U1=  +0.000,  +3.195  SUB
                                    U2=  -3.729,  +0.000  SUB
                                    U3=  +1.000,  +0.000  SUB
                                   U4=+0.000E+00,-1.289E+11  SUB
ROOT#  4     +0.0000, -.0629        U1=  +0.000,   +.020  SUB
                                    U2=   +.196,  +0.000  SUB
                                    U3=  +1.000,  +0.000  SUB
                                   U4=+0.000E+00,+4.779E+08  SUB
ROOT#  5      +.4827, -.7599        U1=   -.849,   +.458 LAYER
                                    U2=  +0.000,  +0.000  LAYER
                                    U3=  +1.000,  +0.000  LAYER
ROOT#  6      -.4827, -.7599        U1=   +.849,   +.458 LAYER
                                    U2=  +0.000,  +0.000  LAYER
                                    U3=  +1.000,  +0.000  LAYER
ROOT#  7      +.4827, +.7599        U1=   -.849,   -.458 LAYER
                                    U2=  +0.000,  +0.000  LAYER
                                    U3=  +1.000,  +0.000  LAYER
ROOT#  8      -.4827, +.7599        U1=   +.849,   -.458 LAYER
                                    U2=  +0.000,  +0.000  LAYER
                                    U3=  +1.000,  +0.000  LAYER
ROOT#  9     +0.0000, -.8685        U1=  +0.000,  +0.000 LAYER
                                    U2=  +1.000,  +0.000  LAYER
                                    U3=  +0.000,  +0.000  LAYER
ROOT# 10     +0.0000, +.8685        U1=  +0.000,  +0.000 LAYER
                                    U2=  +1.000,  +0.000  LAYER
                                    U3=  +0.000,  +0.000  LAYER

WEIGHTING FACTORS
F(1)=-1.544E-01,-3.553E-15     F(2)=+6.623E-02,+9.875E-17
F(3)=+4.445E-01,+2.083E-15     F(4)=+1.961E+01,+1.204E-14
F(5)=+5.207E+00,+4.058E+00     F(6)=+5.207E+00,-4.058E+00
F(7)=+4.778E+00,-4.482E+00     F(8)=+4.778E+00,+4.482E+00
F(9)=+3.357E-01,+0.000E+00     F(10)+1.000E+00,+0.000E+00
```

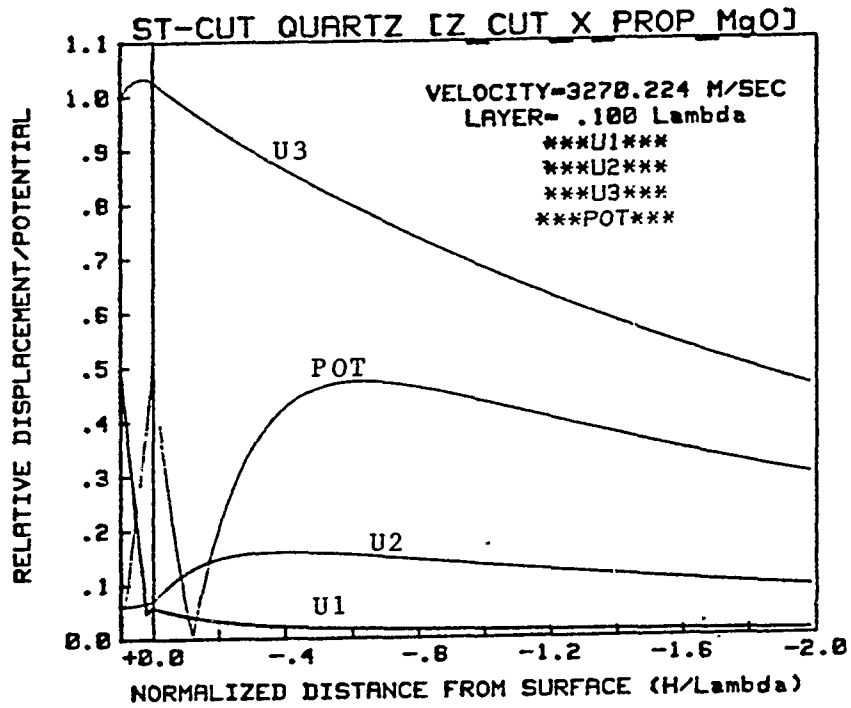

Figure 11- Layered velocity solution for MgO/ST-Quartz when the top layer surface is shorted. Layer thickness is 10% of a wavelength.

```
THE VELOCITY IS W=3270.0601
BC DETERMINANT=-6.596E-09,-1.944E-17

ROOT#  1      +0.0000,-1.2367          U1=  +0.000,  +5.838  SUB
                                        U2=  -2.461,  +0.000  SUB
                                        U3=  +1.000,  +0.000  SUB
                                       U4=+0.000E+00,-5.985E+10  SUB
ROOT#  2      +0.0000,-1.0598          U1=  +0.000,  +2.981  SUB
                                        U2= -18.453,  +0.000  SUB
                                        U3=  +1.000,  +0.000  SUB
                                       U4=+0.000E+00,+4.741E+11  SUB
ROOT#  3      +0.0000,-1.0161          U1=  +0.000,  +3.195  SUB
                                        U2=  -3.728,  +0.000  SUB
                                        U3=  +1.000,  +0.000  SUB
                                       U4=+0.000E+00,-1.290E+11  SUB
ROOT#  4      +0.0000, -.0631          U1=  +0.000,   +.020  SUB
                                        U2=   +.196,  +0.000  SUB
                                        U3=  +1.000,  +0.000  SUB
                                       U4=+0.000E+00,+4.793E+08  SUB
ROOT#  5       +.4827, -.7599          U1=   -.849,   +.458 LAYER
                                        U2=  +0.000,  +0.000  LAYER
                                        U3=  +1.000,  +0.000  LAYER
ROOT#  6       -.4827, -.7599          U1=   +.849,   +.458 LAYER
                                        U2=  +0.000,  +0.000  LAYER
                                        U3=  +1.000,  +0.000  LAYER
ROOT#  7       +.4827, +.7599          U1=   -.849,   -.458 LAYER
                                        U2=  +0.000,  +0.000  LAYER
                                        U3=  +1.000,  +0.000  LAYER
ROOT#  8       -.4827, +.7599          U1=   +.849,   -.458 LAYER
                                        U2=  +0.000,  +0.000  LAYER
                                        U3=  +1.000,  +0.000  LAYER
ROOT#  9      +0.0000, -.8686          U1=  +0.000,  +0.000 LAYER
                                        U2=  +1.000,  +0.000  LAYER
                                        U3=  +0.000,  +0.000  LAYER
ROOT# 10      +0.0000, +.8686          U1=  +0.000,  +0.000 LAYER
                                        U2=  +1.000,  +0.000  LAYER
                                        U3=  +0.000,  +0.000  LAYER

WEIGHTING FACTORS
F(1)=-1.346E-01,-5.329E-15     F(2)=+7.240E-02,-2.970E-16
F(3)=+4.014E-01,+6.941E-16     F(4)=+1.961E+01,-1.452E-13
F(5)=+5.201E+00,+4.054E+00     F(6)=+5.201E+00,-4.054E+00
F(7)=+4.773E+00,-4.477E+00     F(8)=+4.773E+00,+4.477E+00
F(9)=+3.357E-01,+0.000E+00     F(10)+1.000E+00,+0.000E+00
```

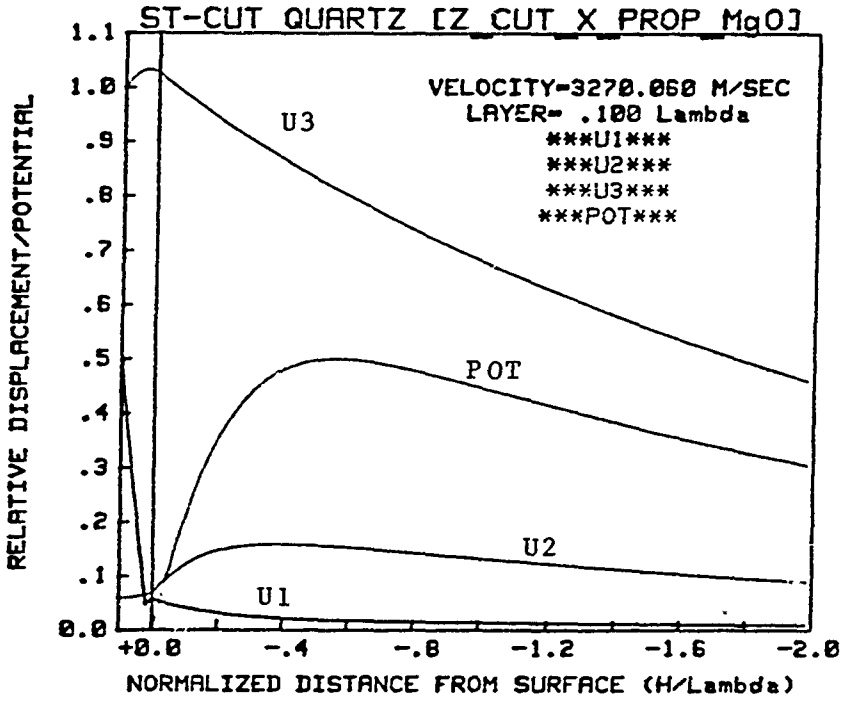

Figure 12- Layered velocity solution for MgO/ST-Quartz when the top layer and interface are shorted. Layer thickness is 10% of a wavelength.

```
THE VELOCITY IS W=3163.1149
BC DETERMINANT=-3.114E-18,+2.044E-11

ROOT#  1     +0.0000,-1.2623          U1=  +0.000,  +5.956  SUB
                                      U2=  -2.523,  +0.000  SUB
                                      U3=  +1.000,  +0.000  SUB
                                     U4=+0.000E+00,-5.521E+10  SUB
ROOT#  2     +0.0000,-1.0761          U1=  +0.000,  +3.311  SUB
                                      U2= -10.681,  +0.000  SUB
                                      U3=  +1.000,  +0.000  SUB
                                     U4=+0.000E+00,+1.555E+11  SUB
ROOT#  3     +0.0000,-1.0185          U1=  +0.000,  +3.098  SUB
                                      U2=  -3.074,  +0.000  SUB
                                      U3=  +1.000,  +0.000  SUB
                                     U4=+0.000E+00,-1.622E+11  SUB
ROOT#  4     +0.0000, -.1367          U1=  +0.000,   +.043  SUB
                                      U2=   +.192,  +0.000  SUB
                                      U3=  +1.000,  +0.000  SUB
                                     U4=+0.000E+00,+1.050E+09  SUB
ROOT#  5      +.4829, -.7679          U1=   -.851,   +.460 LAYER
                                      U2=  +0.000,  +0.000  LAYER
                                      U3=  +1.000,  +0.000  LAYER
ROOT#  6      -.4829, -.7679          U1=   +.851,   +.460 LAYER
                                      U2=  +0.000,  +0.000  LAYER
                                      U3=  +1.000,  +0.000  LAYER
ROOT#  7      +.4829, +.7679          U1=   -.851,   -.460 LAYER
                                      U2=  +0.000,  +0.000  LAYER
                                      U3=  +1.000,  +0.000  LAYER
ROOT#  8      -.4829, +.7679          U1=   +.851,   -.460 LAYER
                                      U2=  +0.000,  +0.000  LAYER
                                      U3=  +1.000,  +0.000  LAYER
ROOT#  9     +0.0000, -.8776          U1=  +0.000,  +0.000 LAYER
                                      U2=  +1.000,  +0.000  LAYER
                                      U3=  +0.000,  +0.000  LAYER
ROOT# 10     +0.0000, +.8776          U1=  +0.000,  +0.000 LAYER
                                      U2=  +1.000,  +0.000  LAYER
                                      U3=  +0.000,  +0.000  LAYER

WEIGHTING FACTORS
F(1)=-3.720E+00,-1.676E-14     F(2)=+4.864E-01,+3.607E-15
F(3)=+2.079E+00,+1.033E-14     F(4)=+2.183E+01,+9.571E-14
F(5)=+6.780E+00,+1.027E+01     F(6)=+6.780E+00,-1.027E+01
F(7)=+3.559E+00,-7.896E-01     F(8)=+3.559E+00,+7.896E-01
F(9)=+9.890E-01,+0.000E+00     F(10)+1.000E+00,+0.000E+00
```

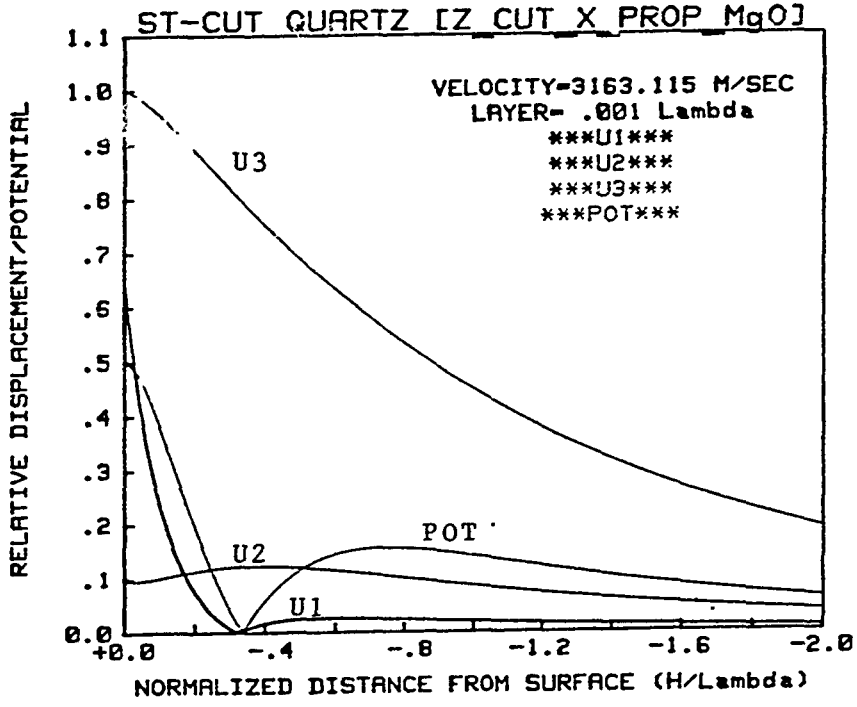

Figure 13- Layered velocity solution for MgO/ST-Quartz when the top layer and interface are unshorted. Layer thickness is 0.1% of a wavelength.

4.1.2 Analysis of Y_2O_3 /ST-Quartz

Layers of yittrium oxide on ST-Quartz substrates were analyzed. Elastic and dielectric constant data for single crystal Y_2O_3 (Appendix I) were used with the crystal c-axis perpendicular to the surface and the X-axis parallel to the Quartz X-axis.

Surface wave velocity vs normalized layer thickness is shown in Figure 14a. Because Y_2O_3 has a velocity only slightly higher than that of the quartz substrate, the velocity of the layered wave becomes constant for large normalized thickness. This implies the wave is entirely in the film and not affected by the substrate. This is confirmed by the coupling shown in Figure 14b where the coupling becomes zero as the thickness approaches a wavelength.

Selected numerical solutions for Y_2O_3 layers 10% of a wavelength are shown in Figures 15-17 under different conditions of shorted and unshorted electric fields at the top layer and interface. Numerically Y_2O_3 /ST-Quartz is governed by equations 9 and 10 of section 3.2 which contain 10 sub-solutions. These are presented in the Tables of Figures 15-17. Displacement/potential vectors associated with each sub-solution root (decay constant) are shown together with the 10 complex weighting factors for the complete summation solution per equation 5 of section 3.1.

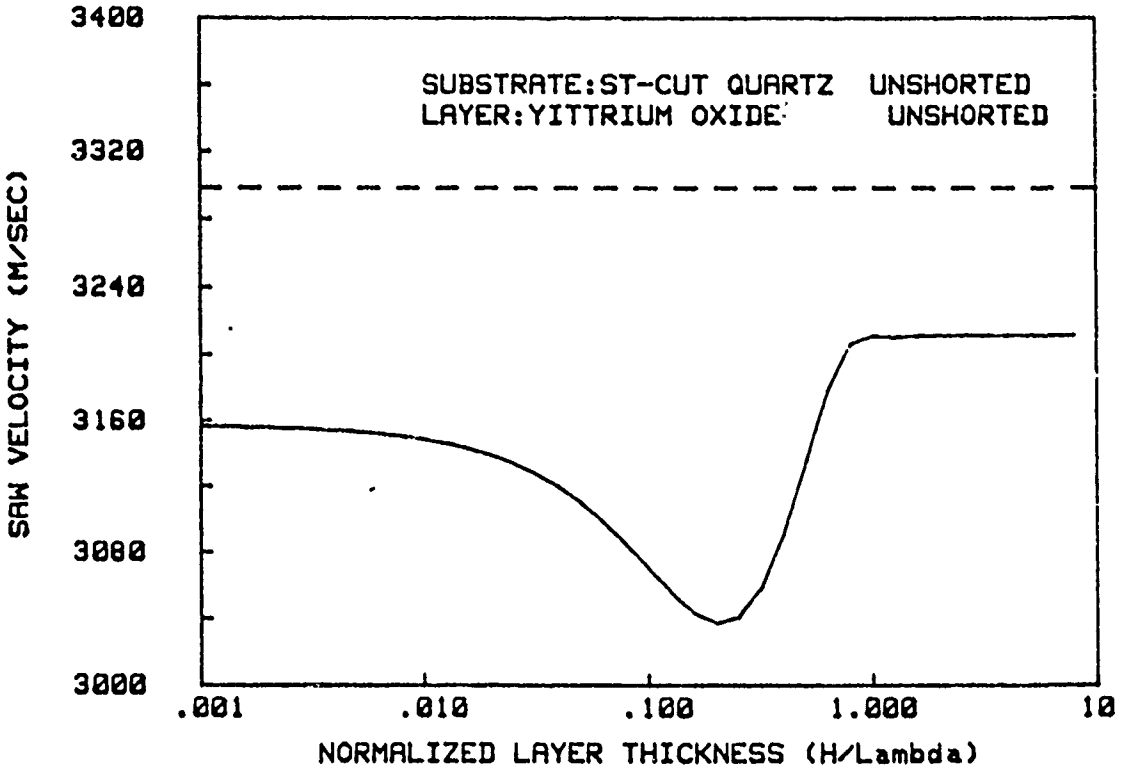

(a)

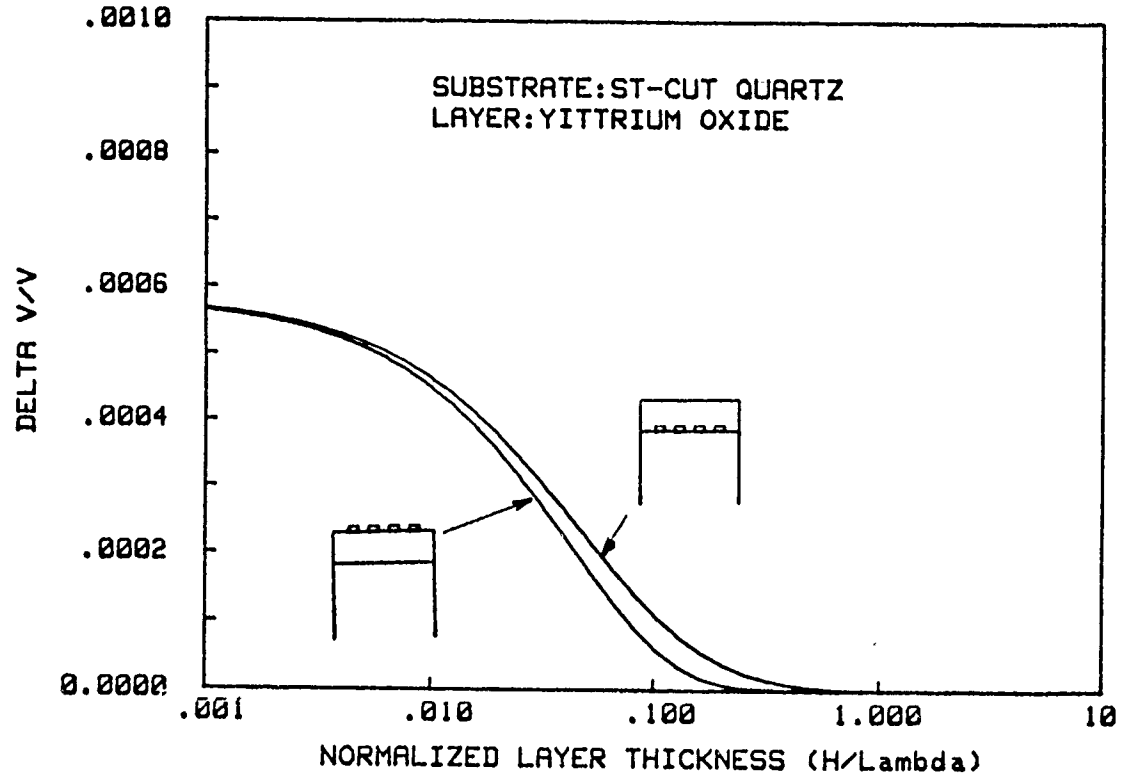

(b)

Figure 14- Velocity dispersion (a) and wave coupling (b) as a function of layer thickness for Y_2O_3/ST-Quartz.

```
THE VELOCITY IS W=3070.4024
BC DETERMINANT=-1.385E-18,+8.484E-14

ROOT#  1      +0.0000,-1.2830
  U1=  +0.000,  +6.047  SUB
  U2=  -2.566,  +0.000  SUB
  U3=  +1.000,  +0.000  SUB
U4=+0.000E+00,-5.208E+10  SUB

ROOT#  2      +0.0000,-1.0919
  U1=  +0.000,  +3.389  SUB
  U2=  -9.367,  +0.000  SUB
  U3=  +1.000,  +0.000  SUB
U4=+0.000E+00,+9.870E+10  SUB

ROOT#  3      +0.0000,-1.0185
  U1=  +0.000,  +2.998  SUB
  U2=  -2.701,  +0.000  SUB
  U3=  +1.000,  +0.000  SUB
U4=+0.000E+00,-1.826E+11  SUB

ROOT#  4      +0.0000, -.1761
  U1=  +0.000,   +.054  SUB
  U2=   +.189,  +0.000  SUB
  U3=  +1.000,  +0.000  SUB
U4=+0.000E+00,+1.364E+09  SUB

ROOT#  5       +.5049, -.4917
  U1=   -.660,   +.438 LAYER
  U2=  +0.000,  +0.000  LAYER
  U3=  +1.000,  +0.000  LAYER

ROOT#  6       -.5049, -.4917
  U1=   +.660,   +.438 LAYER
  U2=  +0.000,  +0.000  LAYER
  U3=  +1.000,  +0.000  LAYER

ROOT#  7       +.5049, +.4917
  U1=   -.660,   -.438 LAYER
  U2=  +0.000,  +0.000  LAYER
  U3=  +1.000,  +0.000  LAYER

ROOT#  8       -.5049, +.4917
  U1=   +.660,   -.438 LAYER
  U2=  +0.000,  +0.000  LAYER
  U3=  +1.000,  +0.000  LAYER

ROOT#  9      +0.0000, -.5581
  U1=  +0.000,  +0.000 LAYER
  U2=  +1.000,  +0.000  LAYER
  U3=  +0.000,  +0.000  LAYER

ROOT# 10      +0.0000, +.5581
  U1=  +0.000,  +0.000 LAYER
  U2=  +1.000,  +0.000  LAYER
  U3=  +0.000,  +0.000  LAYER

WEIGHTING FACTORS
F(1)=-6.857E-01,+7.216E-16    F(2)=+1.998E-01,-2.313E-16
F(3)=+4.533E-01,-1.495E-17    F(4)=+1.498E+01,-1.636E-16
F(5)=+6.211E+00,+5.835E+00    F(6)=+6.211E+00,-5.835E+00
F(7)=+1.265E+00,-1.572E+00    F(8)=+1.265E+00,+1.572E+00
F(9)=+4.959E-01,+0.000E+00    F(10)+1.000E+00,+0.000E+00
```

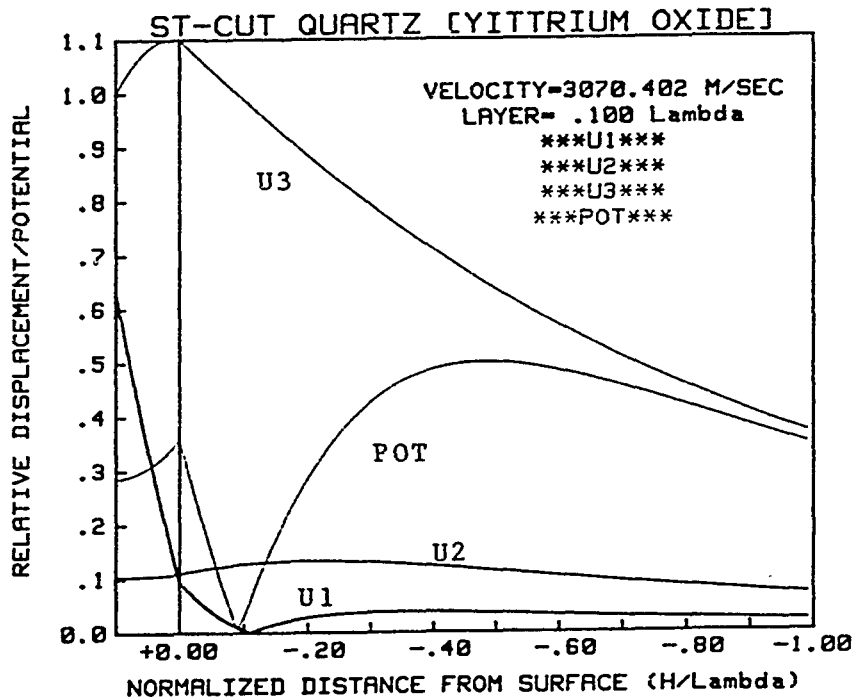

Figure 15- Layered velocity solution for Y_2O_3/ST-Quartz when the top layer and interface are unshorted. Layer thickness is 10% of a wavelength.

```
THE VELOCITY IS W=3070.2139
BC DETERMINANT=+1.304E-18,+0.282E-10

ROOT#  1     +0.0000,-1.2830      U1=  +0.000,  +6.047  SUB
                                  U2=  -2.566,  +0.000  SUB
                                  U3=  +1.000,  +0.000  SUB
                                  U4=+0.000E+00,-5.207E+10  SUB
ROOT#  2     +0.0000,-1.0919      U1=  +0.000,  +3.389  SUB
                                  U2=  -9.365,  +0.000  SUB
                                  U3=  +1.000,  +0.000  SUB
                                  U4=+0.000E+00,+9.863E+10  SUB
ROOT#  3     +0.0000,-1.0185      U1=  +0.000,  +2.998  SUB
                                  U2=  -2.700,  +0.000  SUB
                                  U3=  +1.000,  +0.000  SUB
                                  U4=+0.000E+00,-1.826E+11  SUB
ROOT#  4     +0.0000, -.1762      U1=  +0.000,   +.954  SUB
                                  U2=   +.189,  +0.000  SUB
                                  U3=  +1.000,  +0.000  SUB
                                  U4=+0.000E+00,+1.364E+09  SUB
ROOT#  5      +.5049, -.4918      U1=   -.660,   +.438  LAYER
                                  U2=  +0.000,  +0.000  LAYER
                                  U3=  +1.000,  +0.000  LAYER
ROOT#  6      -.5049, -.4918      U1=   +.660,   +.438  LAYER
                                  U2=  +0.000,  +0.000  LAYER
                                  U3=  +1.000,  +0.000  LAYER
ROOT#  7      +.5049, +.4918      U1=   -.660,   -.438  LAYER
                                  U2=  +0.000,  +0.000  LAYER
                                  U3=  +1.000,  +0.000  LAYER
ROOT#  8      -.5049, +.4918      U1=   +.660,   -.438  LAYER
                                  U2=  +0.000,  +0.000  LAYER
                                  U3=  +1.000,  +0.000  LAYER
ROOT#  9     +0.0000, -.5582      U1=  +0.000,  +0.000  LAYER
                                  U2=  +1.000,  +0.000  LAYER
                                  U3=  +0.000,  +0.000  LAYER
ROOT# 10     +0.0000, +.5582      U1=  +0.000,  +0.000  LAYER
                                  U2=  +1.000,  +0.000  LAYER
                                  U3=  +0.000,  +0.000  LAYER

WEIGHTING FACTORS
F(1)=-6.772E-01,+4.441E-16     F(2)=+2.036E-01,+9.785E-17
F(3)=+4.318E-01,-7.440E-17     F(4)=+1.498E+01,+1.518E-15
F(5)=+6.205E+00,+5.829E+00     F(6)=+6.205E+00,-5.829E+00
F(7)=+1.265E+00,-1.569E+00     F(8)=+1.265E+00,+1.569E+00
F(9)=+4.959E-01,+0.000E+00     F(10)+1.000E+00,+0.000E+00
```

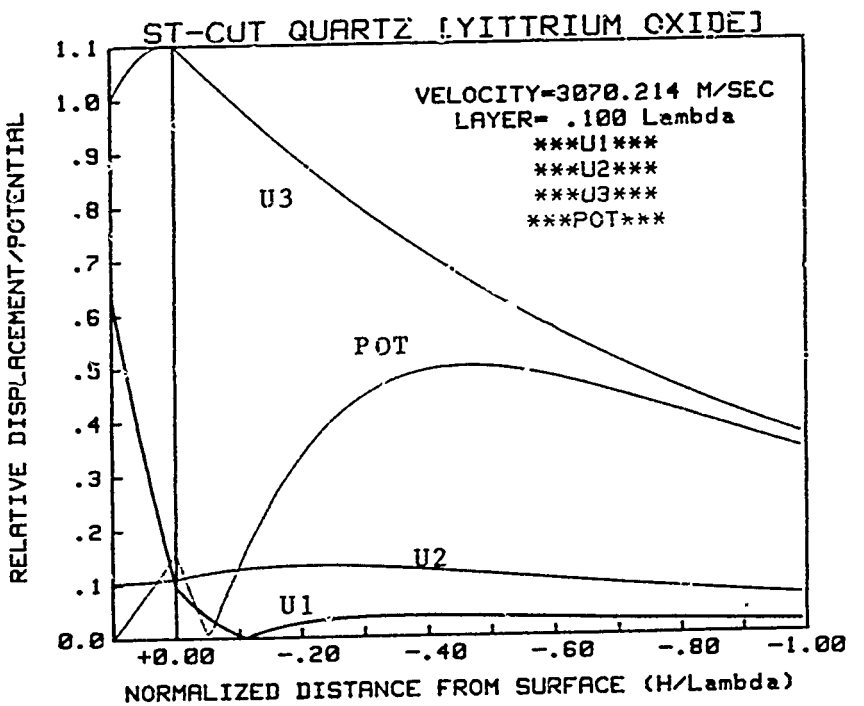

Figure 16- Layered velocity solution for Y_2O_3/ST-Quartz when the top layer surface is shorted. Layer thickness is 10% of a wavelength.

```
THE VELOCITY IS W=3070.0623
BC DETERMINANT=+1.152E-09,+7.170E-18

ROOT#  1      +0.0000,-1.2831          U1=  +0.000,  +6.047  SUB
                                        U2=  -2.567,  +0.000  SUB
                                        U3=  +1.000,  +0.000  SUB
                                       U4=+0.000E+00,-5.207E+10  SUB
ROOT#  2      +0.6000,-1.0919          U1=  +0.000,  +3.389  SUB
                                        U2=  -9.364,  +0.000  SUB
                                        U3=  +1.000,  +0.000  SUB
                                       U4=+0.000E+00,+9.858E+10  SUB
ROOT#  3      +0.0300,-1.0185          U1=  +0.000,  +2.998  SUB
                                        U2=  -2.699,  +0.000  SUB
                                        U3=  +1.000,  +0.000  SUB
                                       U4=+0.000E+00,-1.826E+11  SUB
ROOT#  4      +0.0300, -.1763          U1=  +0.000,   +.054  SUB
                                        U2=   +.189,  +0.000  SUB
                                        U3=  +1.000,  +0.000  SUB
                                       U4=+0.000E+00,+1.365E+09  SUB
ROOT#  5       +.5049, -.4918          U1=   -.660,   +.438 LAYER
                                        U2=  +0.000,  +0.000  LAYER
                                        U3=  +1.000,  +0.000  LAYER
ROOT#  6       -.5049, -.4918          U1=   +.660,   +.438 LAYER
                                        U2=  +0.000,  +0.000  LAYER
                                        U3=  +1.000,  +0.000  LAYER
ROOT#  7       +.5049, +.4918          U1=   -.660,   -.438 LAYER
                                        U2=  +0.000,  +0.000  LAYER
                                        U3=  +1.000,  +0.000  LAYER
ROOT#  8       -.5049, +.4918          U1=   +.660,   -.438 LAYER
                                        U2=  +0.000,  +0.000  LAYER
                                        U3=  +1.000,  +0.000  LAYER
ROOT#  9      +0.0000, -.5583          U1=  +0.000,  +0.000 LAYER
                                        U2=  +1.000,  +0.000  LAYER
                                        U3=  +0.000,  +0.000  LAYER
ROOT# 10      +0.0000, +.5583          U1=  +0.000,  +0.000 LAYER
                                        U2=  +1.000,  +0.000  LAYER
                                        U3=  +0.000,  +0.000  LAYER

WEIGHTING FACTORS
F(1)=-6.704E-01,+6.661E-16      F(2)=+2.067E-01,-2.669E-16
F(3)=+4.146E-01,-2.076E-16      F(4)=+1.498E+01,-2.100E-15
F(5)=+6.199E+00,+5.824E+00      F(6)=+6.199E+00,-5.824E+00
F(7)=+1.264E+00,-1.568E+00      F(8)=+1.264E+00,+1.568E+00
F(9)=+4.958E-01,+0.000E+00      F(10)+1.000E+00,+0.000E+00
```

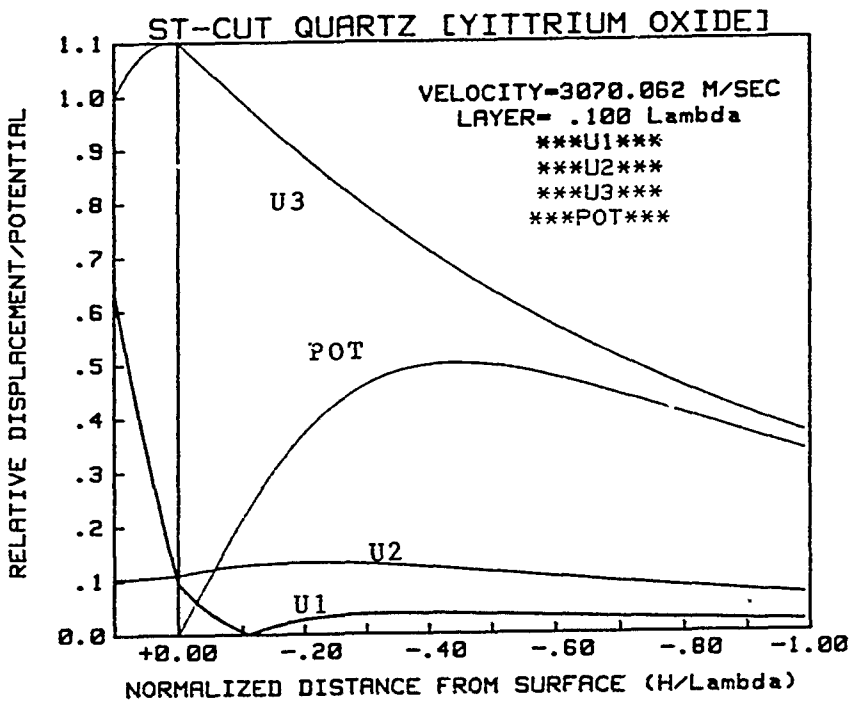

Figure 17- Layered velocity solution for Y_2O_3/ST-Quartz when the top layer and interface are shorted. Layer thickness is 10% of a wavelength.

4.1.3 Analysis of SiO_x/ST-Quartz

Layers of fused quartz on ST-cut Quartz substrates were analyzed. Elastic and dielectric constant data for isotropic fused quartz (Appendix I) were used. Surface wave velocity vs normalized layer thickness is shown in Figure 18a. Because fused quartz is a faster material the velocity increases with layer thickness until reaching the slow shear velocity of the substrate. Surface wave coupling is plotted in Figure 18b for two transducer configurations. The coupling becomes zero for thicknesses greater than half a wavelength.

Selected numerical solutions for fused quartz layers are shown in Figures 19-21. The displacements/potential show penetration increasing with layer thickness. The increased penetration with increasing layer thickness is due to the nearness of the bulk shear wave in the Quartz substrate.

Numerically SiO_x/ST-Quartz is governed by equations 9 and 10 of section 3.2 which contain 10 sub-solutions. Displacement and potential vectors associated with each sub-solution are shown together with the 10 complex weighting factors for the complete summation solution per equation 5 of Section 3.1.

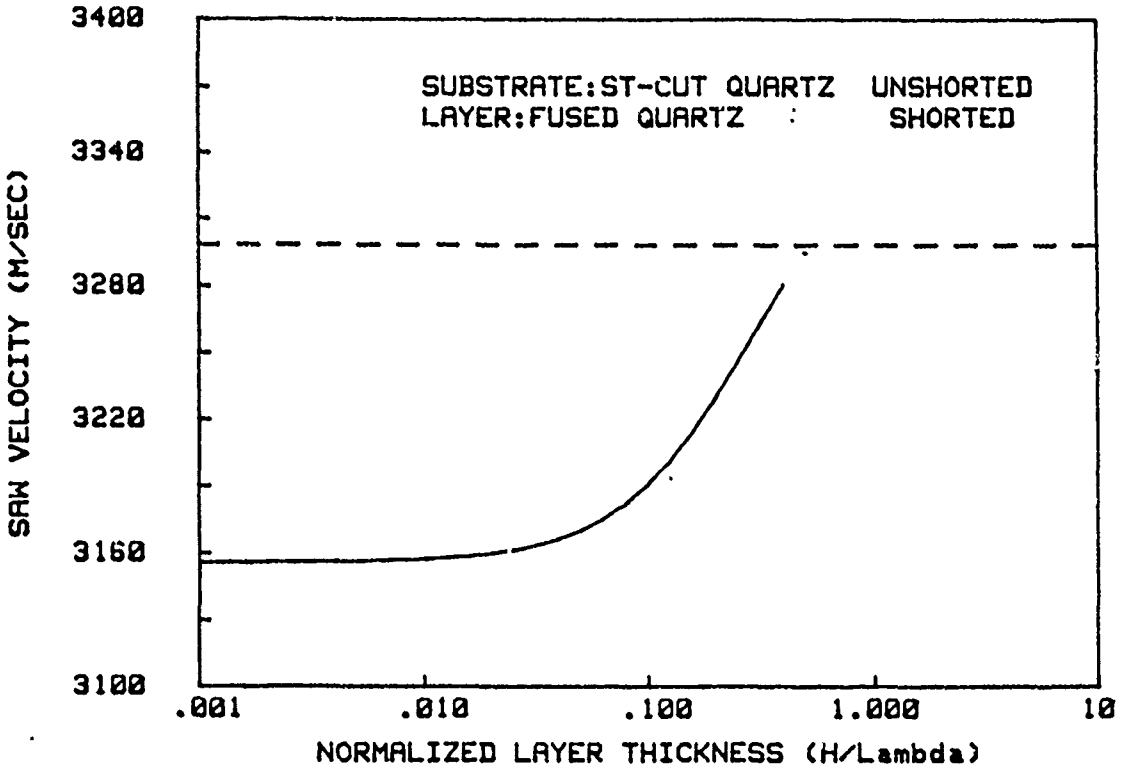

(a)

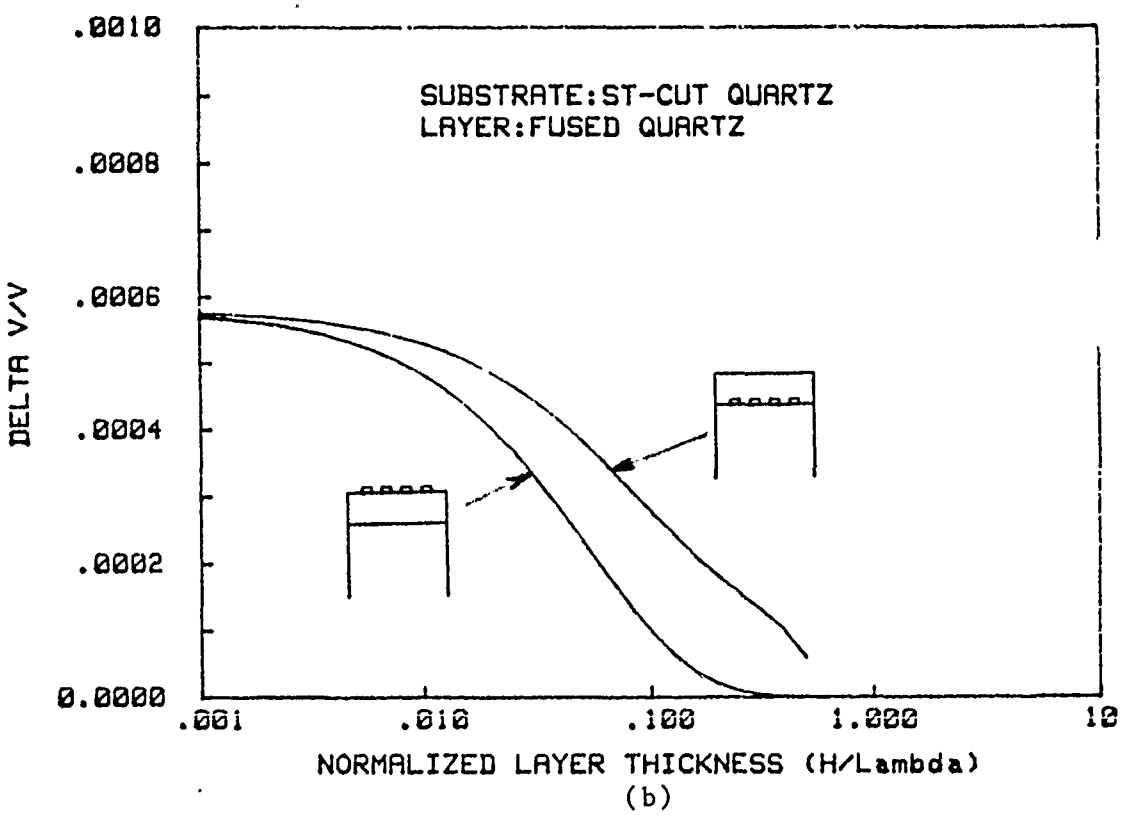

(b)

Figure 18- Velocity dispersion (a) and wave coupling (b) as a function of layer thickness for SiO_x/ST-Quartz.

```
THE VELOCITY IS W=3229.7250
BC DETERMINANT=+0.000E+00,+1.189E-10

ROOT#  1     +0.0000,-1.2466        U1=  +0.000,  +5.884  SUB
                                    U2=  -2.486,  +0.000  SUB
                                    U3=  +1.000,  +0.000  SUB
                                   U4=+0.000E+00,-5.795E+10  SUB
ROOT#  2     +0.0000,-1.0655        U1=  +0.000,  +3.189  SUB
                                    U2= -13.449,  +0.000  SUB
                                    U3=  +1.000,  +0.000  SUB
                                   U4=+0.000E+00,+2.702E+11  SUB
ROOT#  3     +0.0000,-1.0175        U1=  +0.000,  +3.163  SUB
                                    U2=  -3.449,  +0.000  SUB
                                    U3=  +1.000,  +0.000  SUB
                                   U4=+0.000E+00,-1.429E+11  SUB
ROOT#  4     +0.0000, -.0979        U1=  +0.000,   +.031  SUB
                                    U2=   +.194,  +0.000  SUB
                                    U3=  +1.000,  +0.000  SUB
                                   U4=+0.000E+00,+7.473E+08  SUB
ROOT#  5     +0.0000, -.8412        U1=  +0.000,  +1.189 LAYER
                                    U2=  +0.000,  +0.000  LAYER
                                    U3=  +1.000,  +0.000  LAYER
ROOT#  6     +0.0000, -.5143        U1=  +0.000,   +.514 LAYER
                                    U2=  +0.000,  +0.000  LAYER
                                    U3=  +1.000,  +0.000  LAYER
ROOT#  7     +0.0000, +.5143        U1=  +0.000,   -.514 LAYER
                                    U2=  +0.000,  +0.000  LAYER
                                    U3=  +1.000,  +0.000  LAYER
ROOT#  8     +0.0000, +.8412        U1=  +0.000, -1.189 LAYER
                                    U2=  +0.000,  +0.000  LAYER
                                    U3=  +1.000,  +0.000  LAYER
ROOT#  9     +0.0000, -.5143        U1=  +0.000,  +0.000 LAYER
                                    U2=  +1.000,  +0.000  LAYER
                                    U3=  +0.000,  +0.000  LAYER
ROOT# 10     +0.0000, +.5143        U1=  +0.000,  +0.000 LAYER
                                    U2=  +1.000,  +0.000  LAYER
                                    U3=  +0.000,  +0.000  LAYER

WEIGHTING FACTORS
F(1)=-3.966E-01,+0.000E+00     F(2)=+3.412E-02,+0.000E+00
F(3)=+3.455E-01,+0.000E+00     F(4)=+9.983E+00,+0.000E+00
F(5)=-6.128E+00,+0.000E+00     F(6)=+1.407E+01,+0.000E+00
F(7)=+2.432E+00,+0.000E+00     F(8)=-4.050E-31,+0.000E+00
F(9)=+2.746E-01,+0.000E+00     F(10)+1.000E+00,+0.000E+00
```

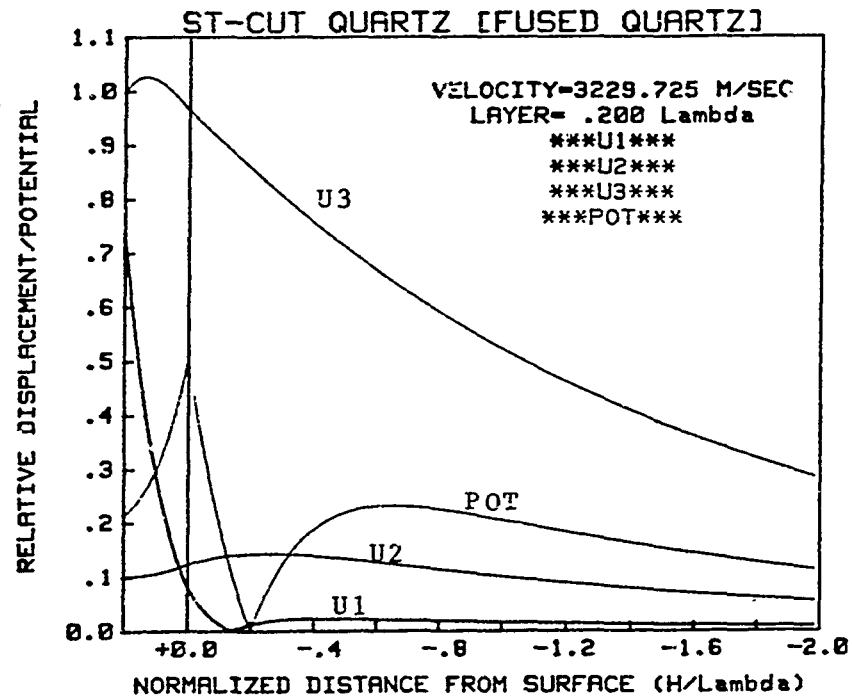

Figure 19- Layered velocity solution for SiO_x/ST-Quartz when the top layer and interface are unshorted. Layer thickness is 20% of a wavelength.

```
THE VELOCITY IS W=3229.6590
BC DETERMINANT=+0.000E+00,+5.098E-10

ROOT#  1     +0.0000,-1.2466        U1=  +0.000,  +5.884  SUB
                                    U2=  -2.486,  +0.000  SUB
                                    U3=  +1.000,  +0.000  SUB
                                   U4=+0.000E+00,-5.794E+10  SUB
ROOT#  2     +0.0000,-1.0655        U1=  +0.000,  +3.189  SUB
                                    U2= -13.445,  +0.000  SUB
                                    U3=  +1.000,  +0.000  SUB
                                   U4=+0.000E+00,+2.700E+11  SUB
ROOT#  3     +0.0000,-1.0175        U1=  +0.000,  +3.163  SUB
                                    U2=  -3.448,  +0.000  SUB
                                    U3=  +1.000,  +0.000  SUB
                                   U4=+0.000E+00,-1.429E+11  SUB
ROOT#  4     +0.0000, -.0980        U1=  +0.000,   +.031  SUB
                                    U2=   +.194,  +0.600  SUB
                                    U3=  +1.000,  +0.000  SUB
                                   U4=+0.000E+00,+7.476E+08  SUB
ROOT#  5     +0.0000, -.8412        U1=  +0.000,  +1.189 LAYER
                                    U2=  +0.000,  +0.000  LAYER
                                    U3=  +1.000,  +0.000  LAYER
ROOT#  6     +0.0000, -.5143        U1=  +0.000,   +.514 LAYER
                                    U2=  +0.000,  +0.000  LAYER
                                    U3=  +1.000,  +0.000  LAYER
ROOT#  7     +0.0000, +.5143        U1=  +0.000,   -.514 LAYER
                                    U2=  +0.000,  +0.000  LAYER
                                    U3=  +1.000,  +0.000  LAYER
ROOT#  8     +0.0000, +.8412        U1=  +0.000,  -1.189 LAYER
                                    U2=  +0.000,  +0.000  LAYER
                                    U3=  +1.000,  +0.000  LAYER
ROOT#  9     +0.0000, -.5143        U1=  +0.000,  +0.000 LAYER
                                    U2=  +1.000,  +0.000  LAYER
                                    U3=  +0.000,  +0.000  LAYER
ROOT# 10     +0.0000, +.5143        U1=  +0.000,  +0.000 LAYER
                                    U2=  +1.000,  +0.000  LAYER
                                    U3=  +0.000,  +0.000  LAYER

WEIGHTING FACTORS
F(1)=-3.937E-01,+0.000E+00     F(2)=+3.530E-02,+0.000E+00
F(3)=+3.388E-01,+0.000E+00     F(4)=+9.982E+00,+0.000E+00
F(5)=-6.126E+00,+0.000E+00     F(6)=+1.406E+01,+0.000E+00
F(7)=+2.432E+00,+0.000E+00     F(8)=-4.046E-01,+0.000E+00
F(9)=+2.746E-01,+0.000E+00     F(10)+1.000E+00,+0.000E+00
```

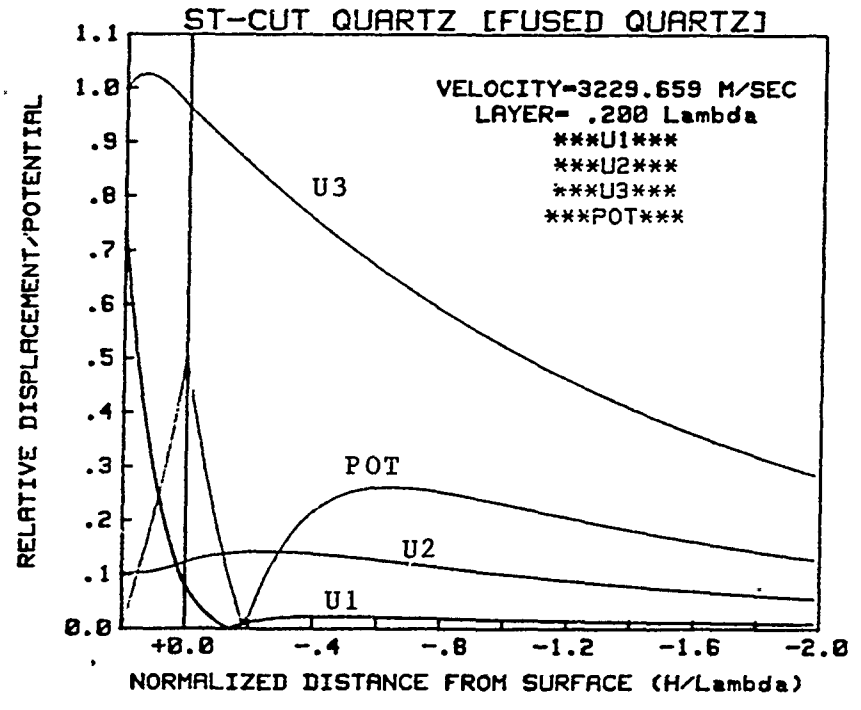

Figure 20- Layered velocity solution for SiO_x/ST-Quartz when the top layer surface is shorted. Layer thickness is 20% of a wavelength.

THE VELOCITY IS W=3229.1370
BC DETERMINANT=-1.899E-10,+0.000E+00

ROOT# 1	+0.0000,-1.2468	U1= +0.000, +5.885 SUB	
		U2= -2.486, +0.000 SUB	
		U3= +1.000, +0.000 SUB	
		U4=+0.000E+00,-5.792E+10 SUB	
ROOT# 2	+0.0000,-1.0656	U1= +0.000, +3.190 SUB	
		U2= -13.407, +0.000 SUB	
		U3= +1.000, +0.000 SUB	
		U4=+0.000E+00,+2.685E+11 SUB	
ROOT# 3	+0.0000,-1.0175	U1= +0.000, +3.162 SUB	
		U2= -3.445, +0.000 SUB	
		U3= +1.000, +0.000 SUB	
		U4=+0.000E+00,-1.431E+11 SUB	
ROOT# 4	+0.0000, -.0983	U1= +0.000, +.031 SUB	
		U2= +.194, +0.000 SUB	
		U3= +1.000, +0.000 SUB	
		U4=+0.000E+00,+7.505E+08 SUB	
ROOT# 5	+0.0000, -.8413	U1= +0.000, +1.189 LAYER	
		U2= +0.000, +0.000 LAYER	
		U3= +1.000, +0.000 LAYER	
ROOT# 6	+0.0000, -.5145	U1= +0.000, +.515 LAYER	
		U2= +0.000, +0.000 LAYER	
		U3= +1.000, +0.000 LAYER	
ROOT# 7	+0.0000, +.5145	U1= +0.000, -.515 LAYER	
		U2= +0.000, +0.000 LAYER	
		U3= +1.000, +0.000 LAYER	
ROOT# 8	+0.0000, +.8413	U1= +0.000, -1.189 LAYER	
		U2= +0.000, +0.000 LAYER	
		U3= +1.000, +0.000 LAYER	
ROOT# 9	+0.0000, -.5145	U1= +0.000, +0.000 LAYER	
		U2= +1.000, +0.000 LAYER	
		U3= +0.000, +0.000 LAYER	
ROOT# 10	+0.0000, +.5145	U1= +0.000, +0.000 LAYER	
		U2= +1.000, +0.000 LAYER	
		U3= +0.000, +0.000 LAYER	

WEIGHTING FACTORS

F(1)=-3.708E-01,+0.000E+00	F(2)=+4.466E-02,+0.000E+00
F(3)=+2.862E-01,+0.000E+00	F(4)=+9.974E+00,+0.000E+00
F(5)=-6.110E+00,+0.000E+00	F(6)=+1.402E+01,+0.000E+00
F(7)=+2.428E+00,+0.000E+00	F(8)=-4.017E-01,+0.000E+00
F(9)=+2.744E-01,+0.000E+00	F(10)+1.000E+00,+0.000E+00

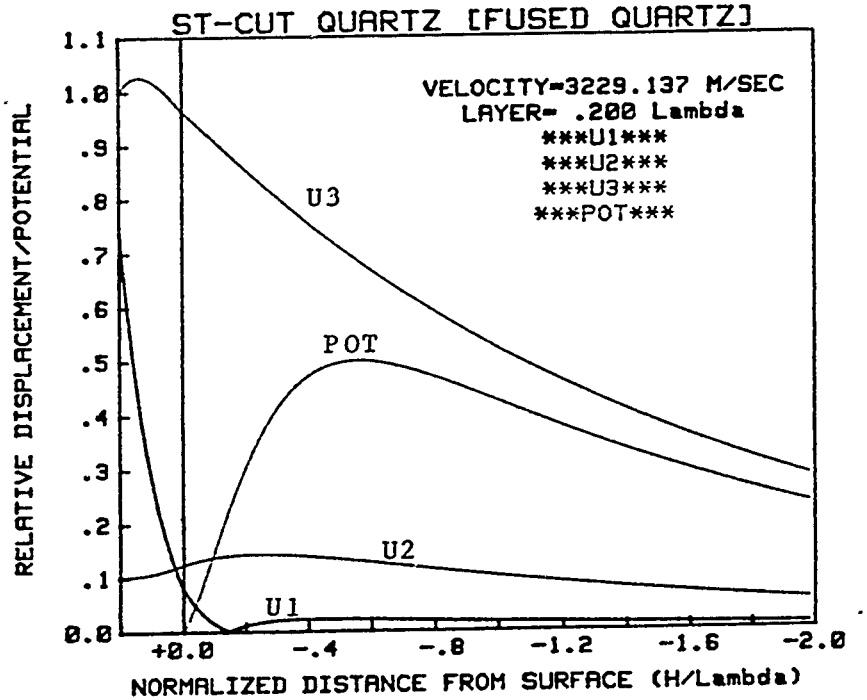

Figure 21- Layered velocity solution for SiO_x/ST-Quartz when the top layer and interface are shorted. Layer thickness is 20% of a wavelength.

4.1.4 Analysis of AlN/ST-Quartz

Layers of aluminum nitride (AlN) deposited on ST-cut Quartz substrates were analyzed. Surface wave velocity vs normalized layer thickness is shown in Figure 22a and 23a for combinations of shorted layer and/or interface. Because AlN is a faster material, the velocity increases with layer thickness until reaching the slow-shear velocity (dotted line) of the ST-Quartz substrate. Because AlN is piezoelectric, four possible transducer configurations are possible. Coupling efficiency to surface waves with only interdigital electrodes at either the interface or top layer surface is shown in Figure 22b. When the interdigital electrodes are at the interface, the coupling is reduced because the wave displacements are located at the top surface. If the electrodes are at the surface and the layer is thick, coupling efficiency improves because of the piezoelectric AlN layer.

For the floating ground plane (either at the surface or interface) the coupling is shown in Figure 23b. Normally, the coupling is low for thin layers. However when the layer thickness is increased, the coupling peaks at 2% of a wavelength.

Numerical solutions for AlN layers are shown in Figures 24-27 for different shorting conditions and thickness equal to 10% of a wavelength. Numerically AlN/ST-Quartz is governed by equations 11 and 12 of section 3.2 which contain 12 sub-solutions. These are presented in the Tables of Figures 24-27. Displacement and potential vectors associated with each sub-solution root are shown together with the 12 complex weighting factors for the complete summation solution per equation 5 of section 3.1.

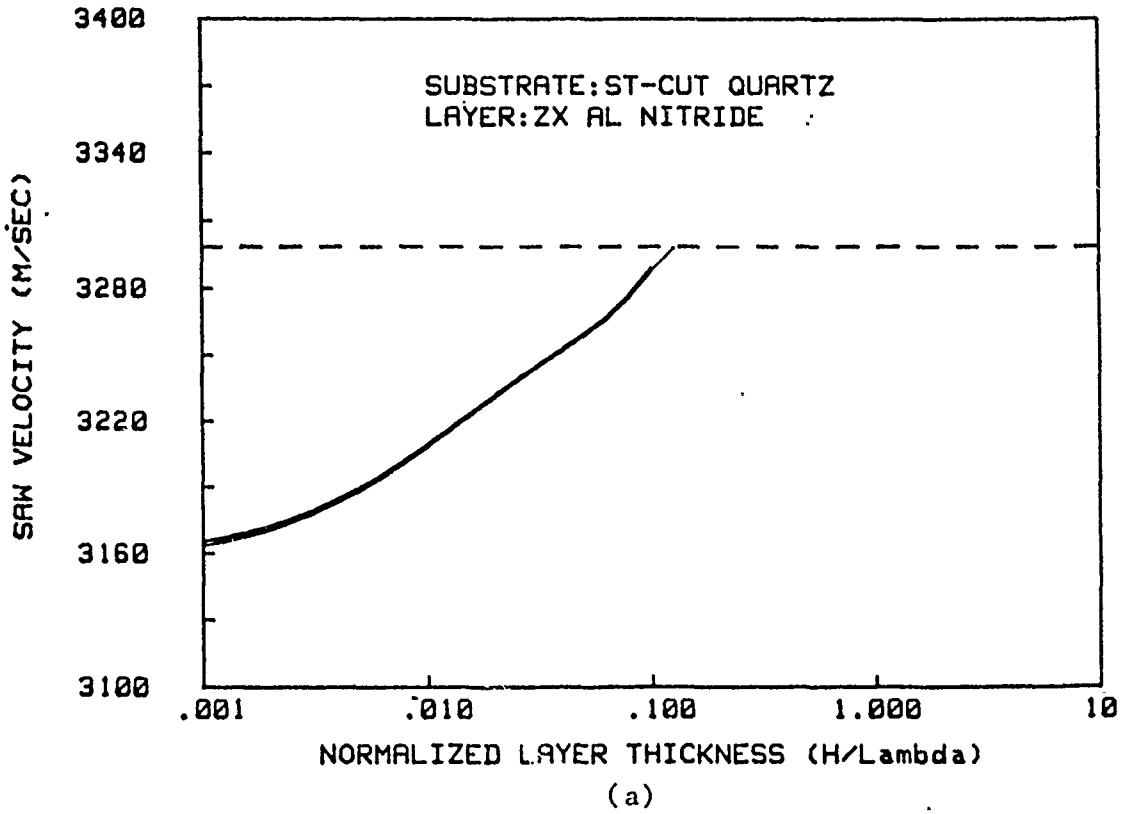

(a)

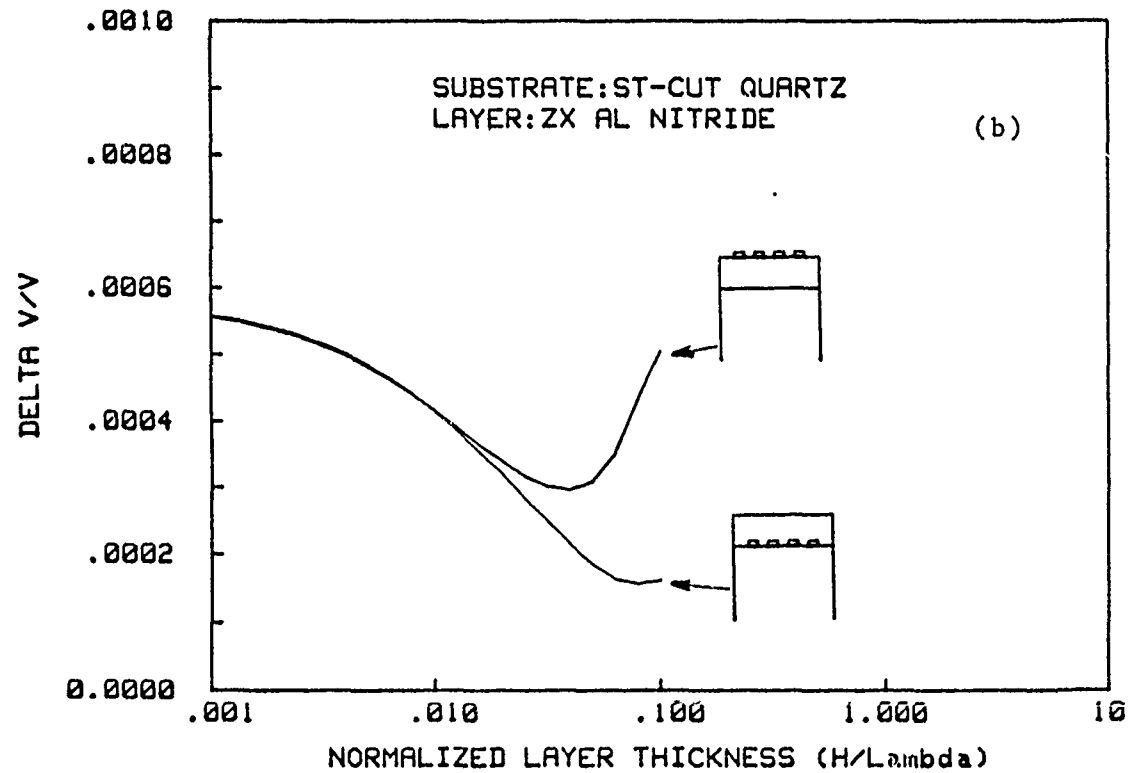

Figure 22- Velocity dispersion (a) and wave coupling (b) as a function of layer thickness for AlN on ST-Quartz with electrodes at either the top or interface surface.

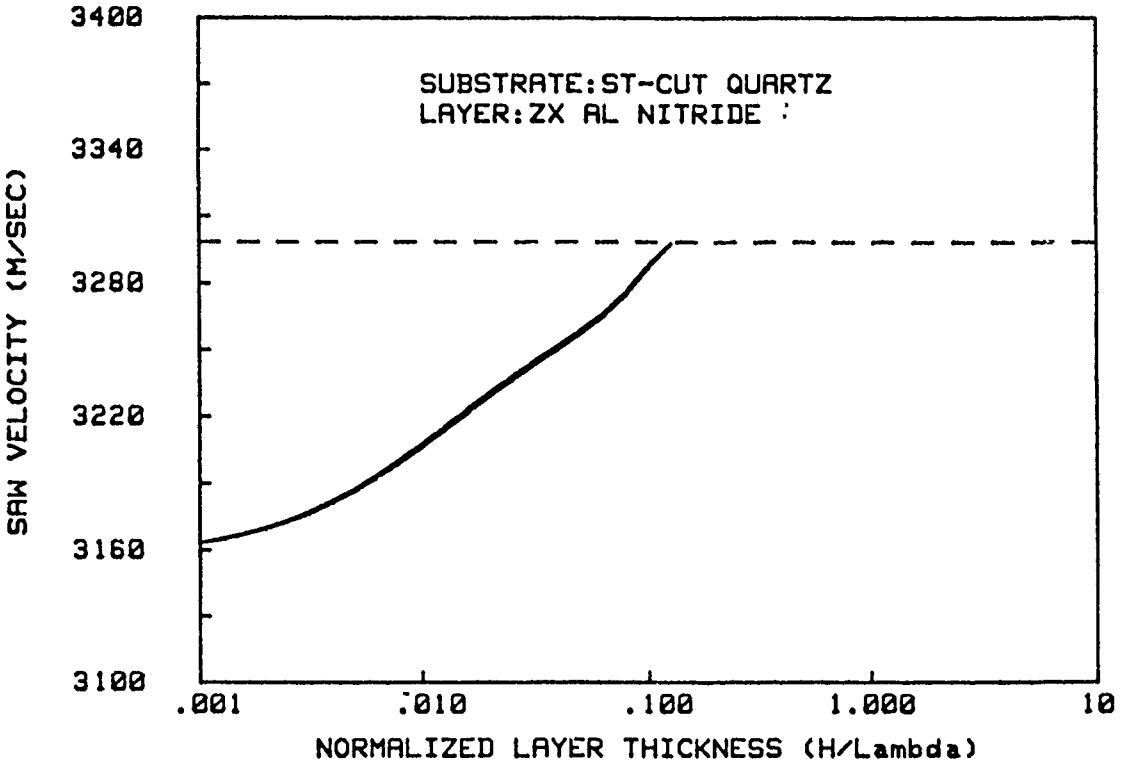

(a)

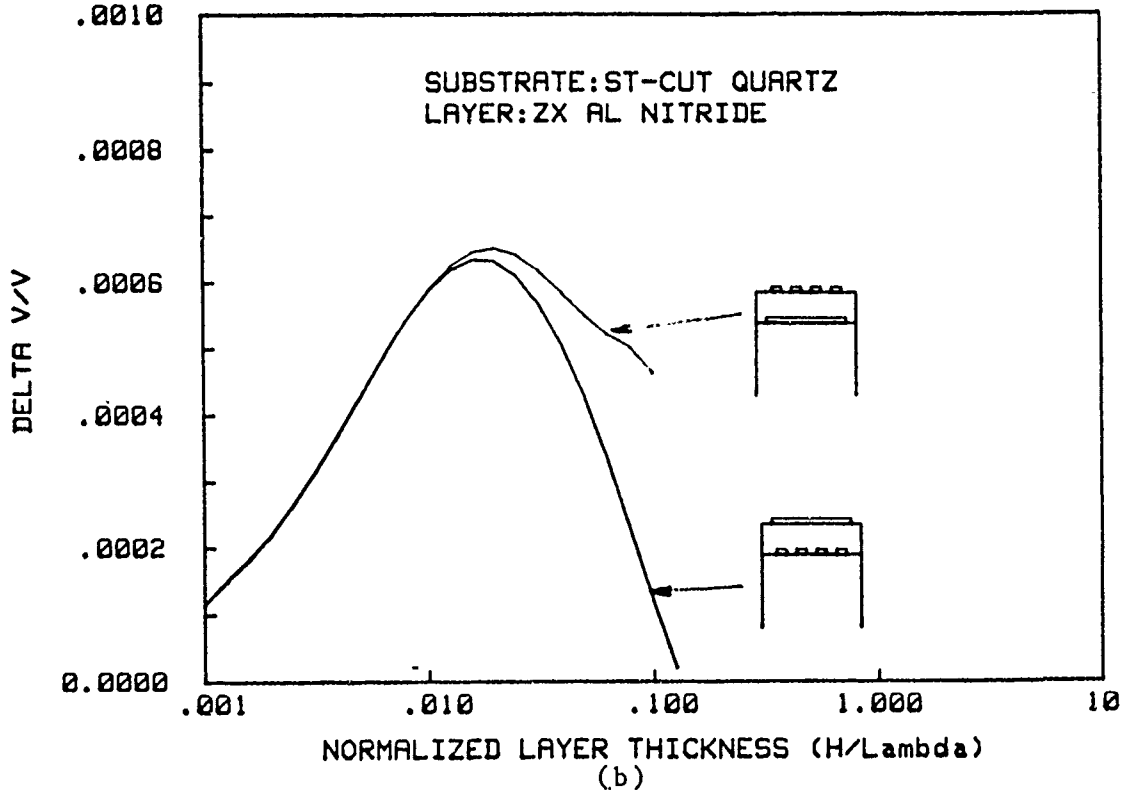

(b)

Figure 23- Velocity dispersion (a) and wave coupling (b) as a function of layer thickness for AlN on ST-Quartz with interdigital electrodes and an opposing ground plane.

```
THE VELOCITY IS W=3288.9303
BC DETERMINANT=+6.913E-11,-5.632E-07

ROOT# 1     +0.0000,-1.2320
                U1=  +0.000,  +5.816  SUB
                U2=  -2.449,  +0.000  SUB
                U3=  +1.000,  +0.000  SUB
               U4=+0.000E+00,-6.083E+10  SUB
ROOT# 2     +0.0000,-1.0575
                U1=  +0.000,  +2.735  SUB
                U2= -24.326,  +0.000  SUB
                U3=  +1.000,  +0.000  SUB
               U4=+0.000E+00,+7.119E+11  SUB
ROOT# 3     +0.0000,-1.0152
                U1=  +0.000,  +3.207  SUB
                U2=  -3.872,  +0.000  SUB
                U3=  +1.000,  +0.000  SUB
               U4=+0.000E+00,-1.220E+11  SUB
ROOT# 4     +0.0000, -.0364
                U1=  +0.000,   +.012  SUB
                U2=   +.196,  +0.000  SUB
                U3=  +1.000,  +0.000  SUB
               U4=+0.000E+00,+2.759E+08  SUB
ROOT# 5     +0.0000,-1.3984
                U1=  +0.000,  +2.843 LAYER
                U2=  +0.000,  +0.000  LAYER
                U3=  +1.000,  +0.000  LAYER
               U4=+7.303E+10,+0.000E+00  LAY
ROOT# 6      +.2352, -.6516
                U1=   -.365,   +.539 LAYER
                U2=  +0.000,  +0.000  LAYER
                U3=  +1.000,  +0.000  LAYER
               U4=-1.215E+10,-2.706E+10  LAY
ROOT# 7      -.2352, -.6516
                U1=   +.365,   +.539 LAYER
                U2=  +0.000,  +0.000  LAYER
                U3=  +1.000,  +0.000  LAYER
               U4=-1.215E+10,+2.706E+10  LAY
ROOT# 8      +.2352, +.6516
                U1=   -.365,   -.539 LAYER
                U2=  +0.000,  +0.000  LAYER
                U3=  +1.000,  +0.000  LAYER
               U4=-1.215E+10,+2.706E+10  LAY
ROOT# 9      -.2352, +.6516
                U1=   +.365,   -.539 LAYER
                U2=  +0.000,  +0.000  LAYER
                U3=  +1.000,  +0.000  LAYER
               U4=-1.215E+10,-2.706E+10  LAY
ROOT# 10    +0.0000,+1.3984
                U1=  +0.000,  -2.843 LAYER
                U2=  +0.000,  +0.000  LAYER
                U3=  +1.000,  +0.000  LAYER
               U4=+7.303E+10,+0.000E+00  LAY
ROOT# 11    +0.0000, -.7958
                U1=  +0.000,  +0.000 LAYER
                U2=  +1.000,  +0.000  LAYER
                U3=  +0.000,  +0.000  LAYER
               U4=+0.000E+00,+0.000E+00  LAY
ROOT# 12    +0.0000, +.7958
                U1=  +0.000,  +0.000 LAYER
                U2=  +1.000,  +0.000  LAYER
                U3=  +0.000,  +0.000  LAYER
               U4=+0.000E+00,+0.000E+00  LAY

WEIGHTING FACTORS
F(1)=+7.786E-03,+8.605E-02     F(2)=+2.169E-02,+1.837E-02
F(3)=+2.563E-01,-1.723E-01     F(4)=+1.480E+01,-4.947E-02
F(5)=-1.221E+00,+4.649E-03     F(6)=+4.519E+00,+3.250E+00
F(7)=+4.379E+00,-3.328E+00     F(8)=+4.294E+00,-3.815E+00
F(9)=+4.590E+00,+3.798E+00     F(10)-1.472E+00,-2.623E-02
F(11)+3.678E-01,+0.000E+00     F(12)+1.000E+00,+0.000E+00
```

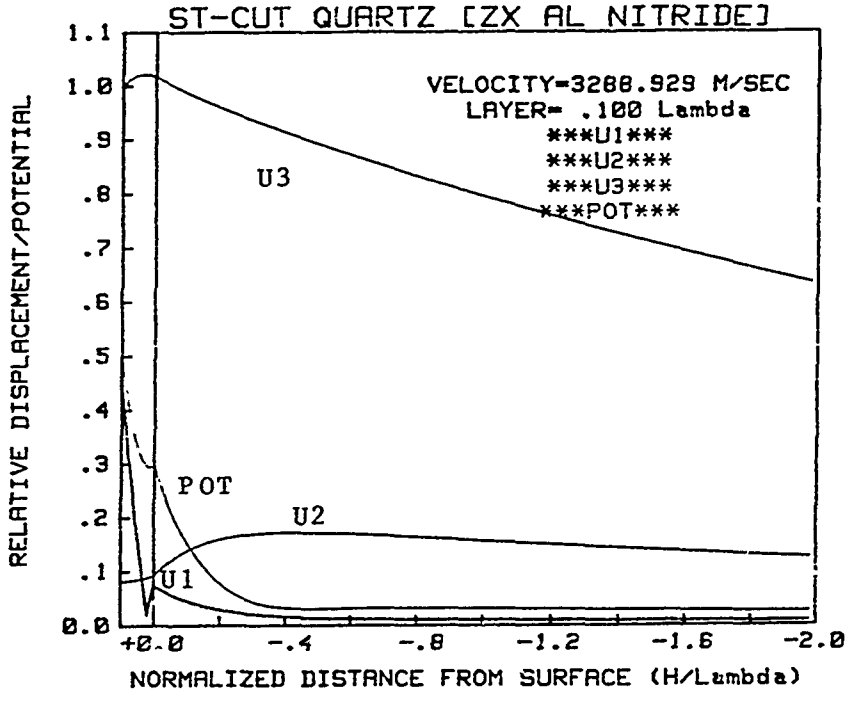

Figure 24- Layered velocity solution for AlN/ST-Quartz when the top layer and inteface are unshorted. Layer thickness is 10% of a wavelength.

```
THE VELOCITY IS W=3287.2710
BC DETERMINANT=-3.546E-19,-6.424E-10

ROOT#  1     +0.0000,-1.2324        U1=  +0.000,  +5.818  SUB
                                    U2=  -2.450,  +0.000  SUB
                                    U3=  +1.000,  +0.000  SUB
                                   U4=+0.000E+00,-6.074E+10  SUB
ROOT#  2     +0.0000,-1.0577        U1=  +0.000,  +2.766  SUB
                                    U2= -23.598,  +0.000  SUB
                                    U3=  +1.000,  +0.000  SUB
                                   U4=+0.000E+00,+6.824E+11  SUB
ROOT#  3     +0.0000,-1.0153        U1=  +0.000,  +3.206  SUB
                                    U2=  -3.859,  +0.000  SUB
                                    U3=  +1.000,  +0.000  SUB
                                   U4=+0.000E+00,-1.226E+11  SUB
ROOT#  4     +0.0000, -.0394        U1=  +0.000,   +.013  SUB
                                    U2=   +.196,  +0.000  SUB
                                    U3=  +1.000,  +0.000  SUB
                                   U4=+0.000E+00,+2.994E+08  SUB
ROOT#  5     +0.0000,-1.3984        U1=  +0.000,  +2.843 LAYER
                                    U2=  +0.000,  +0.000  LAYER
                                    U3=  +1.000,  +0.000  LAYER
                                   U4=+7.302E+10,+0.000E+00  LAY
ROOT#  6      +.2352, -.6517        U1=   -.365,   -.539 LAYER
                                    U2=  +0.000,  +0.000  LAYER
                                    U3=  +1.000,  +0.000  LAYER
                                   U4=-1.215E+10,-2.707E+10  LAY
ROOT#  7      -.2352, -.6517        U1=   +.365,   -.539 LAYER
                                    U2=  +0.000,  +0.000  LAYER
                                    U3=  +1.000,  +0.000  LAYER
                                   U4=-1.215E+10,+2.707E+10  LAY
ROOT#  8      +.2352, +.6517        U1=   -.365,   -.539 LAYER
                                    U2=  +0.000,  +0.000  LAYER
                                    U3=  +1.000,  +0.000  LAYER
                                   U4=-1.215E+10,+2.707E+10  LAY
ROOT#  9      -.2352, +.6517        U1=   +.365,   -.539 LAYER
                                    U2=  +0.000,  +0.000  LAYER
                                    U3=  +1.000,  +0.000  LAYER
                                   U4=-1.215E+10;-2.707E+10  LAY
ROOT# 10     +0.0000,+1.3984        U1=  +0.000,  -2.843 LAYER
                                    U2=  +0.000,  +0.000  LAYER
                                    U3=  +1.000,  +0.000  LAYER
                                   U4=+7.302E+10,+0.000E+00  LAY
ROOT# 11     +0.0000, -.7960        U1=  +0.000,  +0.000 LAYER
                                    U2=  +1.000,  +0.000  LAYER
                                    U3=  +0.000,  +0.000  LAYER
                                   U4=+0.000E+00,+0.000E+00  LAY
ROOT# 12     +0.0000, +.7960        U1=  +0.000,  +0.000 LAYER
                                    U2=  +1.000,  +0.000  LAYER
                                    U3=  +0.000,  +0.000  LAYER
                                   U4=+0.000E+00,+0.000E+00  LAY

WEIGHTING FACTORS
F(1)=-4.897E-03,-2.980E-02     F(2)=+2.800E-02,-5.329E-03
F(3)=+2.368E-01,+5.277E-02     F(4)=+1.493E+01,+2.482E-02
F(5)=-1.152E+00,+3.991E-03     F(6)=+4.402E+00,+3.692E+00
F(7)=+4.493E+00,-3.679E+00     F(8)=+4.351E+00,-3.915E+00
F(9)=+4.526E+00,+3.972E+00     F(10)-1.433E+00,-3.203E-02
F(11)+3.678E-01,+0.000E+00     F(12)+1.000E+00,+0.000E+00
```

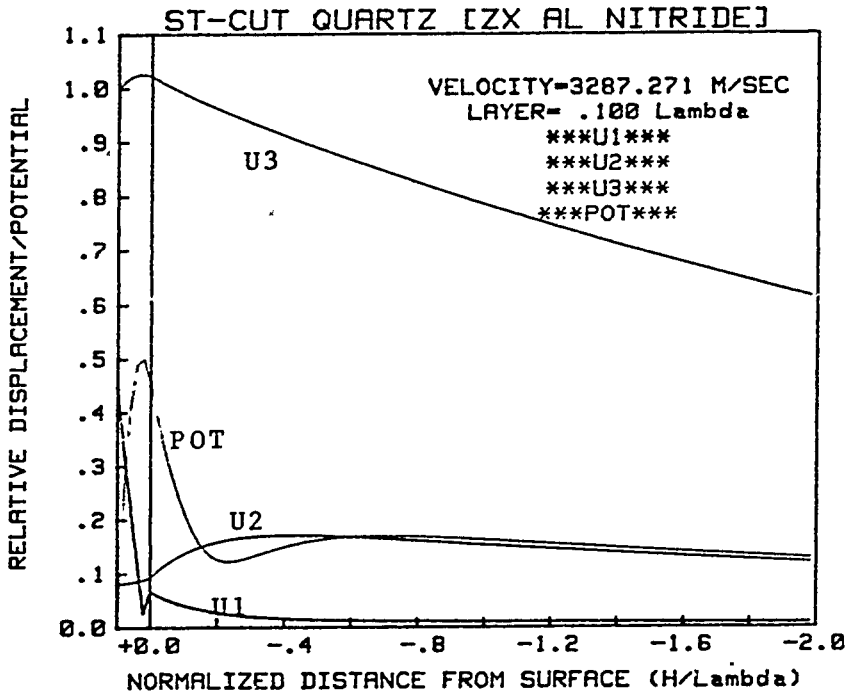

Figure 25- Layered velocity solution for AlN/ST-Quartz when the top layer is shorted and the interface is unshorted. Layer thickness is 10% of a wavelength.

```
THE VELOCITY IS W=3288.3990
BC DETERMINANT=+1.505E-19,-1.244E-09

ROOT# 1      +0.0000,-1.2321          U1=  +0.000,  +5.816  SUB
                                      U2=  -2.449,  +0.000  SUB
                                      U3=  +1.000,  +0.000  SUB
                                     U4=+0.000E+00,-6.080E+10  SUB
ROOT# 2      +0.0000,-1.0576          U1=  +0.000,  +2.745  SUB
                                      U2= -24.086,  +0.000  SUB
                                      U3=  +1.000,  +0.000  SUB
                                     U4=+0.000E+00,+7.022E+11  SUB
ROOT# 3      +0.0000,-1.0152          U1=  +0.000,  +3.206  SUB
                                      U2=  -3.868,  +0.000  SUB
                                      U3=  +1.000,  +0.000  SUB
                                     U4=+0.000E+00,-1.222E+11  SUB
ROOT# 4      +0.0000, -.0374          U1=  +0.000,   +.012  SUB
                                      U2=   +.196,  +0.000  SUB
                                      U3=  +1.000,  +0.000  SUB
                                     U4=+0.000E+00,+2.837E+08  SUB
ROOT# 5      +0.0000,-1.3984          U1=  +0.000,  +2.843 LAYER
                                      U2=  +0.000,  +0.000  LAYER
                                      U3=  +1.000,  +0.000  LAYER
                                     U4=+7.303E+10,+0.000E+00  LAY
ROOT# 6       +.2352, -.6516          U1=   -.365,   +.539 LAYER
                                      U2=  +0.000,  +0.000  LAYER
                                      U3=  +1.000,  +0.000  LAYER
                                     U4=-1.215E+10,-2.706E+10  LAY
ROOT# 7       -.2352, -.6516          U1=   +.365,   +.539 LAYER
                                      U2=  +0.000,  +0.000  LAYER
                                      U3=  +1.000,  +0.000  LAYER
                                     U4=-1.215E+10,+2.706E+10  LAY
ROOT# 8       +.2352, +.6516          U1=   -.365,   -.539 LAYER
                                      U2=  +0.000,  +0.000  LAYER
                                      U3=  +1.000,  +0.000  LAYER
                                     U4=-1.215E+10,+2.706E+10  LAY
ROOT# 9       -.2352, +.6516          U1=   +.365,   -.539 LAYER
                                      U2=  +0.000,  +0.000  LAYER
                                      U3=  +1.000,  +0.000  LAYER
                                     U4=-1.215E+10,-2.706E+10  LAY
ROOT# 10     +0.0000,+1.3984          U1=  +0.000,  -2.843 LAYER
                                      J2=  +0.000,  +0.000  LAYER
                                      J3=  +1.000,  +0.000  LAYER
                                     U4=+7.303E+10,+0.000E+00  LAY
ROOT# 11     +0.0000, -.7959          U1=  +0.000,  +0.000 LAYER
                                      J2=  +1.000,  +0.000  LAYER
                                      J3=  +0.000,  +0.000  LAYER
                                     U4=+0.000E+00,+0.000E+00  LAY
ROOT# 12     +0.0000, +.7959          J1=  +0.000,  +0.000 LAYER
                                      J2=  +1.000,  +0.000  LAYER
                                      J3=  +0.000,  +0.000  LAYER
                                     U4=+0.000E+00,+0.000E+00  LAY

WEIGHTING FACTORS
F(1)=+4.245E-02,+7.493E-16      F(2)=+2.989E-02,-2.110E-16
F(3)=+1.850E-01,-1.574E-15      F(4)=+1.481E+01,-6.202E-15
F(5)=-1.201E+00,+3.845E-16      F(6)=+4.442E+00,+3.370E+00
F(7)=+4.442E+00,-3.370E+00      F(8)=+4.383E+00,-4.080E+00
F(9)=+4.383E+00,+4.080E+00      F(10)-1.384E+00,-5.652E-17
F(11)+3.678E-01,+0.000E+00      F(12)+1.000E+00,+0.000E+00
```

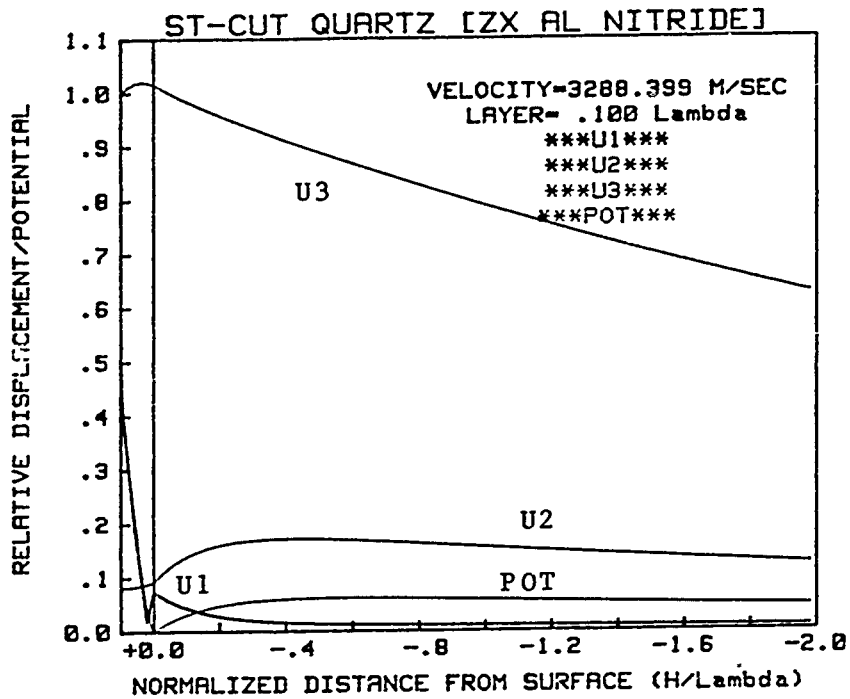

Figure 26- Layered velocity solution for AlN/ST-Quartz when the top layer is unshorted and the inteface is shorted. Layer thickness is 10% of a wavelength.

```
THE VELOCITY IS W=3286.8760
BC DETERMINANT=+6.519E-10,+2.319E-19

ROOT#  1     +0.0000,-1.2325        U1=  +0.000,  +5.818  SUB
                                    U2=  -2.450,  +0.000  SUB
                                    U3=  +1.000,  +0.000  SUB
                                   U4=+0.000E+00,-6.072E+10  SUB
ROOT#  2     +0.0000,-1.0578        U1=  +0.000,  +2.773  SUB
                                    U2= -23.433,  +0.000  SUB
                                    U3=  +1.000,  +0.000  SUB
                                   U4=+0.000E+00,+6.757E+11  SUB
ROOT#  3     +0.0000,-1.0153        U1=  +0.000,  +3.205  SUB
                                    U2=  -3.856,  +0.000  SUB
                                    U3=  +1.000,  +0.000  SUB
                                   U4=+0.000E+00,-1.228E+11  SUB
ROOT#  4     +0.0000, -.0401        U1=  +0.000,   +.013  SUB
                                    U2=   +.196,  +0.000  SUB
                                    U3=  +1.000,  +0.000  SUB
                                   U4=+0.000E+00,+3.047E+08  SUB
ROOT#  5     +0.0000,-1.3985        U1=  +0.000,  +2.843 LAYER
                                    U2=  +0.000,  +0.000  LAYER
                                    U3=  +1.000,  +0.000  LAYER
                                   U4=+7.302E+10,+0.000E+00  LAY
ROOT#  6      +.2352, -.6517        U1=   -.365,   +.539 LAYER
                                    U2=  +0.000,  +0.000  LAYER
                                    U3=  +1.000,  +0.000  LAYER
                                   U4=-1.215E+10,-2.707E+10  LAY
ROOT#  7      -.2352, -.6517        U1=   +.365,   +.539 LAYER
                                    U2=  +0.000,  +0.000  LAYER
                                    U3=  +1.000,  +0.000  LAYER
                                   U4=-1.215E+10,+2.707E+10  LAY
ROOT#  8      +.2352, +.6517        U1=   -.365,   -.539 LAYER
                                    U2=  +0.000,  +0.000  LAYER
                                    U3=  +1.000,  +0.000  LAYER
                                   U4=-1.215E+10,+2.707E+10  LAY
ROOT#  9      -.2352, +.6517        U1=   +.365,   -.539 LAYER
                                    U2=  +0.000,  +0.000  LAYER
                                    U3=  +1.000,  +0.000  LAYER
                                   U4=-1.215E+10,-2.707E+10  LAY
ROOT# 10     +0.0000,+1.3985        U1=  +0.000,  -2.843 LAYER
                                    U2=  +0.000,  +0.000  LAYER
                                    U3=  +1.000,  +0.000  LAYER
                                   U4=+7.302E+10,+0.000E+00  LAY
ROOT# 11     +0.0000, -.7961        U1=  +0.000,  +0.000 LAYER
                                    U2=  +1.000,  +0.000  LAYER
                                    U3=  +0.000,  +0.000  LAYER
                                   U4=+0.000E+00,+0.000E+00  LAY
ROOT# 12     +0.0000, +.7961        U1=  +0.000,  +0.000 LAYER
                                    U2=  +1.000,  +0.000  LAYER
                                    U3=  +0.000,  +0.000  LAYER
                                   U4=+0.000E+00,+0.000E+00  LAY

WEIGHTING FACTORS
F(1)=-7.606E-04,-7.494E-16      F(2)=+3.192E-02,-7.248E-17
F(3)=+2.132E-01,-1.444E-16      F(4)=+1.496E+01,-2.537E-14
F(5)=-1.141E+00,+1.127E-15      F(6)=+4.442E+00,+3.746E+00
F(7)=+4.442E+00,-3.746E+00      F(8)=+4.468E+00,-3.787E+00
F(9)=+4.468E+00,+3.787E+00      F(10)-1.478E+00,+2.670E-15
F(11)+3.677E-01,+0.000E+00      F(12)+1.000E+00,+0.000E+00
```

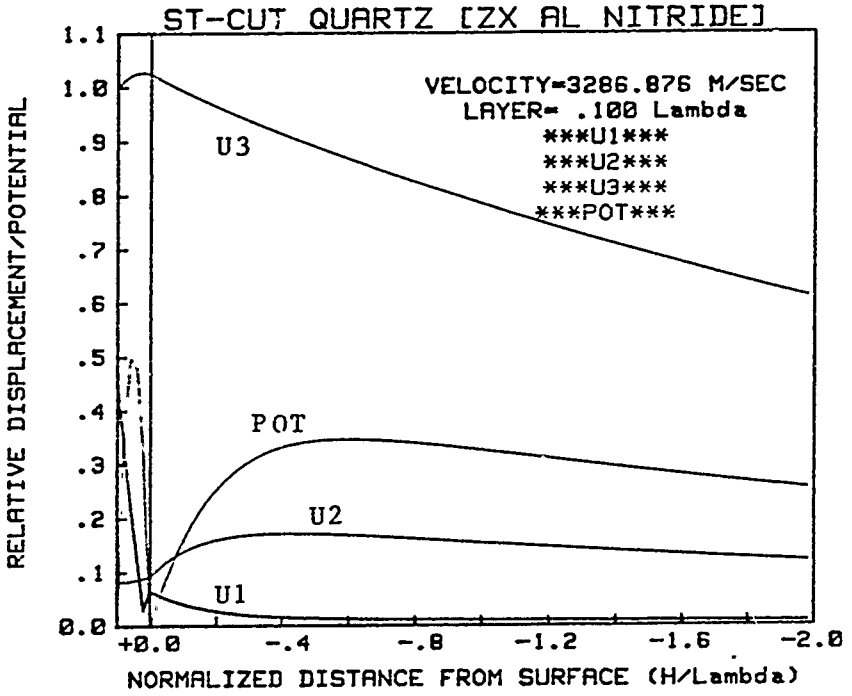

Figure 27- Layered velocity solution for AlN/ST-Quartz when the top and interface layers are shorted. Layer thickness is 10% of a wavelength.

4.1.5 Analysis of TiO_2/ST-Quartz

Layers of rutile (TiO_2) on ST-cut Quartz substrates were analyzed. Elastic and dielectric constant data for rutile were used (Appendix I). Surface wave velocity vs normalized layer thickness is shown in Figure 28a. Because rutile is a faster material the velocity increases with layer thickness until reaching the slow shear velocity of the substrate. Surface wave coupling is plotted in Figure 28b for two transducer configurations. The coupling becomes zero for layers greater than 10% of a wavelength.

Selected numerical solutions for rutile layers are shown in Figures 29-31. The displacements/potential show penetration increasing with layer thickness. The increased penetration with increasing layer thickness is due to the nearness of the bulk shear wave in the substrate.

Numerically TiO_2/ST-Quartz is governed by equations 9 and 10 of section 3.2 which contain 10 sub-solutions. Displacement and potential vectors associated with each sub-solution are shown together with the 10 complex weighting factors for the complete summation solution per equation 5 of Section 3.1.

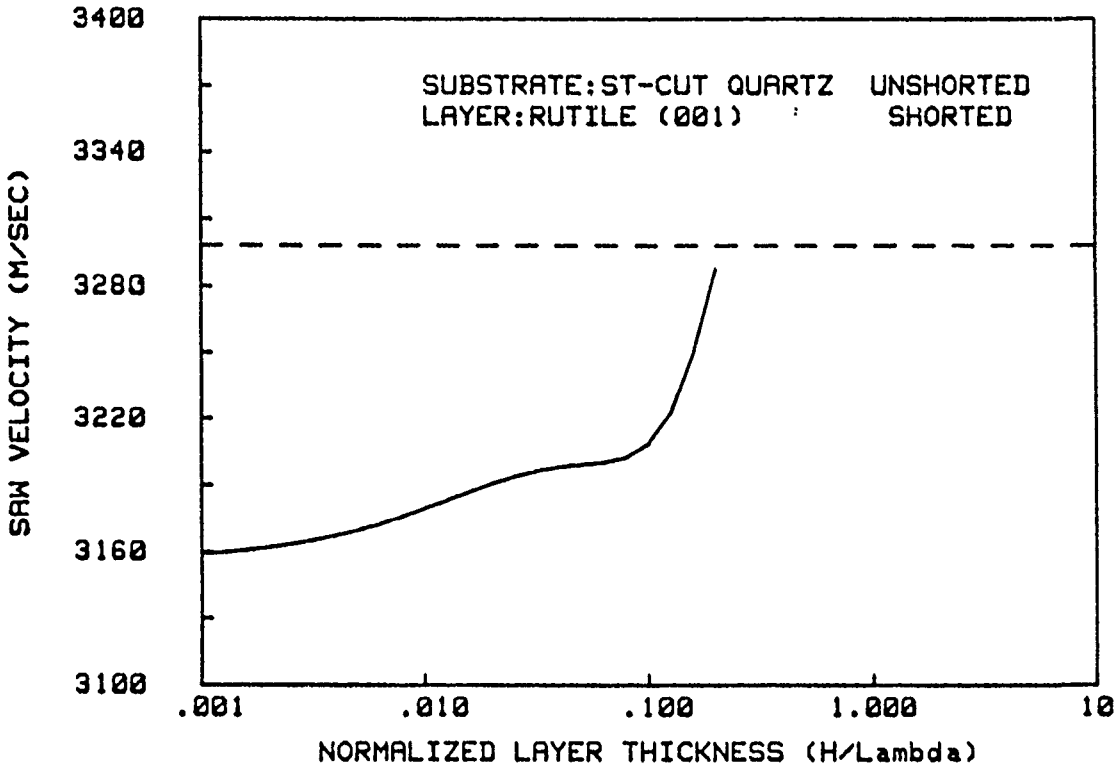

(a)

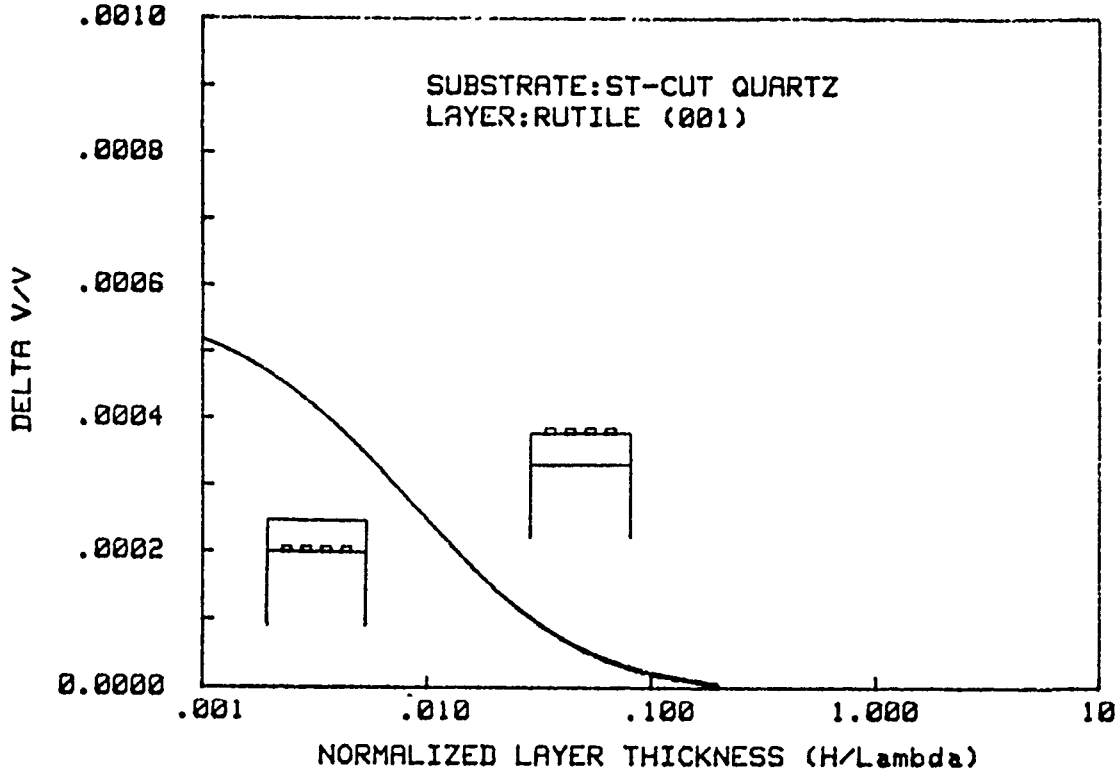

(b)

Figure 28- Velocity dispersion (a) and wave coupling (b) as a function of layer thickness for Rutile (TiO_2) on ST-Quartz.

```
THE VELOCITY IS W=3288.2486
BC DETERMINANT=-1.308E-17,-9.609E-10

ROOT# 1     +0.0000,-1.2322      U1=  +0.000,  +5.816  SUB
                                 U2=  -2.449,  +0.000  SUB
                                 U3=  +1.000,  +0.000  SUB
                                U4=+0.000E+00,-6.079E+10  SUB
ROOT# 2     +0.0000,-1.0576      U1=  +0.000,  +2.748  SUB
                                 U2= -24.020,  +0.000  SUB
                                 U3=  +1.000,  +0.000  SUB
                                U4=+0.000E+00,+6.995E+11  SUB
ROOT# 3     +0.0000,-1.0152      U1=  +0.000,  +3.206  SUB
                                 U2=  -3.866,  +0.000  SUB
                                 U3=  +1.000,  +0.000  SUB
                                U4=+0.000E+00,-1.222E+11  SUB
ROOT# 4     +0.0000, -.0377      U1=  +0.000,   +.012  SUB
                                 U2=   +.196,  +0.000  SUB
                                 U3=  +1.000,  +0.000  SUB
                                U4=+0.000E+00,+2.858E+08  SUB
ROOT# 5      +.2762, -.6819      U1=   -.652,   +.856 LAYER
                                 U2=  +0.000,  +0.000  LAYER
                                 U3=  +1.000,  +0.000  LAYER
ROOT# 6      -.2762, -.6819      U1=   +.652,   +.856 LAYER
                                 U2=  +0.000,  +0.000  LAYER
                                 U3=  +1.000,  +0.000  LAYER
ROOT# 7      +.2762, +.6819      U1=   -.652,   -.856 LAYER
                                 U2=  +0.000,  +0.000  LAYER
                                 U3=  +1.000,  +0.000  LAYER
ROOT# 8      -.2762, +.6819      U1=   +.652,   -.856 LAYER
                                     +0.000,  +0.000  LAYER
                                 U3=  +1.000,  +0.000  LAYER
ROOT# 9     +0.0000,-1.0728      U1=  +0.000,  +0.000 LAYER
                                 U2=  +1.000,  +0.000  LAYER
                                 U3=  +0.000,  +0.000  LAYER
ROOT# 10    +0.0000,+1.0728      U1=  +0.000,  +0.000 LAYER
                                 U2=  +1.000,  +0.000  LAYER
                                 U3=  +0.000,  +0.000  LAYER

WEIGHTING FACTORS
F(1)=+9.645E-01,-3.331E-15      F(2)=+4.411E-02,+3.085E-16
F(3)=-1.675E-01,+4.509E-15      F(4)=+1.957E+01,-6.924E-16
F(5)=+4.989E+00,+5.889E+00      F(6)=+4.989E+00,-5.889E+00
F(7)=+5.214E+00,-1.035E+01      F(8)=+5.214E+00,+1.035E+01
F(9)=+6.745E-02,+0.000E+00      F(10)+1.000E+00,+0.000E+00
```

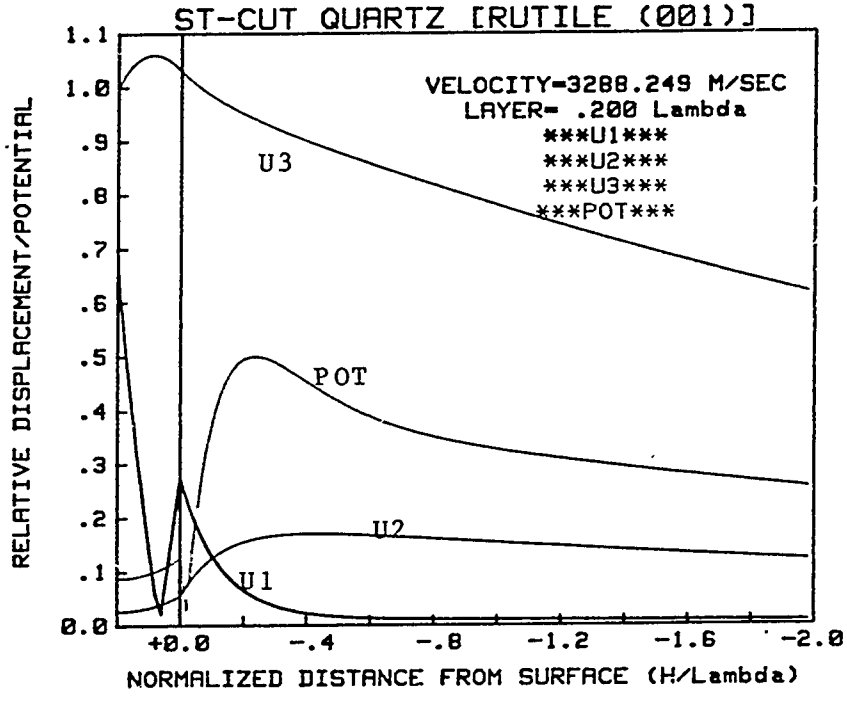

Figure 29- Layered velocity solution for TiO_2/ST-Quartz when the top and interface surface are unshorted. Layer thickness is 20% of a wavelength.

```
THE VELOCITY IS W=3288.2384
BC DETERMINANT=+4.752E-19,-4.526E-12

ROOT#  1     +0.0000,-1.2322        U1=  +0.000,  +5.816  SUB
                                    U2=  -2.449,  +0.000  SUB
                                    U3=  +1.000,  +0.000  SUB
                                   U4=+0.000E+00,-6.079E+10  SUB
ROOT#  2     +0.0000,-1.0576        U1=  +0.000,  +2.748  SUB
                                    U2= -24.015,  +0.000  SUB
                                    U3=  +1.000,  +0.000  SUB
                                   U4=+0.000E+00,+6.993E+11  SUB
ROOT#  3     +0.0000,-1.0152        U1=  +0.000,  +3.206  SUB
                                    U2=  -3.866,  +0.000  SUB
                                    U3=  +1.000,  +0.000  SUB
                                   U4=+0.000E+00,-1.222E+11  SUB
ROOT#  4     +0.0000, -.0377        U1=  +0.000,   +.012  SUB
                                    U2=   +.196,  +0.000  SUB
                                    U3=  +1.000,  +0.000  SUB
                                   U4=+0.000E+00,+2.860E+08  SUB
ROOT#  5      +.2762, -.6819        U1=   -.652,   +.856 LAYER
                                    U2=  +0.000,  +0.000  LAYER
                                    U3=  +1.000,  +0.000  LAYER
ROOT#  6      -.2762, -.6819        U1=   +.652,   +.856 LAYER
                                    U2=  +0.000,  +0.000  LAYER
                                    U3=  +1.000,  +0.000  LAYER
ROOT#  7      +.2762, +.6819        U1=   -.652,   -.856 LAYER
                                    U2=  +0.000,  +0.000  LAYER
                                    U3=  +1.000,  +0.000  LAYER
ROOT#  8      -.2762, +.6819        U1=   +.652,   -.856 LAYER
                                    U2=  +0.000,  +0.000  LAYER
                                    U3=  +1.000,  +0.000  LAYER
ROOT#  9     +0.0000,-1.0728        U1=  +0.000,  +0.000 LAYER
                                    U2=  +1.000,  +0.000  LAYER
                                    U3=  +0.000,  +0.000  LAYER
ROOT# 10     +0.0000,+1.0728        U1=  +0.000,  +0.000 LAYER
                                    U2=  +1.000,  +0.000  LAYER
                                    U3=  +0.000,  +0.000  LAYER

WEIGHTING FACTORS
F(1)=+9.666E-01,-1.776E-15     F(2)=+4.465E-02,+1.028E-16
F(3)=-1.722E-01,+1.127E-15     F(4)=+1.956E+01,-3.047E-14
F(5)=+4.989E+00,+5.889E+00     F(6)=+4.989E+00,-5.889E+00
F(7)=+5.213E+00,-1.035E+01     F(8)=+5.213E+00,+1.035E+01
F(9)=+6.745E-02,+0.000E+00     F(10)=1.000E+00,+0.000E+00
```

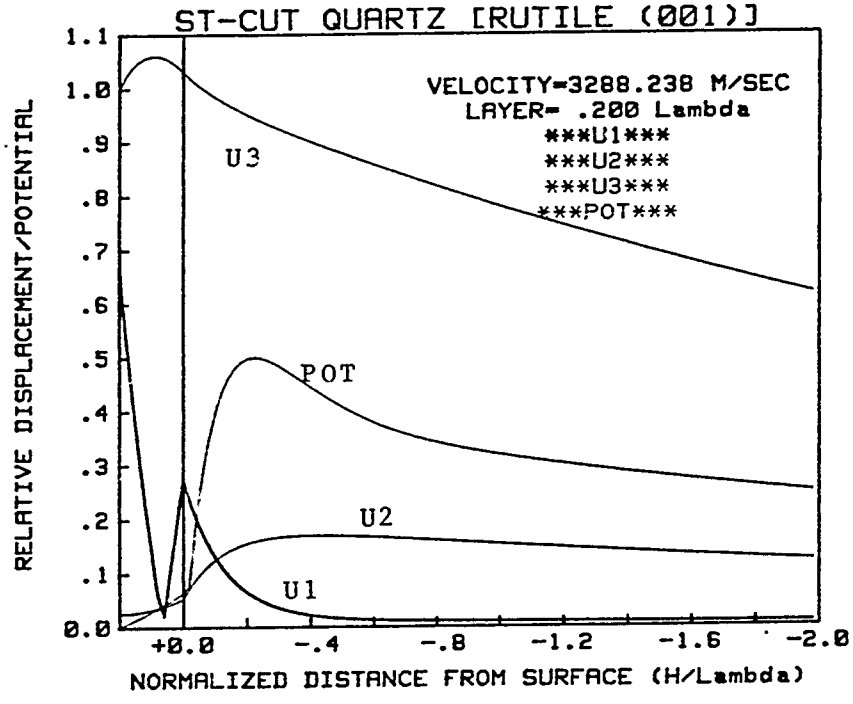

Figure 30- Layered velocity solution for TiO_2/ST-Quartz when the top surface is shorted and the interface is unshorted. Layer thickness is 20% of a wavelength.

```
THE VELOCITY IS W=3288.2271
BC DETERMINANT=-5.389E-12,-2.366E-18

ROOT# 1     +0.0000,-1.2322        U1=  +0.000,  +5.816  SUB
                                   U2=  -2.449,  +0.000  SUB
                                   U3=  +1.000,  +0.000  SUB
                                  U4=+0.000E+00,-6.079E+10  SUB
ROOT# 2     +0.0000,-1.0576        U1=  +0.000,  +2.749  SUB
                                   U2= -24.010,  +0.000  SUB
                                   U3=  +1.000,  +0.000  SUB
                                  U4=+0.000E+00,+6.991E+11  SUB
ROOT# 3     +0.0000,-1.0152        U1=  +0.000,  +3.206  SUB
                                   U2=  -3.866,  +0.000  SUB
                                   U3=  +1.000,  +0.000  SUB
                                  U4=+0.000E+00,-1.223E+11  SUB
ROOT# 4     +0.0000, -.0377        U1=  +0.000,   +.012  SUB
                                   U2=   +.196,  +0.000  SUB
                                   U3=  +1.000,  +0.000  SUB
                                  U4=+0.000E+00,+2.861E+08  SUB
ROOT# 5      +.2762, -.6819        U1=   -.652,   +.856 LAYER
                                   U2=  +0.000,  +0.000  LAYER
                                   U3=  +1.000,  +0.000  LAYER
ROOT# 6      -.2762, -.6819        U1=   +.652,   +.856 LAYER
                                   U2=  +0.000,  +0.000  LAYER
                                   U3=  +1.000,  +0.000  LAYER
ROOT# 7      +.2762, +.6819        U1=   -.652,   -.856 LAYER
                                   U2=  +0.000,  +0.000  LAYER
                                   U3=  +1.000,  +0.000  LAYER
ROOT# 8      -.2762, +.6819        U1=   +.652,   -.856 LAYER
                                   U2=  +0.000,  +0.000  LAYER
                                   U3=  +1.000,  +0.000  LAYER
ROOT# 9     +0.0000,-1.0728        U1=  +0.000,  +0.000 LAYER
                                   U2=  +1.000,  +0.000  LAYER
                                   U3=  +0.000,  +0.000  LAYER
ROOT# 10    +0.0000,+1.0728        U1=  +0.000,  +0.000 LAYER
                                   U2=  +1.000,  +0.000  LAYER
                                   U3=  +0.000,  +0.000  LAYER

WEIGHTING FACTORS
F(1)=+9.690E-01,+4.441E-16     F(2)=+4.524E-02,+4.115E-16
F(3)=-1.773E-01,+2.254E-15     F(4)=+1.956E+01,-1.616E-14
F(5)=+4.988E+00,+5.888E+00     F(6)=+4.988E+00,-5.888E+00
F(7)=+5.213E+00,-1.035E+01     F(8)=+5.213E+00,+1.035E+01
F(9)=+6.745E-02,+0.000E+00     F(10)+1.000E+00,+0.000E+00
```

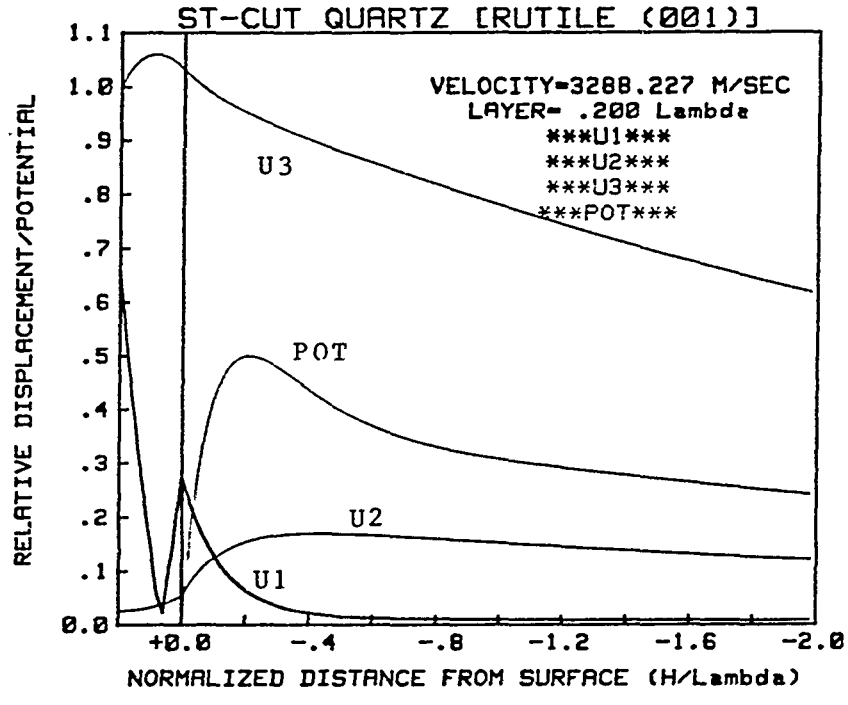

Figure 31- Layered velocity solution for TiO_2/ST-Quartz when the top surface is unshorted and the interface is shorted. Layer thickness is 20% of a wavelength.

4.1.6 Analysis of Al_2O_3/ST-Quartz

Layers of sapphire (Al_2O_3) on ST-cut Quartz substrates were analyzed. Elastic and dielectric constant data for c-axis oriented sapphire were used (Appendix I). Surface wave velocity vs normalized layer thickness is shown in Figure 32a. Because sapphire is a fast material the velocity increases with layer thickness until reaching the slow shear velocity of the substrate. Surface wave coupling is plotted in Figure 32b for two transducer configurations. The coupling becomes zero for layers greater than 10% of a wavelength.

Selected numerical solutions for sapphire layers are shown in Figures 33-35. The displacements and potential show penetration increasing with layer thickness. The increased penetration with increasing layer thickness is due to the proximity of the bulk shear wave in the substrate.

Numerically Al_2O_3/ST-Quartz is governed by equations 9 and 10 of section 3.2 which contain 10 sub-solutions. Displacement and potential vectors associated with each sub-solution are shown together with the 10 complex weighting factors for the complete summation solution per equation 5 cf section 3.1.

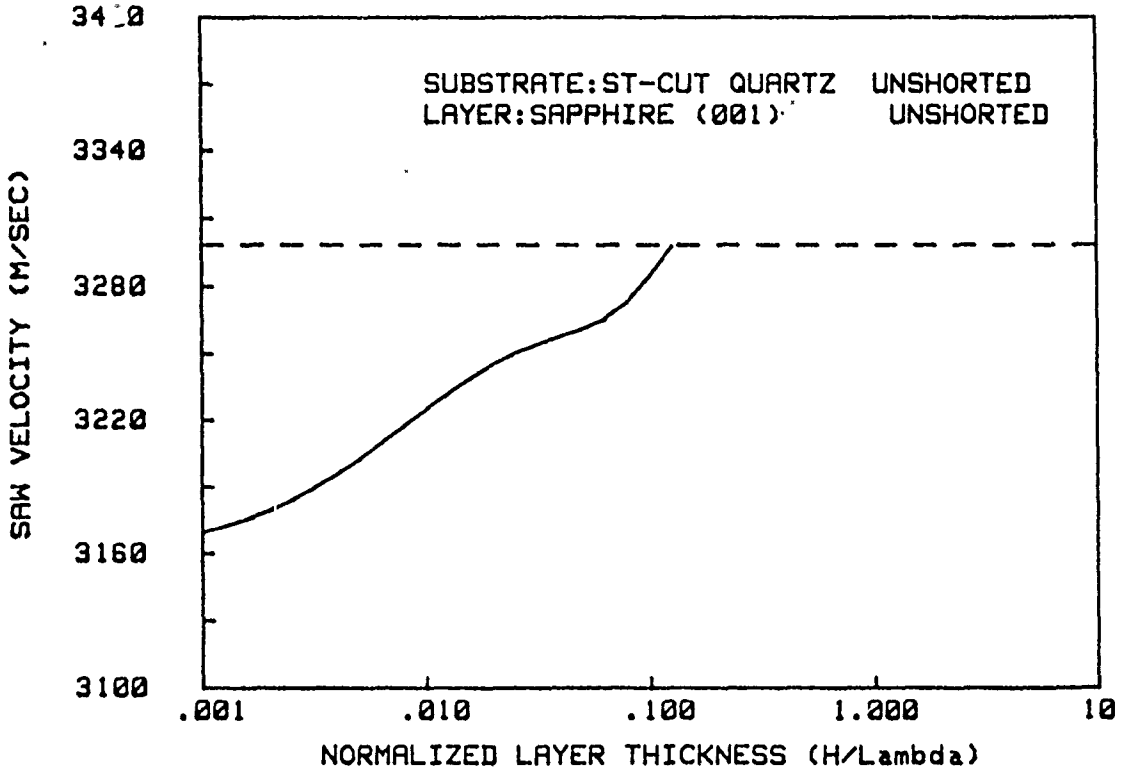

(a)

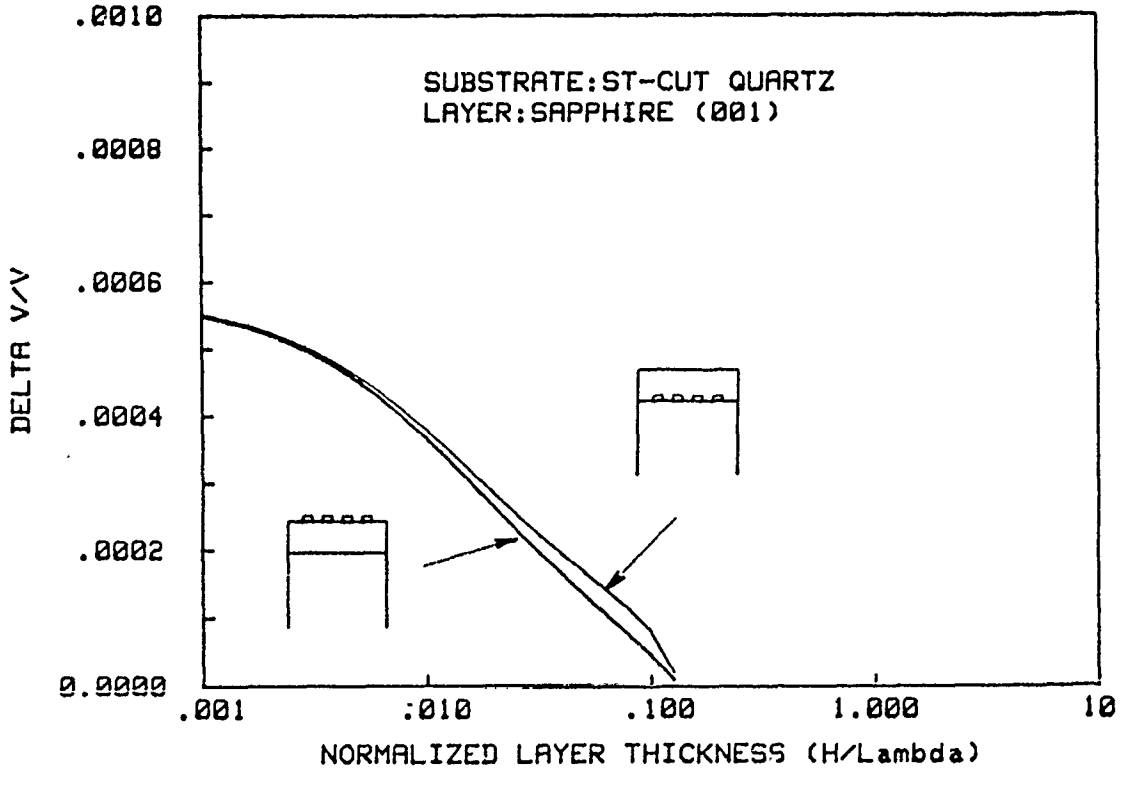

(b)

Figure 32- Velocity dispersion (a) and wave coupling (b) as a function of layer thickness for Sapphire (Al_2O_3) on ST-Quartz.

```
THE VELOCITY IS W=3285.0520
BC DETERMINANT=+0.000E+00,+2.173E-10

ROOT#  1     +0.0000,-1.2330        U1=  +0.000,  +5.820  SUB
                                    U2=  -2.451,  +0.000  SUB
                                    U3=  +1.000,  +0.000  SUB
                                   U4=+0.000E+00,-6.062E+10  SUB
ROOT#  2     +0.0000,-1.0580        U1=  +0.000,  +2.803  SUB
                                    U2= -22.709,  +0.000  SUB
                                    U3=  +1.000,  +0.000  SUB
                                   U4=+0.000E+00,+6.465E+11  SUB
ROOT#  3     +0.0000,-1.0154        U1=  +0.000,  +3.204  SUB
                                    U2=  -3.842,  +0.000  SUB
                                    U3=  +1.000,  +0.000  SUB
                                   U4=+0.000E+00,-1.234E+11  SUB
ROOT#  4     +0.0000, -.0432        U1=  +0.000,   +.014  SUB
                                    U2=   +.196,  +0.000  SUB
                                    U3=  +1.000,  +0.000  SUB
                                   U4=+0.000E+00,+3.282E+08  SUB
ROOT#  5     +0.0000,-1.3414        U1=  +0.000,  +2.210 LAYER
                                    U2=  -1.155,  +0.000  LAYER
                                    U3=  +1.000,  +0.000  LAYER
ROOT#  6     +0.0000,-1.0264        U1=  +0.000,  +1.339 LAYER
                                    U2=  -2.813,  +0.000  LAYER
                                    U3=  +1.000,  +0.000  LAYER
ROOT#  7     +0.0000, -.5233        U1=  +0.000,   +.304 LAYER
                                    U2=   +.372,  +0.000  LAYER
                                    U3=  +1.000,  +0.000  LAYER
ROOT#  8     +0.0000, +.5233        U1=  +0.000,   -.304 LAYER
                                    U2=   +.372,  +0.000  LAYER
                                    U3=  +1.000,  +0.000  LAYER
ROOT#  9     +0.0000,+1.0264        U1=  +0.000,  -1.339 LAYER
                                    U2=  -2.813,  +0.000  LAYER
                                    U3=  +1.000,  +0.000  LAYER
ROOT# 10     +0.0000,+1.3414        U1=  +0.000,  -2.210 LAYER
                                    U2=  -1.155,  +0.000  LAYER
                                    U3=  +1.000,  +0.000  LAYER

WEIGHTING FACTORS
F(1)=-4.415E-02,+0.000E+00     F(2)=-4.968E-03,+0.000E+00
F(3)=-3.733E-02,+0.000E+00     F(4)=-3.608E+00,+0.000E+00
F(5)=+7.004E-01,+0.000E+00     F(6)=-5.111E-01,+0.000E+00
F(7)=-2.021E+00,+0.000E+00     F(8)=-2.235E+00,+0.000E+00
F(9)=-6.279E-01,+0.000E+00     F(10)+1.000E+00,+0.000E+00
```

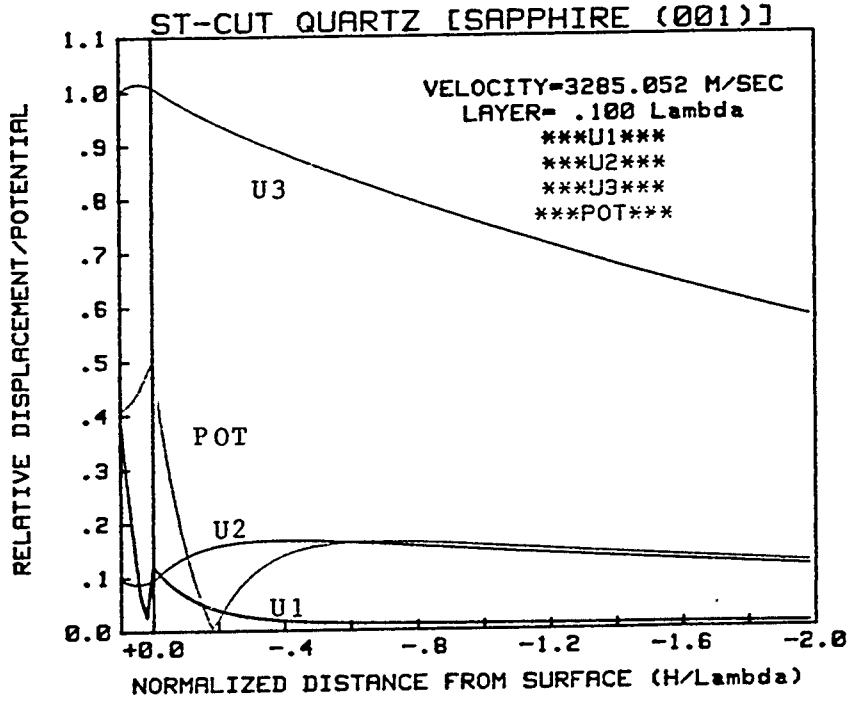

Figure 33- Layered velocity solution for Al_2O_3/ST-Quartz when the top and interface surface are unshorted. Layer thickness is 10% of a wavelength.

```
THE VELOCITY IS W=3284.9010
BC DETERMINANT=+0.000E+00,-4.084E-09

ROOT#  1     +0.0000,-1.2330        U1=  +0.000,  +5.820  SUB
                                    U2=  -2.451,  +0.000  SUB
                                    U3=  +1.000,  +0.000  SUB
                                   U4=+0.000E+00,-6.061E+10  SUB
ROOT#  2     +0.0000,-1.0580        U1=  +0.000,  +2.806  SUB
                                    U2= -22.652,  +0.000  SUB
                                    U3=  +1.000,  +0.000  SUB
                                   U4=+0.000E+00,+6.441E+11  SUB
ROOT#  3     +0.0000,-1.0154        U1=  +0.000,  +3.204  SUB
                                    U2=  -3.841,  +0.000  SUB
                                    U3=  +1.000,  +0.000  SUB
                                   U4=+0.000E+00,-1.235E+11  SUB
ROOT#  4     +0.0000, -.0435        U1=  +0.000,   +.014  SUB
                                    U2=   +.196,  +0.000  SUB
                                    U3=  +1.000,  +0.000  SUB
                                   U4=+0.000E+00,+3.301E+08  SUB
ROOT#  5     +0.0000,-1.3414        U1=  +0.000,  +2.210 LAYER
                                    U2=  -1.155,  +0.000  LAYER
                                    U3=  +1.000,  +0.000  LAYER
ROOT#  6     +0.0000,-1.0264        U1=  +0.000,  +1.339 LAYER
                                    U2=  -2.813,  +0.000  LAYER
                                    U3=  +1.000,  +0.000  LAYER
ROOT#  7     +0.0000, -.5233        U1=  +0.000,   +.304 LAYER
                                    U2=   +.372,  +0.000  LAYER
                                    U3=  +1.000,  +0.000  LAYER
ROOT#  8     +0.0000, +.5233        U1=  +0.000,   -.304 LAYER
                                    U2=   +.372,  +0.000  LAYER
                                    U3=  +1.000,  +0.000  LAYER
ROOT#  9     +0.0000,+1.0264        U1=  +0.000,  -1.339 LAYER
                                    U2=  -2.813,  +0.000  LAYER
                                    U3=  +1.000,  +0.000  LAYER
ROOT# 10     +0.0000,+1.3414        U1=  +0.000,  -2.210 LAYER
                                    U2=  -1.155,  +0.000  LAYER
                                    U3=  +1.000,  +0.000  LAYER

WEIGHTING FACTORS
F(1)=-4.882E-02,+0.000E+00     F(2)=-6.137E-03,+0.000E+00
F(3)=-2.766E-02,+0.000E+00     F(4)=-3.612E+00,+0.000E+00
F(5)=+7.005E-01,+0.000E+00     F(6)=-5.112E-01,+0.000E+00
F(7)=-2.021E+00,+0.000E+00     F(8)=-2.235E+00,+0.000E+00
F(9)=-6.278E-01,+0.000E+00     F(10)+1.000E+00,+0.000E+00
```

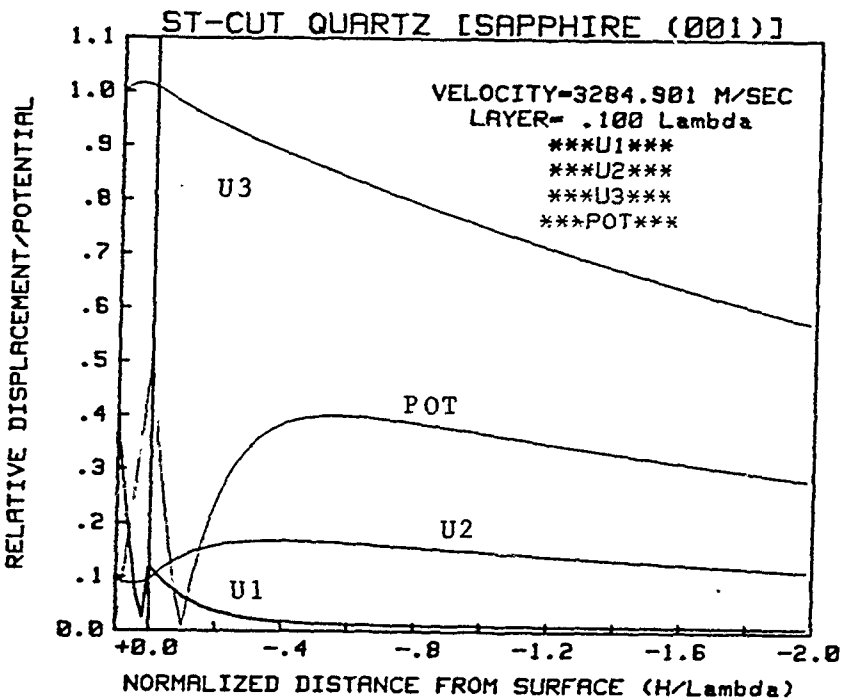

Figure 34- Layered velocity solution for Al_2O_3/ST-Quartz when the top surface is shorted and the interface is unshorted. Layer thickness is 10% of a wavelength.

```
THE VELOCITY IS W=3284.7881
BC DETERMINANT=+2.381E-10,+0.000E+00

ROOT#  1     +0.0000,-1.2330        U1=  +0.000,  +5.821  SUB
                                    U2=  -2.452,  +0.000  SUB
                                    U3=  +1.000,  +0.000  SUB
                                   U4=+0.000E+00,-6.061E+10  SUB
ROOT#  2     +0.0000,-1.0580        U1=  +0.000,  +2.807  SUB
                                    U2= -22.609,  +0.000  SUB
                                    U3=  +1.000,  +0.000  SUB
                                   U4=+0.000E+00,+6.424E+11  SUB
ROOT#  3     +0.0000,-1.0154        U1=  +0.000,  +3.204  SUB
                                    U2=  -3.840,  +0.000  SUB
                                    U3=  +1.000,  +0.000  SUB
                                   U4=+0.000E+00,-1.225E+11  SUB
ROOT#  4     +0.0000, -.0437        U1=  +0.000,   +.014  SUB
                                    U2=   +.196,  +0.000  SUB
                                    U3=  +1.000,  +0.000  SUB
                                   U4=+0.000E+00,+3.314E+08  SUB
ROOT#  5     +0.0000,-1.3414        U1=  +0.000,  +2.210 LAYER
                                    U2=  -1.155,  +0.000  LAYER
                                    U3=  +1.000,  +0.000  LAYER
ROOT#  6     +0.0000,-1.0264        U1=  +0.000,  +1.339 LAYER
                                    U2=  -2.813,  +0.000  LAYER
                                    U3=  +1.000,  +0.000  LAYER
ROOT#  7     +0.0000, -.5233        U1=  +0.000,   +.304 LAYER
                                    U2=   +.372,  +0.000  LAYER
                                    U3=  +1.000,  +0.000  LAYER
ROOT#  8     +0.0000, +.5233        U1=  +0.000,   -.304 LAYER
                                    U2=   +.372,  +0.000  LAYER
                                    U3=  +1.000,  +0.000  LAYER
ROOT#  9     +0.0000,+1.0264        U1=  +0.000,  -1.339 LAYER
                                    U2=  -2.813,  +0.000  LAYER
                                    U3=  +1.000,  +0.000  LAYER
ROOT# 10     +0.0000,+1.3414        U1=  +0.000,  -2.210 LAYER
                                    U2=  -1.155,  +0.000  LAYER
                                    U3=  +1.000,  +0.000  LAYER

WEIGHTING FACTORS
F(1)=-5.228E-02,+0.000E+00     F(2)=-7.007E-03,+0.000E+00
F(3)=-2.049E-02,+0.000E+00     F(4)=-3.616E+00,+0.000E+00
F(5)=+7.006E-01,+0.000E+00     F(6)=-5.112E-01,+0.000E+00
F(7)=-2.022E+00,+0.000E+00     F(8)=-2.235E+00,+0.000E+00
F(9)=-6.278E-01,+0.000E+00     F(10)+1.000E+00,+0.000E+00
```

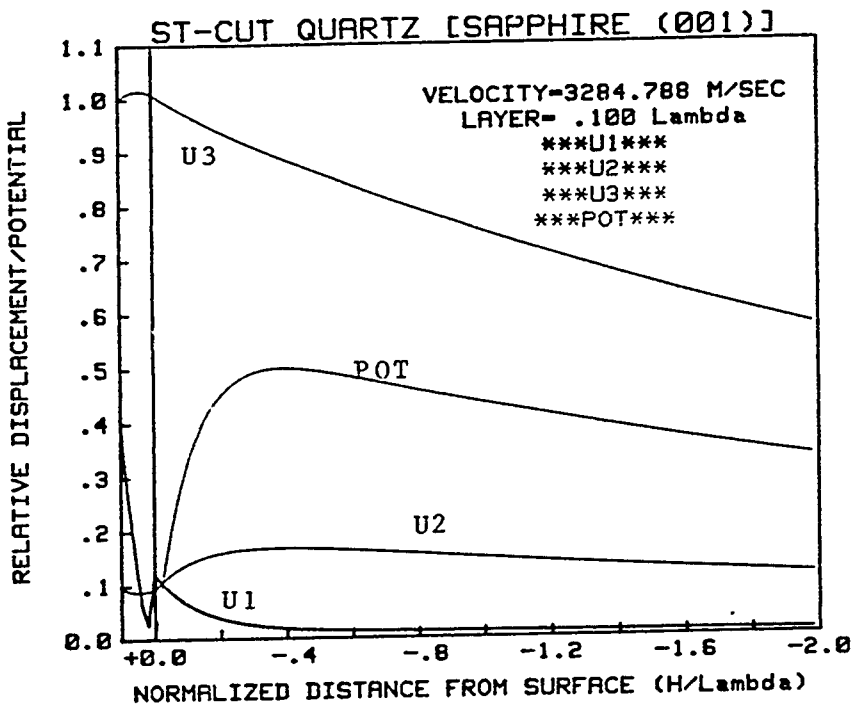

Figure 35- Layered velocity solution for Al_2O_3/ST-Quartz when the top and interface surface are shorted. Layer thickness is 10% of a wavelength.

4.2 Interfacial Wave Analyses

In this section highlights of a study of Stoneley waves in anisotropic crystals are presented. For illustration, data on copper and quartz crystals is presented. Copper was selected to establish a basis with previous publications. Quartz is of particular interest because it is synonymous with frequency control and stability.

The approach taken in this interfacial wave study is shown in Figure 36 where a view along the X_3 direction (normal to the $X_1 X_2$ plane) is shown. This plane is called the interface plane.

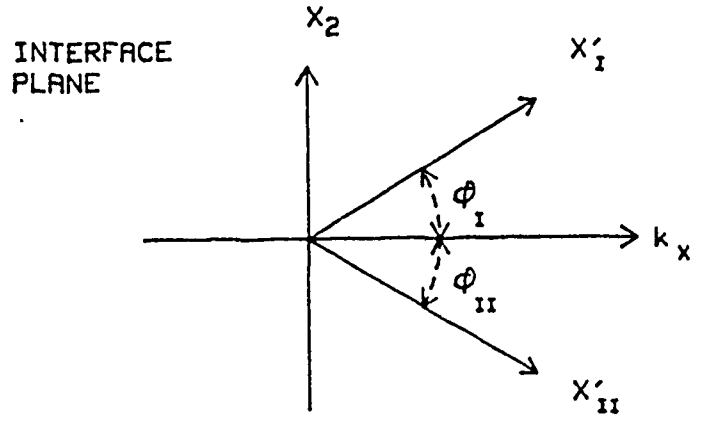

Figure 36- Coordinate system relative to the interface plane plane for Stoneley wave analysis. Crystal material parameters are rotated with respect to the k_x direction along which the interface wave propagates.

In order to obtain interface waves in a single material two different orientations of the same crystal must be used. As shown in Figure 36 each orientation (top and bottom material) is obtained by rotating the crystal material parameters with respect to the wave propagation vector. Typically the top material is rotated by a negative angle and the bottom material by a positive angle. The objective of our study was to determine their properties and how best to search for interface waves.

4.2.1 Analysis of Copper

The interface wave velocity as a function of material rotation is shown in Figure 37. Unrotated material constants for copper (Appendix I) were used. The top and bottom material constants were obtained by rotating negative and positive amounts respectively.

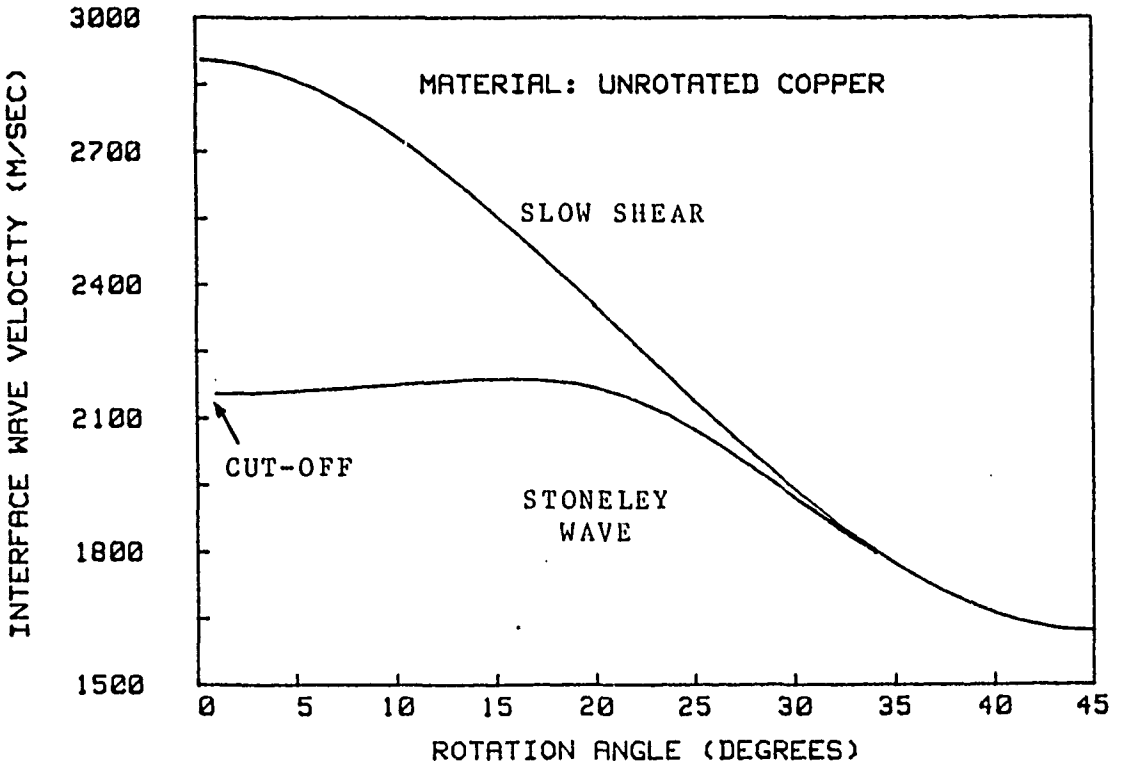

Figure 37- Stoneley wave velocity vs material rotation angle in single crystal copper (001 plane).

Two points are of interest: (1) the larger angles result in large bulk like shears at the interface and (2) angles less than cut-off do not possess Stoneley wave solutions.

A Stoneley wave search technique was developed based upon the prediction of cut-off using techniques of Barnett and Lothe (Appendix II). This search method does not require complete solution of the wave boundary equations and greatly simplified the Stoneley wave searches.

Stonely wave solutions for two different angles are shown in Figure 38. AT $\pm$ 10° the displacements are not strongly bound to the interface however, at $\pm$ 20° the wave is well bound and decays within 3-5 wavelengths of the interface.

Stoneley wave solutions were found to be strongly influenced by the material anisotropy as defined by

$$2\ C_{44}\ /(C_{11}\ -C_{12}\ )$$

Normal copper possesses an anisotropy of 3.2 however, artificially changing C_{44} to obtain an anisotropy of 1.52 and the effects this has on Stoneley wave solutions is shown in Figure 39. Lower anisotropy lowers the cut-off angle and causes the wave to be more closely bound to the interface.

4.2.2 Analysis of Quartz

Using the above search techniques (Appendix II) a study was performed on single crystal Quartz. Although these waves were not found to exist on all cuts of quartz they have for the first time been found in quartz. The data indicates piezoelectrically active and well bound waves are possible. This result suggests a potentially useful resonator structure with electrodes encapsulated at the material interface.

A complete listing of all numerical search data within this report is not possible due to length restrictions hence only one Stoneley wave solution for quartz will be presented. Shown in Figures 40 and 41 are the velocity solutions for X-cut, Z propagating Stoneley waves with a rotation angle of $\pm$ 20°. The effects of shorting the electric field at the interface are shown in the detailed plots of Figure 42.

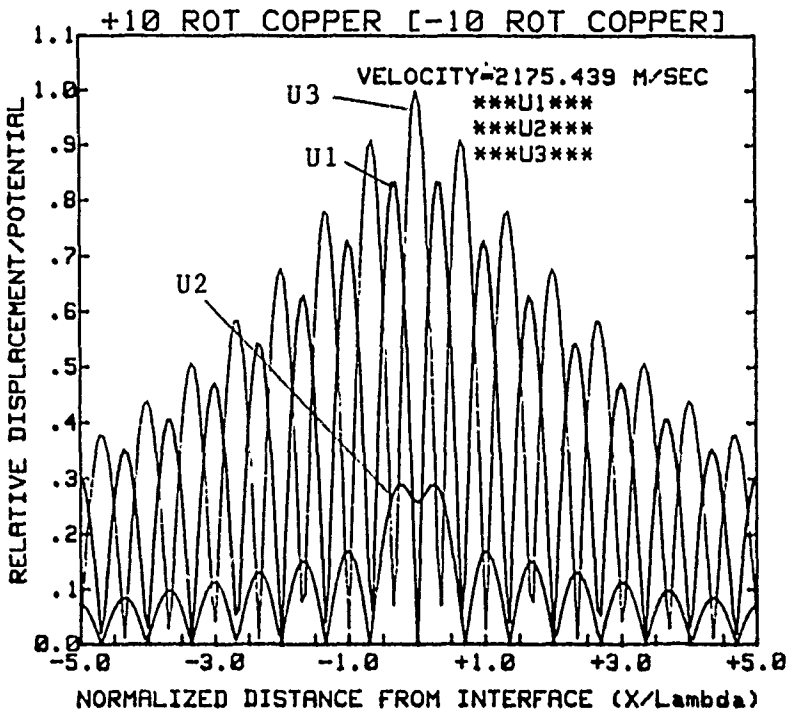

(a)

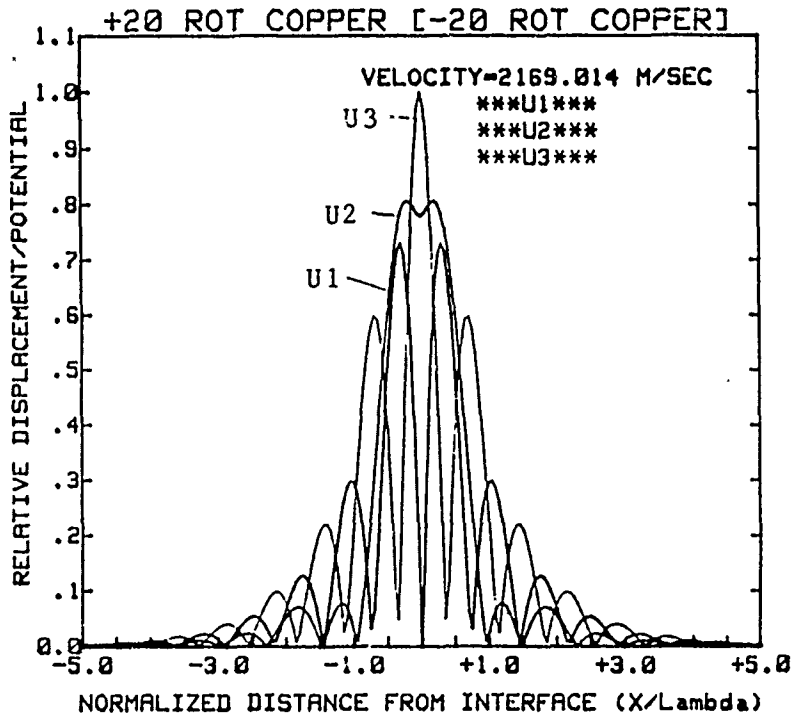

(b)

Figure 38- Stoneley wave solution on Copper for a rotation angle of (a) $\pm$ 10° and (b) $\pm$ 20°.

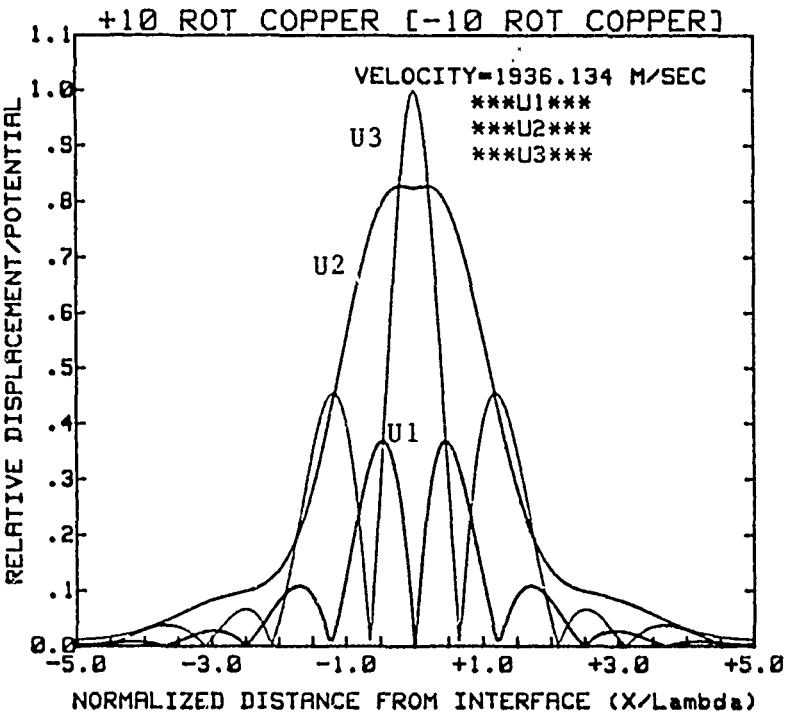

(a)

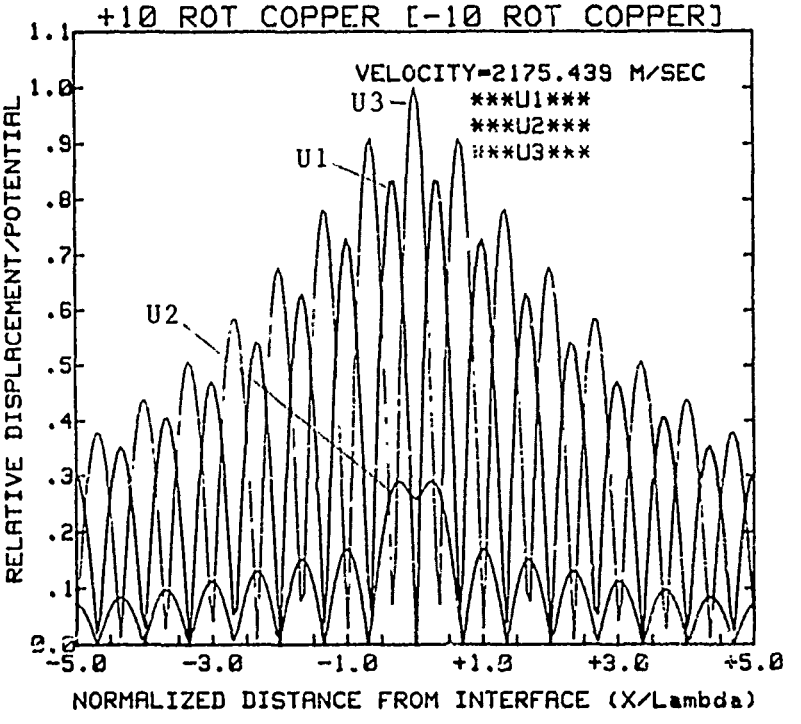

(b)

Figure 39- Stoneley wave solution for (a) modified Copper (anisotropy=1.52) and (b) normal Copper with (anisotropy=3.2) rotation angle of $\pm$ 10°.

```
THE VELOCITY IS W=3988.5199
BC DETERMINANT=-8.247E-13,-2.637E-17

ROOT#  1      +0.0000,-1.0225          U1=  +1.000,  +0.000  BOT
                                        U2=    -.963,   +0.000  BOT
                                        U3=   +0.000,    -.014  BOT
                                       U4=+0.000E+00,+5.238E+11  SUB

ROOT#  2       +.4578, -.3766          U1=  +1.000,  +0.000  BOT
                                        U2=    -.637,  -1.455  BOT
                                        U3=   -1.380,    -.515  BOT
                                       U4=+2.043E+09,-9.990E+08  SUB

ROOT#  3       -.4578, -.3766          U1=  +1.000,  +0.000  BOT
                                        U2=    -.637,  +1.455  BOT
                                        U3=   +1.380,    -.515  BOT
                                       U4=-2.043E+09,-9.990E+08  SUB

ROOT#  4      +0.0000, -.2045          U1=  +1.000,  +0.000  BOT
                                        U2=  +35.669,   +0.000  BOT
                                        U3=   +0.000,   -5.954  BOT
                                       U4=+0.000E+00,+7.543E+09  SUB

ROOT#  5      +0.0000,+1.4576          U1=  +1.000,  +0.000 TOP
                                        U2=    +.636,   +0.000  TOP
                                        U3=   +0.000,    +.163  TOP
                                       U4=+0.000E+00,-6.420E+09  TOP

ROOT#  6      +0.0000,+1.0047          U1=  +1.000,  +0.000 TOP
                                        U2=    +.618,   +0.000  TOP
                                        U3=   +0.000,    +.742  TOP
                                       U4=+0.000E+00,+2.265E+11  TOP

ROOT#  7       +.2616, +.1275          U1=  +1.000,  +0.000 TOP
                                        U2=   -2.389,    +.182  TOP
                                        U3=   -4.005,   +1.291  TOP
                                       U4=-1.331E+09,+3.720E+08  TOP

ROOT#  8       -.2616, +.1275          U1=  +1.000,  +0.000 TOP
                                        U2=   -2.389,    -.182  TOP
                                        U3=   +4.005,   +1.291  TOP
                                       U4=+1.331E+09,+3.720E+08  TOP

WEIGHTING FACTORS
F(1)=-7.372E-04,-6.694E-04     F(2)=-7.756E-01,+1.529E+00
F(3)=+1.447E+00,-9.190E-01     F(4)=-1.771E-01,-1.608E-01
F(5)=-6.008E-01,-5.455E-01     F(6)=-1.465E-03,-1.331E-03
F(7)=+9.618E-02,+9.954E-01     F(8)=+1.000E+00,+0.000E+00
```

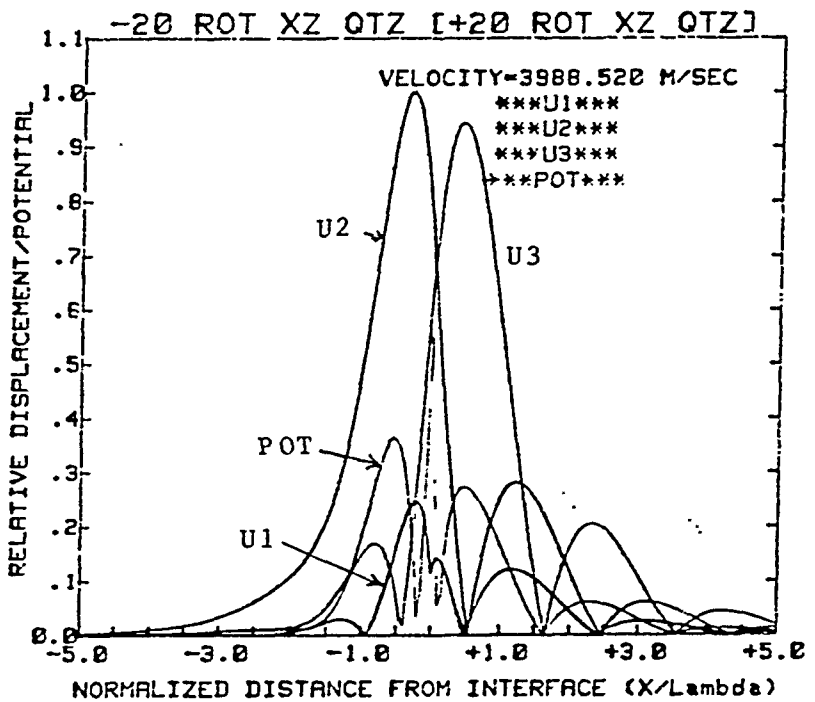

Figure 40- Stoneley wave velocity solution for XZ-Quartz when the interface is unshorted.

```
THE VELOCITY IS W=3988.7167
BC DETERMINANT=-9.087E-18,+4.812E-12

ROOT# 1     +0.0000,-1.0225          U1=  +1.000,   +0.000  BOT
                                     U2=    -.963,   +0.000  BOT
                                     U3=   +0.000,    -.014  BOT
                                    U4=+0.000E+00,+5.238E+11  SUB
ROOT# 2      +.4578, -.3765          U1=  +1.000,   +0.000  BOT
                                     U2=    -.637,   -1.455  BOT
                                     U3=   -1.380,    -.515  BOT
                                    U4=+2.042E+09,-9.983E+08  SUB
ROOT# 3      -.4578, -.3765          U1=  +1.000,   +0.000  BOT
                                     U2=    -.637,   +1.455  BOT
                                     U3=   +1.380,    -.515  BOT
                                    U4=-2.042E+09,-9.983E+08  SUB
ROOT# 4     +0.0000, - 2037          U1=  +1.000,   +0.000  BOT
                                     U2=  +36.050,   +0.000  BOT
                                     U3=   +0.000,   -5.999  BOT
                                    U4=+0.000E+00,+7.600E+09  SUB
ROOT# 5     +0.0000,+1.4575          U1=  +1.000,   +0.000 TOP
                                     U2=    +.636,   +0.000  TOP
                                     U3=   +0.000,    +.163  TOP
                                    U4=+0.000E+00,-6.420E+09  TOP
ROOT# 6     +0.0000,+1.0047          U1=  +1.000,   +0.000 TOP
                                     U2=    +.618,   +0.000  TOP
                                     U3=   +0.000,    +.742  TOP
                                    U4=+0.000E+00,+2.265E+11  TOP
ROOT# 7      +.2616, +.1272          U1=  +1.000,   +0.000 TOP
                                     U2=   -2.389,    +.182  TOP
                                     U3=   -4.008,   +1.290  TOP
                                    U4=-1.331E+09,+3.712E+08  TOP
ROOT# 8      -.2616, +.1272          U1=  +1.000,   +0.000 TOP
                                     U2=   -2.389,    -.182  TOP
                                     U3=   +4.008,   +1.290  TOP
                                    U4=+1.331E+09,+3.712E+08  TOP

WEIGHTING FACTORS
F(1)=-5.677E-03,-5.107E-03     F(2)=-7.587E-01,+1.527E+00
F(3)=+1.438E+00,-9.155E-01     F(4)=-1.757E-01,-1.581E-01
F(5)=-5.949E-01,-5.351E-01     F(6)=-1.283E-02,-1.154E-02
F(7)=+1.055E-01,+9.944E-01     F(8)=+1.000E+00,+0.000E+00
```

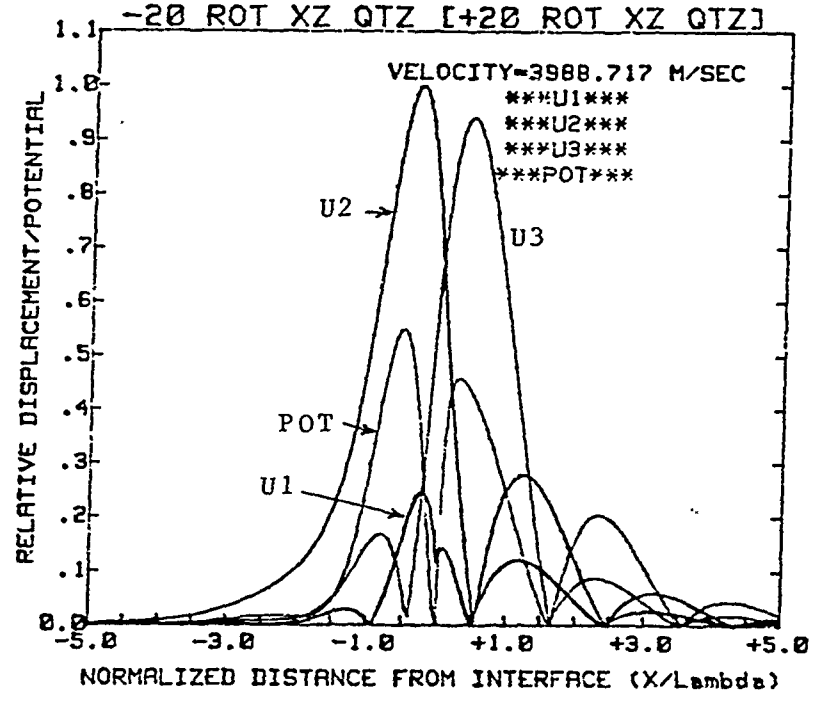

Figure 41- Stoneley wave velocity solution for XZ-Quartz when the interface is shorted.

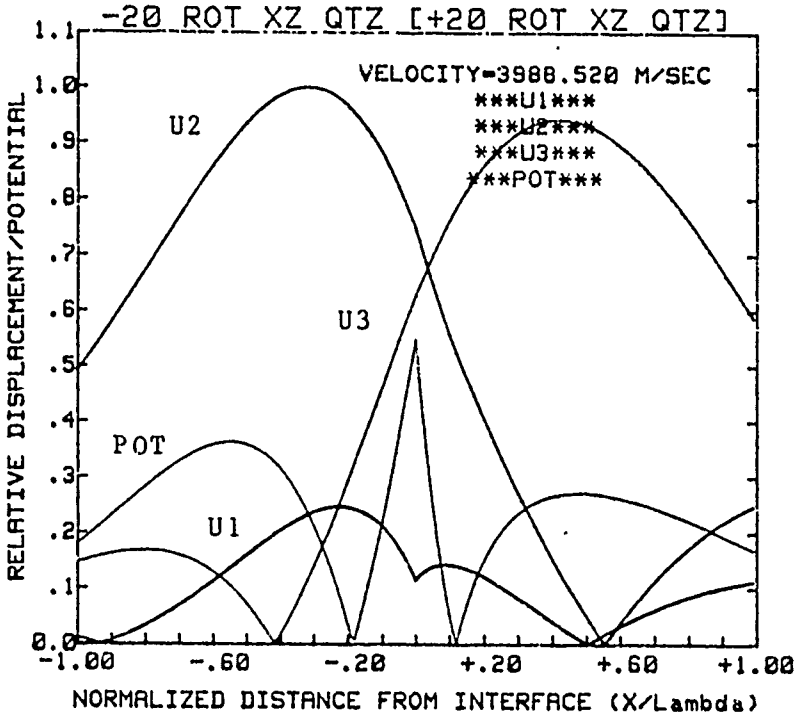

(a)

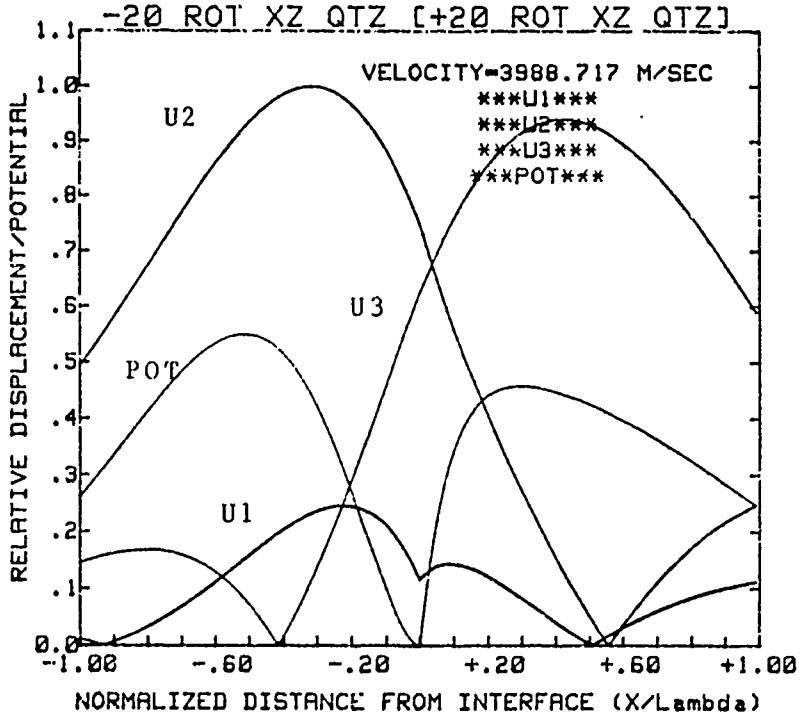

(b)

Figure 42- Expanded plot of the displacements and potential of Stoneley waves on XZ-Quartz when the interface is (a) unshorted and (b) shorted.

4.3 Stoneley Interface-Wave Accelerometer

A Stoneley wave is a type of elastic wave that is propagated along the interface of two elastic solids. Because its energy remains at or near the interface, it can be generated, reflected and detected at the interface. Since Stoneley wave, derived from surface acoustic wave (SAW) technology, is also a planar technology, and hence can be fabricated by photolithographic techniques. That is why Stoneley wave devices can be fabricated at costs comparable to those for integrated circuits.

The interface Stoneley wave resonator consists of a pair of reflective gratings on a surface, defining a resonant cavity for interface acoustic waves. These waves can be generated and detected by an interdigital transducer, which is piezoelectrically coupled to the interface strain variations of the acoustic waves. This resonant cavity, shown in Fig.43, is coupled to a feedback amplifier to maintain the energy in the cavity.

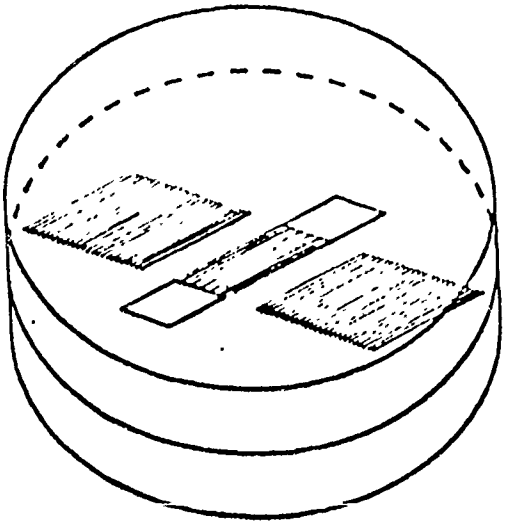

Figure 43- Stoneley Interface Wave Configuration

The bit quantization for an interface-wave accelerometer is in the same range as those of high precision accelerometers. For an interface wave accelerometer with 320 MHz frequency and proof mass loading to produce 200 ppm strain at 20g input acceleration, the bit quantization will be:

$$\frac{(20\ g)\ (32\ fps/sec/g)}{(320 \times 10^{6}\ bit/sec)\ (200 \times 10^{-6}\ p/p)} = 0.01\ fps/bit$$

The short-term stability of the interface wave resonator (assuming for the worst case is similar to surface acoustic wave) is in the order of 0.1 parts per billion.

For the above example, this gives a comparable short-term stability of:

$$\frac{10^{-4}\ ppm}{200\ ppm\ /\ 20\ g} = 10\ micro\text{-}g$$

and gives a dynamic range of

$$\frac{20}{10 \times 10^{-6}} = 2 \times 10^{6}$$

The accelerometer overall design has a direct bearing on the complexity of the inertial guidance system. The digital nature of the interface wave accelerometer output results in an extremely simple system architecture. Shown in Fig.44 is a baseline guidance system block diagram which shows how the interface wave accelerometer signals are processed to generate not only acceleration but also velocity and displacement signals (words) for the guidance system.

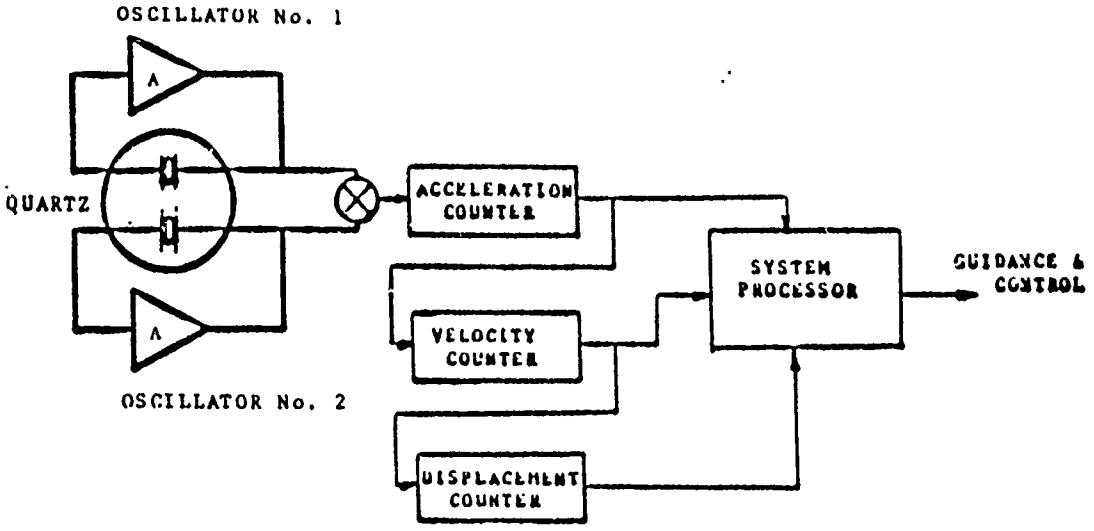

Figure 44- Proposed Baseline Interface Wave Accelerometer in Inertial Guidance System

The mixer output is a frequency proportional to acceleration and the acceleration counter generates a binary count with each clock reset from the microprocessor. The output of the acceleration counter is summed (integrated) in another counter which then generates a binary word representing velocity. Displacement is computed by summing the velocity counter output and transmitting the displacement word to the microprocessor. The microprocessor provides the appropriate scaling and generates the needed guidance and control signals.

The digital system proposed is capable of providing acceleration signals with more than 12 bits accuracy due to the large dynamic range of such proposed accelerometer. The system is unique in that 12 bit accuracy is provided without using analog-to-digital converters. This, in turn, will enable the design of a system with minimum power requirements. Starting with this baseline system, the detailed design will be the subject for the proposed study.

4.4 Comparison With Experimental Results

The theoretical results of Section 4.1 were compared with experimentally published results. The experimental method consisted of monitoring the frequency (proportional to velocity), resonant resistance, and quality factor (Q) of SAW resonators while a crystalline film was deposited (sputtered) under vacuum. The following films were evaluated by this method: MgO, SiO_x, Y_2O_3, and AlN. The experimental results are shown in Figures 45 and 46.

Because the experimental results are based upon time of deposition and not absolute film thickness it was difficult to compare directly theory and experiment. Nevertheless it can be assumed that thickness is proportional to time for discussion purposes. Comparing the theoretical results (MgO) of Figure 9 with Figure 45, several points are noted:(1) the velocity or frequency increases with film thickness and (2) after an initial drop in Q the loss is relatively constant with only a small increase with thickness. The increase in frequency with thickness is predicted because we believe the film grown was considerably less than 10% of a wavelength.

Experimental results for SiO_x films are compared to theoretical predictions using Figure 18. The important points are: (1) experimental frequency drops with film thickness in contrast to theory which predicts an increase with film thickness and (2) experimental results indicate a sharp increase in loss at an intermediate thickness. The later is compatible with what is predict-

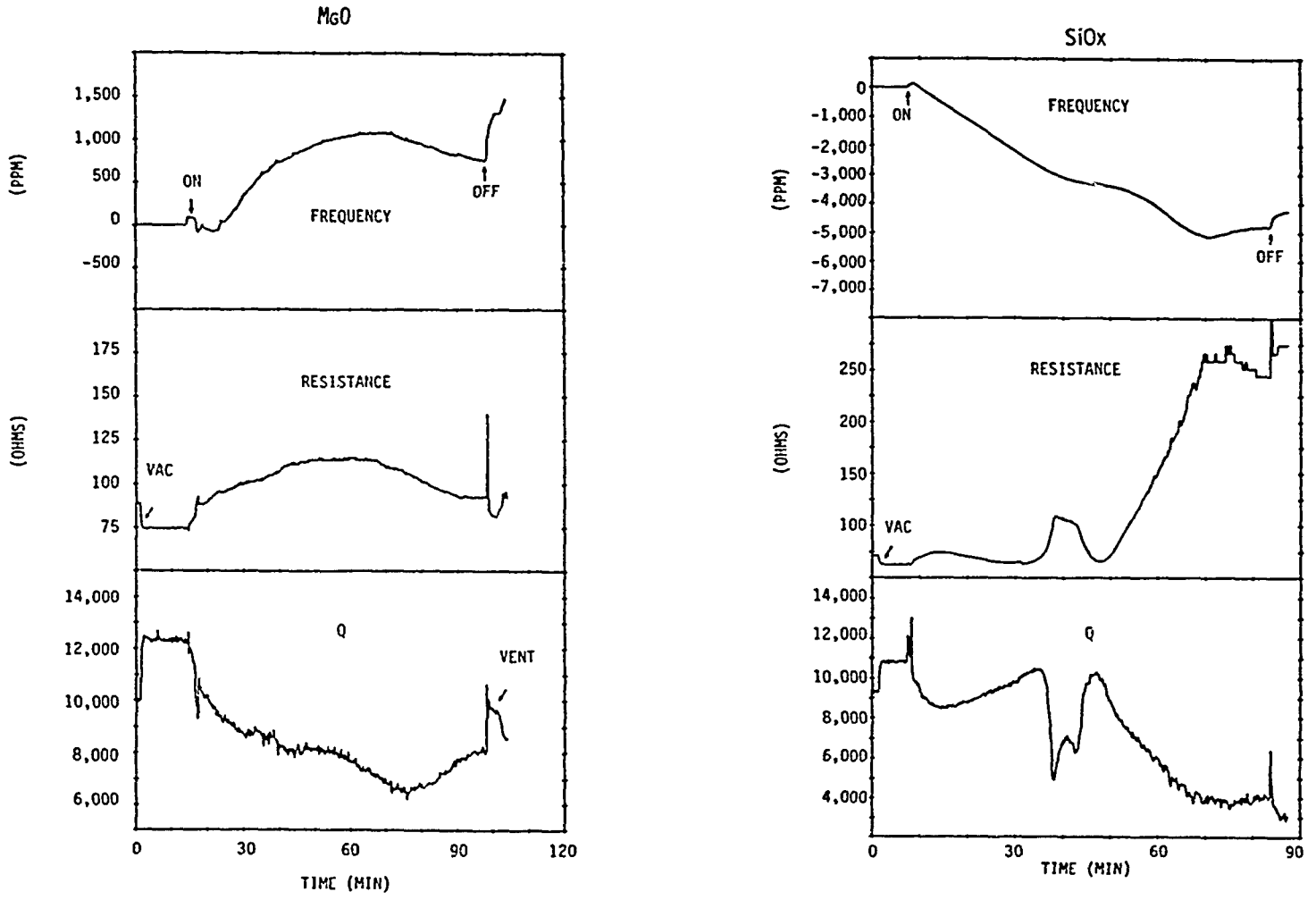

Figure 45- Experimentally measured frequency, resistance, and Q for SAW resonators on ST-Quartz with sputtered films of (a)MgO and (b) SiO_x.

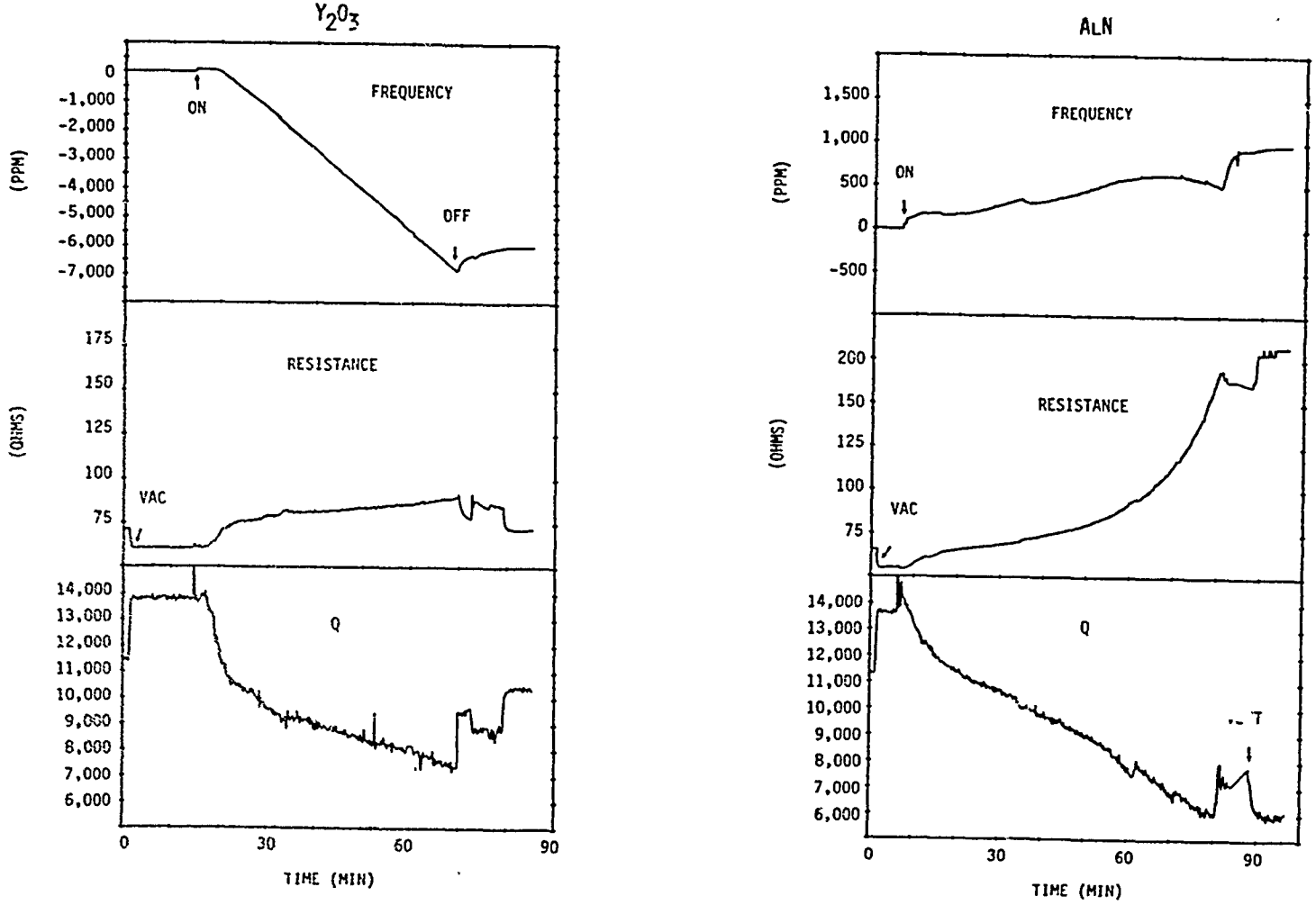

Figure 46- Experimentally measured frequency, resistance, and Q for SAW resonators on ST-Quartz with sputtered films of (a)Y_2O_3 and (b) AlN.

ed for film thickness in the range than 5-10% of a wavelength. The discrepency between the frequency behavior is explained as follows: For film thickness less than 5% of a wavelength the frequency changes by a very small amount, however this is masked by a relatively large temperature increase during sputtering. Half way into the film deposition there is a decrease in the rate of frequency drop and at the same time the loss increases dramatically. We believe this is where the film thickness is approaching 5-10% of a wavelength resulting in increased wave penetration and a sharp drop in coupling.

Experimentally films of Y_2O_3 were the most well behaved with a uniform drop in frequency during deposition, a relatively small increase in resistance, and a drop in Q. The decrease in frequency and the low loss was predicted because the surface wave does not couple into a bulk wave for Y_2O_3 layers at any thickness.

Experimentaly films of AlN showed an increase in frequency and a uniform increase in loss during deposition. Near the end of the deposition the resistance increase was accelerated. Theoretically the increase in frequency was predicted. The large increase in resonator resistance and loss near the end of the depositon indicates the film was near 5-10% of a wavelength hence the piezoelectric coupling drops and coupling to a bulk wave occurs.

5.0 CONCLUSIONS AND RECOMMENDATIONS

This study has established the theoretical foundations for using higher order Rayleigh and interfacial (Stoneley) waves for acoustic devices such as SAW resonators and sensors. Techniques for analyzing layered SAW devices as well as multi-layered interfacial waves were developed and applied to many anisotropic materials as part of this study.

Layered SAW device performance using materials such as MgO, SiO_x, AlN, Y_2O_3, Al_2O_3, and TiO_2 was theoretically analyzed and the results compared with experimental results. Shifts in frequency, loss to bulk mode coupling, and changes in piezoelectric coupling can now be predicted for any layer material. From this study it is concluded that passivation , for the first order Rayleigh mode cannot be achieved using layers of material. This is due to the fact that the particle displacements of the surface wave are at the surface of any deposited layer and hence a decrease in piezoelectric coupling because of the separation between the elastic displacements of the wave and the potential generating electrodes at the interface.

For future studies of layered SAW devices it is recommended that temperature effects and power flow calculations be added to the existing analysis techniques. These properties can be used to predict temperature compensated materials and determine orientations where power flow is co-linear with the wave vector.

An analysis of interfacial waves in multi-layered media was completed during this phase I study. A method of analyzing interfacial waves was developed which included search methods which greatly reduced the time needed to determine the existence of Stoneley waves. Using these methods, Stoneley waves were for the first time predicted in single crystal quartz. Stoneley waves which are well bound and piezoelectrically active were found to exist for several orientations of quartz. This is an important discovery since it may result in a new class of acoustic resonators and sensors with stability superior to existing SAW devices. Unlike layered SAW devices, Stoneley wave structures are well passivated and require no hermetic enclosure; thus they will have better stability and lower cost.

Based upon the results of this phase I study, recommendations for future work are:

1. To add temperature sensitivity and power flow analysis to the existing theoeretical techniques.
2. To design, fabricate, and test interface wave resonators and to compare their characteristics with theoretical predictions.
3. To design, fabricate, and test interface wave sensors as inertial navigation (acceleration) sensors.

6.Ø REFERENCES

1. E.J. Staples and T.C. Lim, "3ØØ MHz Oscillators Using SAW Resonators and Delay Lines," Proceedings of the 31st Annual Symposium on Frequency Control, U.S. Army Electronics Com. Ft. Monmouth, NJ, pp.371-373, 1977.

2. E.J. Staples, J. Wise, and A.P. Andrews, "Inertial Guidance and Underwater Sound Detection Using SAW Sensors," 36th Annual Frequency Control Symposium, U.S. Army Electronics Command, Ft. Monmouth, NJ, June 1982.

3. [illegible] chematic Society Proceedings, V. 17, p. 4.

4. W.M. Ewing, W.S. Jardetzky and F. Press, "Elastic Waves in Layered Media," McGraw-Hill, 1957.

5. T.C. Lim andl M.P. Musgrave, "Stoneley Waves in anisotropic Media," Nature, V. 225, 1970, p.372.

6. R. Stoneley, "Elastic Waves at the Surface of Separation of Two solides," Proc. Royal Soc. (London), V. A245, 1924, p. 213.

7. G.W. Farnell and E.L. Adler, "Elastic Wave Propagation in Thin Layers," in Physical Acoustics, V. IX, Edited by W.P. Mason and R.N. Thurston , Academic Press, 1972.

8. K. Yamanouchi and S. Hayama, "SAW Properties of SiO_2/128° YX $LiNbO_3$ Structure Fabricated by the Magnetron Sputtering Technique," IEEE Transactions on Sonics and Ultrasonics, SU-31, No. 1, January 1984, p. 51-57.

9. G.W. Farnell, "Symmetry Considerations for Elastic Layer Modes Propagating in Anisotropic Piezoelectric Crystals," IEEE Transactions on Sonics and Ultrasonics, SU-17, No. 4, October 1970, p.229-238.

1Ø. J. Lothe and D.M. Barnett, "On the Existence of Surface Wave Solutions for Anisotropic Elastic Half-Spaces with Free Surface," Journal of Applied Physics, V. 47, No. 2, February 1976, p. 428-433.

7.0 APPENDICES

7.1 Appendix I

The following arrays of material constants were used to perform the studies contained in this report. The constants are arranged by title, elastic constants, piezoelectric constants, dielectric constants and density.

THE MATERIAL IS ST-CUT QUARTZ

+8.670E+10	+2.749E+10	-8.587E+09	-1.038E+09	+0.000E+00	+0.000E+00
+2.749E+10	+9.653E+10	-4.830E+09	-1.339E+10	+0.000E+00	+0.000E+00
-8.587E+09	-4.830E+09	+1.306E+11	+1.872E+09	+0.000E+00	+0.000E+00
-1.038E+09	-1.339E+10	+1.872E+09	+4.117E+10	+0.000E+00	+0.000E+00
+0.000E+00	+0.000E+00	+0.000E+00	+0.000E+00	+3.032E+10	-7.593E+09
+0.000E+00	+0.000E+00	+0.000E+00	+0.000E+00	-7.593E+09	+6.743E+10

+1.710E-01	-3.832E-02	-1.327E-01	-8.205E-02	+0.000E+00	+0.000E+00
+0.000E+00	+0.000E+00	+0.000E+00	+0.000E+00	-6.653E-02	-9.903E-02
+0.000E+00	+0.000E+00	+0.000E+00	+0.000E+00	-7.197E-02	-1.071E-01

+3.920E-11	+0.000E+00	+0.000E+00
+0.000E+00	+4.017E-11	-8.972E-13
+0.000E+00	-8.972E-13	+4.003E-11

DENSITY = 2650

THE MATERIAL IS FUSED QUARTZ

+7.850E+10	+1.610E+10	+1.610E+10	+0.000E+00	+0.000E+00	+0.000E+00
+1.610E+10	+7.850E+10	+1.610E+10	+0.000E+00	+0.000E+00	+0.000E+00
+1.610E+10	+1.610E+10	+7.850E+10	+0.000E+00	+0.000E+00	+0.000E+00
+0.000E+00	+0.000E+00	+0.000E+00	+3.120E+10	+0.000E+00	+0.000E+00
+0.000E+00	+0.000E+00	+0.000E+00	+0.000E+00	+3.120E+10	+0.000E+00
+0.000E+00	+0.000E+00	+0.000E+00	+0.000E+00	+0.000E+00	+3.120E+10

+0.000E+00	+0.000E+00	+0.000E+00	+0.000E+00	+0.000E+00	+0.000E+00
+0.000E+00	+0.000E+00	+0.000E+00	+0.000E+00	+0.000E+00	+0.000E+00
+0.000E+00	+0.000E+00	+0.000E+00	+0.000E+00	+0.000E+00	+0.000E+00

+3.320E-11	+0.000E+00	+0.000E+00
+0.000E+00	+3.320E-11	+0.000E+00
+0.000E+00	+0.000E+00	+3.320E-11

DENSITY = 2200

THE MATERIAL IS YITTRIUM OXIDE

+2.270E+11	+1.380E+11	+1.380E+11	+0.000E+00	+0.000E+00	+0.000E+00
+1.380E+11	+2.270E+11	+1.380E+11	+0.000E+00	+0.000E+00	+0.000E+00
+1.380E+11	+1.380E+11	+2.270E+11	+0.000E+00	+0.000E+00	+0.000E+00
+0.000E+00	+0.000E+00	+0.000E+00	+6.860E+10	+0.000E+00	+0.000E+00
+0.000E+00	+0.000E+00	+0.000E+00	+0.000E+00	+6.860E+10	+0.000E+00
+0.000E+00	+0.000E+00	+0.000E+00	+0.000E+00	+0.000E+00	+6.860E+10

+0.000E+00	+0.000E+00	+0.000E+00	+0.000E+00	+0.000E+00	+0.000E+00
+0.000E+00	+0.000E+00	+0.000E+00	+0.000E+00	+0.000E+00	+0.000E+00
+0.000E+00	+0.000E+00	+0.000E+00	+0.000E+00	+0.000E+00	+0.000E+00

+1.151E-10	+0.000E+00	+0.000E+00
+0.000E+00	+1.151E-10	+0.000E+00
+0.000E+00	+0.000E+00	+1.151E-10

DENSITY = 5010

THE MATERIAL IS UNROTATED COPPER

+1.710E+11	+1.239E+11	+1.239E+11	+0.000E+00	+0.000E+00	+0.000E+00
+1.239E+11	+1.710E+11	+1.239E+11	+0.000E+00	+0.000E+00	+0.000E+00
+1.239E+11	+1.239E+11	+1.710E+11	+0.000E+00	+0.000E+00	+0.000E+00
+0.000E+00	+0.000E+00	+0.000E+00	+7.560E+10	+0.000E+00	+0.000E+00
+0.000E+00	+0.000E+00	+0.000E+00	+0.000E+00	+7.560E+10	+0.000E+00
+0.000E+00	+0.000E+00	+0.000E+00	+0.000E+00	+0.000E+00	+7.560E+10

+0.000E+00	+0.000E+00	+0.000E+00	+0.000E+00	+0.000E+00	+0.000E+00
+0.000E+00	+0.000E+00	+0.000E+00	+0.000E+00	+0.000E+00	+0.000E+00
+0.000E+00	+0.000E+00	+0.000E+00	+0.000E+00	+0.000E+00	+0.000E+00

+0.000E+00	+0.000E+00	+0.000E+00
+0.000E+00	+0.000E+00	+0.000E+00
+0.000E+00	+0.000E+00	+0.000E+00

DENSITY = 8950

THE MATERIAL IS RUTILE (001)

+2.660E+11	+1.730E+11	+1.360E+11	+0.000E+00	+0.000E+00	+0.000E+00
+1.730E+11	+2.660E+11	+1.360E+11	+0.000E+00	+0.000E+00	+0.000E+00
+1.360E+11	+1.360E+11	+4.700E+11	+0.000E+00	+0.000E+00	+0.000E+00
+0.000E+00	+0.000E+00	+0.000E+00	+1.240E+11	+0.000E+00	+0.000E+00
+0.000E+00	+0.000E+00	+0.000E+00	+0.000E+00	+1.240E+11	+0.000E+00
+0.000E+00	+0.000E+00	+0.000E+00	+0.000E+00	+0.000E+00	+1.890E+11

+0.000E+00	+0.000E+00	+0.000E+00	+0.000E+00	+0.000E+00	+0.000E+00
+0.000E+00	+0.000E+00	+0.000E+00	+0.000E+00	+0.000E+00	+0.000E+00
+0.000E+00	+0.000E+00	+0.000E+00	+0.000E+00	+0.000E+00	+0.000E+00

+7.610E-10	+0.000E+00	+0.000E+00
+0.000E+00	+7.610E-10	+0.000E+00
+0.000E+00	+0.000E+00	+1.504E-09

DENSITY = 4280

THE MATERIAL IS Z_CUT_X_PROP_MgO

```
+2.964E+11  +9.500E+10  +9.500E+10  +0.000E+00  +0.000E+00  +0.000E+00
+9.500E+10  +2.964E+11  +9.500E+10  +0.000E+00  +0.000E+00  +0.000E+00
+9.500E+10  +9.500E+10  +2.964E+11  +0.000E+00  +0.000E+00  +0.000E+00
+0.000E+00  +0.000E+00  +0.000E+00  +1.560E+11  +0.000E+00  +0.000E+00
+0.000E+00  +0.000E+00  +0.000E+00  +0.000E+00  +1.560E+11  +0.000E+00
+0.000E+00  +0.000E+00  +0.000E+00  +0.000E+00  +0.000E+00  +1.560E+11

+0.000E+00  +0.000E+00  +0.000E+00  +0.000E+00  +0.000E+00  +0.000E+00
+0.000E+00  +0.000E+00  +0.000E+00  +0.000E+00  +0.000E+00  +0.000E+00
+0.000E+00  +0.000E+00  +0.000E+00  +0.000E+00  +0.000E+00  +0.000E+00

+8.544E-11  +0.000E+00  +0.000E+00
+0.000E+00  +8.544E-11  +0.000E+00
+0.000E+00  +0.000E+00  +8.544E-11
```

DENSITY = 3583

THE MATERIAL IS SAPPHIRE (001)

```
+4.970E+11  +1.640E+11  +1.110E+11  -2.350E+10  +0.000E+00  +0.000E+00
+1.640E+11  +4.970E+11  +1.110E+11  +2.350E+10  +0.000E+00  +0.000E+00
+1.110E+11  +1.110E+11  +4.980E+11  +0.000E+00  +0.000E+00  +0.000E+00
-2.350E+10  +2.350E+10  +0.000E+00  +1.470E+11  +0.000E+00  +0.000E+00
+0.000E+00  +0.000E+00  +0.000E+00  +0.000E+00  +1.470E+11  -2.350E+10
+0.000E+00  +0.000E+00  +0.000E+00  +0.000E+00  -2.350E+10  +1.665E+11

+0.000E+00  +0.000E+00  +0.000E+00  +0.000E+00  +0.000E+00  +0.000E+00
+0.000E+00  +0.000E+00  +0.000E+00  +0.000E+00  +0.000E+00  +0.000E+00
+0.000E+00  +0.000E+00  +0.000E+00  +0.000E+00  +0.000E+00  +0.000E+00

+8.280E-11  +0.000E+00  +0.000E+00
+0.000E+00  +8.280E-11  +0.000E+00
+0.000E+00  +0.000E+00  +1.020E-10
```

DENSITY = 3980

THE MATERIAL IS ZX AL NITRIDE

```
+3.450E+11  +1.250E+11  +1.200E+11  +0.000E+00  +0.000E+00  +0.000E+00
+1.250E+11  +3.450E+11  +1.200E+11  +0.000E+00  +0.000E+00  +0.000E+00
+1.200E+11  +1.200E+11  +3.950E+11  +0.000E+00  +0.000E+00  +0.000E+00
+0.000E+00  +0.000E+00  +0.000E+00  +1.180E+11  +0.000E+00  +0.000E+00
+0.000E+00  +0.000E+00  +0.000E+00  +0.000E+00  +1.180E+11  +0.000E+00
+0.000E+00  +0.000E+00  +0.000E+00  +0.000E+00  +0.000E+00  +1.100E+11

+0.000E+00  +0.000E+00  +0.000E+00  +0.000E+00  -4.800E-01  +0.000E+00
+0.000E+00  +0.000E+00  +0.000E+00  -4.800E-01  +0.000E+00  +0.000E+00
-5.800E-01  -5.800E-01  +1.550E+00  +0.000E+00  +0.000E+00  +0.000E+00

+8.000E-11  +0.000E+00  +0.000E+00
+0.000E+00  +8.000E-11  +0.000E+00
+0.000E+00  +0.000E+00  +9.500E-11
```

DENSITY = 3260

7.2 Appendix II

The basis of a search technique for Stoneley waves is contained in the paper reprinted in this appendix. The importance of formulating the wave impedance is discussed in considerable detail by the authors. Using these techniques a search method for Stoneley waves in piezoelectric materials was developed.

On the existence of surface-wave solutions for anisotropic elastic half-spaces with free surface

J. Lothe

Institute of Physics, University of Oslo, Oslo, Norway

D. M. Barnett

Department of Materials Science and Engineering, Stanford University, Stanford, California 94305

A proof is developed that for a given direction of propagation on the free surface of a half-infinite anisotropic crystal, a surface-wave solution with a certain phase velocity $v_R < v_L$, where v_L is the limiting velocity, will always exist, except in the special case when the bulk wave defining the limiting velocity satisfies the condition of a free surface. The proof is in terms of the surface impedance, which relates the amplitude at the surface of a surface wave with the external forces needed at the surface. The properties of the impedance as a function of phase velocity determines whether a surface wave not requiring external forces at the surface exists for a certain phase velocity. The proof is valid also in the case of degeneracies in the eigenvalue problem entering the analysis.

I. INTRODUCTION

Recently the present authors[1] provided a proof for the existence of surface-wave solutions for elastic half-spaces with a free boundary. However, the proof was in terms of the Lagrangian for moving dislocations, a quantity not well known among surface-wave researchers. Here an alternative proof in terms of the so-called surface-wave impedance is given. Usually a surface wave with given phase velocity and given amplitude at the surface requires external forces at the surface. The surface impedance relates amplitude at the surface with external forces needed at the surface. However, when the impedance satisfies certain requirements, surface waves which do not require external forces at the surface may exist. In this paper we will analyze the impedance as a function of velocity to see whether for certain phase velocities the impedance satisfies the requirements for surface waves in the case of free surfaces.

In Secs. II and III an integral form of the general theory for surface waves maintained by external forces is developed and, in particular, a convenient integral expression for the impedance is derived. As in our previous paper[1] the analysis presupposes no degeneracy in the eigenvalue problem appearing. In Sec. IV the complications that arise with degeneracy are considered and it is concluded that the integral expression for the impedance remains valid. In Sec. V the properties of the impedance are listed. Finally, in Sec. VI we turn to the special problem of surface-wave propagation on *free* surfaces. This is the real problem to which we are addressing ourselves in this paper. It will be shown how this problem can be discussed in terms of the properties of the impedance developed in Secs. III—V. The first sections of the paper are necessary prerequisites for the discussion in Sec. VI.

The exposition in what follows will be kept quite brief by appropriate reference to earlier work.

II. INTRODUCTORY THEORY

The surface has normal $\mathbf{n}^0$, see Fig. 1. We consider harmonic waves traveling along the surface in the $\mathbf{m}^0$ direction

$$\mathbf{u}(\mathbf{x}) = \mathbf{A}(\mathbf{n}^0\mathbf{x}) \exp[ik(\mathbf{m}^0\mathbf{x} - vt)], \tag{2.1}$$

where v is the phase velocity for propagation along the surface, $\mathbf{x}$ is the position vector with a point on the surface as origin, and $\mathbf{n}^0\mathbf{x}$ is thus the depth below the surface. With respect to a fixed external Cartesian laboratory set of unit vectors, $\mathbf{x}$ has components x_1, x_2, and x_3.

The amplitude $\mathbf{A}$ as a function of depth depends on the boundary conditions at the surface and the boundary conditions at infinite depth. For given $k, \mathbf{m}, \mathbf{n}$, and v, several independent waves of the type (2.1) will be possible. These are derived in Secs. III and IV.

Referring also the elastic coefficients to the external laboratory system, the elastic force per unit area parallel with the surface is

$$J_j = n_i^0 C_{ijkl} \frac{\partial u_k}{\partial x_l} \tag{2.2}$$

or, by Eq. (2.1)

$$J_j = ik(n_i^0 C_{ijkl} m_l^0) A_k + (n_i^0 C_{ijkl} n_l^0) \frac{\partial A_k}{\partial y}, \tag{2.3}$$

where

$$y = \mathbf{n}^0\mathbf{x} \tag{2.4}$$

is a convenient notation for the depth below the surface.

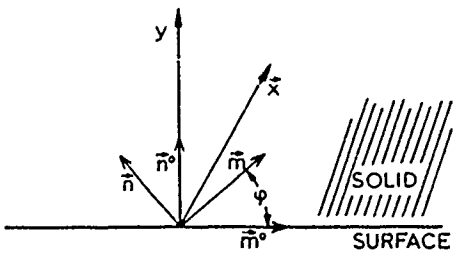

FIG. 1. Coordinate systems for the description of surface waves in a half-infinite crystal. $\mathbf{n}^0$ is the inner unit normal.

If an observer travels with a wave with the phase velocity v of the wave, he sees a stationary wave field, and the condition for dynamic equilibrium can be stated similarly to the condition for equilibrium in the static case as

$$C'_{ijkl}\frac{\partial^2 u_k}{\partial x_j \partial x_l}=0, \tag{2.5}$$

where C'_{ijkl} are the dynamic elastic coefficients

$$C'_{ijkl}=C_{ijkl}-\rho v^2 m_i^0 m_l^0 \delta_{jk}. \tag{2.6}$$

Introducing the vectors

$$\mathbf{L}=ik^{-1}\mathbf{J}, \tag{2.7}$$

the equilibrium condition (2.5) can be expressed in the form

$$\mathbf{N}^0\xi=-ik^{-1}\frac{\partial}{\partial y}\xi, \tag{2.8}$$

where ξ is the six-dimensional vector

$$\xi=\begin{pmatrix}\mathbf{A}\\ \mathbf{L}\end{pmatrix} \tag{2.9}$$

and $\mathbf{N}^0$ is the 6×6 matrix

$$\mathbf{N}^0=-\begin{pmatrix}(n^0n)^{-1}(n^0m^0) & (n^0n^0)^{-1}\\ (m^0n^0)(n^0n^0)^{-1}(n^0m^0)-(m^0m^0) & (m^0n^0)(n^0n^0)^{-1}\end{pmatrix}. \tag{2.10}$$

The 3×3 matrices (ab) occurring in the block representation of $\mathbf{N}^0$ are defined by

$$(ab)_{jk}=a_i C'_{ijkl} b_l. \tag{2.11}$$

The symmetry of C'_{ijkl} is such that

$$(ab)=(ba)^T,$$

where T means transposition.

The above is essentially the formalism of Stroh[2] and Ingebrigtsen and Tonning.[3]

In terms of the above notation, the relation between $\mathbf{L}$ and $\mathbf{A}$ can be written

$$\mathbf{L}=-(n^0m^0)\mathbf{A}+ik^{-1}(n^0n^0)\frac{\partial}{\partial y}\mathbf{A}. \tag{2.12}$$

Now formally construct the operator $\mathbf{N}$ by the prescription (2.10) in terms of a unit vector system $(\mathbf{m},\mathbf{n})$ rotated by ϕ relative to the system $(\mathbf{m}^0,\mathbf{n}^0)$. However, note that $\mathbf{m}^0$ in the definition (2.6) of C'_{ijkl} is kept *fixed* as parallel with the surface and the direction of wave propagation. The resulting $\mathbf{N}$ is a function of ϕ, $\mathbf{N}(\phi)$, and as shown by Barnett and Lothe[4]

$$\frac{\partial}{\partial\phi}\mathbf{N}=-(\mathbf{I}+\mathbf{N}^2). \tag{2.13}$$

The operator $\mathbf{N}(\phi)$ exists for all ϕ up to the limiting velocity v_L. The limiting velocity is the lowest velocity for which there exists an orientation for the unit vector $\mathbf{m}$, $\mathbf{m}_L$ such that

$$\|(m_L m_L)\|=0, \tag{2.14}$$

allowing a bulk wave of amplitude $\mathbf{A}_L$ satisfying

$$(m_L m_L)\mathbf{A}_L=0 \tag{2.15}$$

and traveling in the $\mathbf{m}_L$ direction. In the static case, i.e., with $v=0$ in Eq. (2.6), (mm) is positive definite by elastic stability,

$$\|(mm)\|>0, \quad v=0. \tag{2.16}$$

Thus

$$\|mm\|>0, \quad v<v_L, \text{ all } \phi \tag{2.17}$$

and likewise

$$\|(m)\|>0, \quad \text{all } \phi \text{ when } v<v_L$$

so that $(nn)^{-1}$ and also $\mathbf{N}(\phi)$ exist for all ϕ when $v<v_L$.

The preceding is general. Now we will discuss separately the case of no degeneracy and degeneracy and show that the same integral expression for the surface-wave impedance applies in either case.

III. NO DEGENERACY

Assume that $\mathbf{A}(\mathbf{n}^0\mathbf{x})=\mathbf{A}(y)$ in Eq. (2.1) is of the form

$$\mathbf{A}(y)=\mathbf{A}_\alpha \exp(ikp_\alpha^0 y). \tag{3.1}$$

Then Eq. (2.8) leads to the eigenvalue problem

$$\mathbf{N}^0\xi_\alpha=p_\alpha^0\xi_\alpha, \tag{3.2}$$

which shows that the p_α^0 must be the roots of

$$\|\mathbf{N}^0-p_\alpha^0\mathbf{I}\|=0. \tag{3.3}$$

This is a sixth-order equation with real coefficients, so there will be six roots occurring in pairs of complex conjugates. Real roots cannot occur for $v<v_L$. At $v=v_L$, one pair of roots coalesces into one real root.

When all p_α are *different* (no degeneracy), it can be asserted by general theorems (Nering[5] and Pease[6]) that

the six ξ_α form a complete set, (3.4)

or said in a more detailed fashion, the six ξ_α are linearly independent and any vector ξ in the six-dimensional vector space can be represented by a linear combination of the six ξ_α. This explains the meaning of the word "complete" in theorem (3.4).

Thus in the case of all p_α different, the general solution of Eq. (2.8) can indeed be constructed by a superposition of partial solutions of the type (3.1).

Now consider the eigenvalue problem

$$\mathbf{N}(\phi)\xi_\alpha=p_\alpha(\phi)\xi_\alpha. \tag{3.5}$$

From Eq. (2.13) it follows that the eigenvectors for Eq. (3.5) are the *same* as the ξ_α of Eq. (3.2). The eigenvectors ξ_α are *invariant* to rotation.

The eigenvalues must vary with ϕ as

$$\frac{\partial p_\alpha}{\partial\phi}=-(1+p_\alpha^2) \tag{3.6}$$

according to Eq. (2.13). From Eq. (3.6) it follows that

$$\overline{p_\alpha}=\frac{1}{2\pi}\int_0^{2\pi} p_\alpha\, d\phi=\pm i, \tag{3.7}$$

+ or − according to whether we consider roots with a positive or negative imaginary part.

Introducing

$$\overline{\mathbf{N}}=\frac{1}{2\pi}\int_0^{2\pi}\mathbf{N}\,d\phi=\begin{pmatrix}\mathbf{S} & \mathbf{Q}\\ \mathbf{B} & \mathbf{S}^T\end{pmatrix}, \tag{3.8}$$

where

$$\mathbf{S}=-\frac{1}{2\pi}\int_0^{2\pi}(m)^{-1}(nm)\,d\phi, \tag{3.9}$$

$$\mathbf{Q}=-\frac{1}{2\pi}\int_0^{2\pi}(m)^{-1}\,d\phi, \tag{3.10}$$

$$\mathbf{B}=-\frac{1}{2\pi}\int_0^{2\pi}[(mn)(m)^{-1}(nm)-(nm)]\,d\phi, \tag{3.11}$$

it now follows that

$$\bar{\mathbf{N}}\xi_\alpha=\pm i\xi_\alpha. \tag{3.12}$$

The first three of these equations are

$$\mathbf{S}\mathbf{A}_\alpha+\mathbf{Q}\mathbf{L}_\alpha=\pm i\mathbf{A}_\alpha. \tag{3.13}$$

For $v<v_L$, $(m)^{-1}$ is positive definite and consequently $\mathbf{Q}$ is negative definite. Thus $\mathbf{Q}^{-1}$ exists and

$$\mathbf{L}_\alpha=\mathbf{Q}^{-1}(\pm i\mathbf{I}-\mathbf{S})\mathbf{A}_\alpha. \tag{3.14}$$

Let $\alpha=1,2,3$ be the solutions with positive imaginary part in p_α. These are the solutions which show exponential decay with increasing y and which are to be used in the construction of surface waves. For these solutions

$$\mathbf{L}_\alpha=\mathbf{Q}^{-1}(i\mathbf{I}-\mathbf{S})\mathbf{A}_\alpha,\quad \alpha=1,2,3. \tag{3.15}$$

Now suppose that the three $\mathbf{A}_\alpha$ are linearly dependent. But then by Eq. (3.15), the same linear dependence would exist between the corresponding $\mathbf{L}_\alpha$ and consequently between the corresponding ξ_α, in contradiction with theorem (3.4).

Thus the three $\mathbf{A}_\alpha$, $\alpha=1,2,3$, form a *complete* set in three-dimensional space for all $v<v_L$. The same conclusion was reached by Stroh[7] by more intricate reasoning.

Since $\mathbf{A}_\alpha$, $\alpha=1,2,3$, form a complete set, an arbitrary amplitude $\mathbf{A}$ on the surface can be obtained by superposition of exponentially decaying solutions provided a force amplitude

$$\mathbf{J}=-ik\mathbf{L}=k(\mathbf{Q}^{-1}+i\mathbf{Q}^{-1}\mathbf{S})\mathbf{A} \tag{3.16}$$

is maintained at the surface. We can write

$$\mathbf{J}=-Z\mathbf{A}, \tag{3.17}$$

where

$$\mathbf{Z}=-k(\mathbf{Q}^{-1}+i\mathbf{Q}^{-1}\mathbf{S}) \tag{3.18}$$

will be called the surface impedance. A similar concept was introduced by Ingebrigtsen and Tonning,[3] but in an eigenvector representation. In Sec. IV, the above integral expression for $\mathbf{Z}$ will be shown to be valid also in cases of degeneracy.

The matrices $\mathbf{S}$, $\mathbf{Q}$, and $\mathbf{B}$ introduced in the foregoing, are not independent, but obey certain completeness relations. From Eq. (3.12), applying $\mathbf{N}$ twice gives

$$\bar{\mathbf{N}}^2\xi_\alpha=-\xi_\alpha, \tag{3.19}$$

and since the ξ_α form a complete set

$$\bar{N}^2\xi=-\xi, \tag{3.20}$$

where ξ is an arbitrary six-dimensional vector. Thus

$$\bar{N}^2+\begin{pmatrix}\mathbf{I} & \mathbf{0}\\ \mathbf{0} & \mathbf{I}\end{pmatrix}=0, \tag{3.21}$$

where $\mathbf{I}$ is block notation for a three-dimensional unit matrix.

Written out in components Eq. (3.21) yields

$$\mathbf{Q}\mathbf{B}+\mathbf{S}^2+\mathbf{I}=0, \tag{3.22}$$

$$\mathbf{S}\mathbf{Q}+\mathbf{Q}\mathbf{S}^T=0, \tag{3.23}$$

$$\mathbf{B}\mathbf{S}+\mathbf{S}^T\mathbf{B}=0, \tag{3.24}$$

$$\mathbf{B}\mathbf{Q}+(\mathbf{S}^T)^2+\mathbf{I}=0. \tag{3.25}$$

From Eq. (3.23) it follows that $\mathbf{Q}^{-1}\mathbf{S}$ is antisymmetric. Thus since $\mathbf{Q}^{-1}$ is symmetric the impedance $\mathbf{Z}$, Eq. (3.18), is Hermitian,

$$\mathbf{Z}=(\mathbf{Z}^T)^*, \tag{3.26}$$

where * indicates complex conjugation.

IV. DEGENERACY

The considerations in Sec. III were largely based on the fact that the ξ_α form a complete set when all p_α are different. However, degeneracy may occur. For definiteness, suppose that

$$\left.\begin{matrix}p_1\neq p_2=p_3\\ p_4\neq p_5=p_6\end{matrix}\right\},\quad p_4=p_1^*,\quad p_5=p_2^*. \tag{4.1}$$

The degeneracy may either occur for reasons of symmetry or accidentally for a definite velocity.

If the degenerate $\mathbf{N}$ still possesses six independent eigenvectors, the considerations of Sec. III apply *in toto*.

However, with degeneracy one is not assured that six independent eigenvectors exist as in the nondegenerate case, for which theorem (3.4) applies. When the degenerate $\mathbf{N}$ does not possess six independent eigenvectors, we say that we have the case of nonsimple degeneracy. Static deformation [i.e., $v=0$ in Eq. (2.6)] in elastically isotropic bodies is such a case.[8]

In the case of nonsimple degeneracy, one forms a complete set by the introduction of generalized eigenvectors associated with the degenerate eigenvectors. Suppose the degenerate $\mathbf{N}$ corresponding to the example (4.1) only allows four independent eigenvectors ξ_1, ξ_2, ξ_4, and ξ_5. Generalized eigenvectors ξ_3 and ξ_6 associated with the degenerate eigenvectors ξ_2 and ξ_5 can then be formed according to the scheme

$$(\mathbf{N}-p_2\mathbf{I})\xi_3=\xi_2, \tag{4.2}$$

$$(\mathbf{N}-p_5\mathbf{I})\xi_6=\xi_5. \tag{4.3}$$

General theorems exist[5,6] stating that

> the eigenvectors together with their associated generalized eigenvectors form a complete set. (4.4)

Let $\xi_3(y)$ be the condition at depth y below the surface when the force-displacement condition at the surface is ξ_3, and similarly let $\xi_2(y)$ correspond to ξ_2 at the surface. Combination of Eqs. (4.2) and (2.8) show, since $\mathbf{N}$ and $\mathbf{N}$-$p_2\mathbf{I}$ commute, that

$$(\mathbf{N}-p_2\mathbf{I})\xi_3(y)=\xi_2(y). \tag{4.5}$$

$\xi_3(y)$ remains the generalized eigenvector associated with $\xi_2(y)$. The explicit y dependence of $\xi_3(y)$ is obtained by integration of

$$\frac{\partial}{\partial y}\,\xi_3(y) = ik\mathbf{N}\xi_3(y) = ik[p_2\xi_3(y) + \xi_2(y)], \tag{4.6}$$

which, since

$$\xi_2(y) = \exp(ikp_2y)\xi_2, \tag{4.7}$$

yields

$$\xi_3(y) = \exp(ikp_2y)\,\xi_3 + iky\exp(ikp_2y)\,\xi_2. \tag{4.8}$$

It is apparent that since $\xi_2(y)$ is decaying with increasing y because $\mathrm{Im}\,p_2 > 0$, $\xi_3(y)$ will also vanish as $y \to \infty$. Thus $\xi_3(y)$ is also an allowed component in a surface-wave construction.

Next consider ξ_3 as a function of the angle ϕ in $\mathbf{N}(\phi)$, $\xi_3(\phi)$. ξ_3 is not invariant to rotations ϕ and the question arises whether Eq. (3.12), which is the basis for the integral impedance expression, holds for ξ_3.

$\xi_3(\phi)$ obeys the equation

$$[\mathbf{N}(\phi) - p_2(\phi)\mathbf{I}]\xi_3(\phi) = \xi_2, \tag{4.9}$$

where ξ_2 is independent of ϕ. Differentiating this equation with respect to ϕ and using Eqs. (2.13) and (3.6) (which holds for p_2), we obtain

$$(\mathbf{N}^2 - p_2^2\mathbf{I})\xi_3 = (\mathbf{N} - p_2\mathbf{I})\frac{\partial}{\partial\phi}\,\xi_3, \tag{4.10}$$

from which follows, by combination with Eq. (4.9),

$$(\mathbf{N} - p_2\mathbf{I})\frac{\partial}{\partial\phi}\,\xi_3 = 2p_2\xi_2. \tag{4.11}$$

Comparing Eqs. (4.11) and (4.9) one sees that

$$\frac{\partial}{\partial\phi}\,\xi_3 = 2p_2\xi_3 + \gamma\xi_2. \tag{4.12}$$

where γ is constant. Actually ξ_3 is not unique; it is unique on to within an arbitrary component of ξ_2. We may choose $\gamma = 0$. Integration of Eq. (4.12) then yields

$$\xi_3(\phi) = \xi_3(0)\exp[\kappa(\phi)], \tag{4.13}$$

where

$$\frac{\partial\kappa}{\partial\phi} = 2p_2, \tag{4.14}$$

i.e.,

$$\kappa(\phi) = 2\int_0^{\phi} p_2(\phi)\,d\phi. \tag{4.15}$$

Consider now $\mathbf{N}(\phi)\xi_3(0)$. By Eqs. (4.9) and (4.13)

$$\begin{aligned}\mathbf{N}(\phi)\xi_3(0) &= \exp[-\kappa(\phi)]\mathbf{N}(\phi)\,\xi_3(\phi)\\ &= \exp[-\kappa(\phi)][p_2(\phi)\,\xi_3(\phi) + \xi_2]\\ &= p_2(\phi)\,\xi_3(0) + \exp[-\kappa(\phi)]\xi_2.\end{aligned} \tag{4.16}$$

Thus making angular averages

$$\bar{\mathbf{N}}\xi_3(0) = i\xi_3(0) + \overline{\exp[-\kappa(\phi)]}\,\xi_2. \tag{4.17}$$

From Eqs. (4.15) and (3.6)

$$\kappa(\phi) = -2\int_{p_2(0)}^{p_2(\phi)} \frac{p\,dp}{1+p^2} = -\ln\frac{1+p_2^2(\phi)}{1+p_2^2(0)}, \tag{4.18}$$

so

$$\exp[-\kappa(\phi)] = \frac{1+p_2^2(\phi)}{1+p_2^2(0)}. \tag{4.19}$$

From Eq. (3.6)

$$\overline{1+p_2^2} = 0, \tag{4.20}$$

so finally

$$\overline{\exp[-\kappa(\phi)]} = 0. \tag{4.21}$$

[The special case $p_2(0) = i$ must be considered separately, but the conclusion is the same.]

Equation (4.17) thus reduces to

$$\bar{\mathbf{N}}\xi_3(0) = i\xi_3(0) \tag{4.22}$$

and we have reached the important conclusion that Eq. (3.12) applies *both* to eigenvectors and associated generalized eigenvectors. Thus, Eq. (3.14) also applies to eigenvectors as well as generalized eigenvectors. Recalling theorem (4.4) as the equivalent of theorem (3.4), it also follows, by reasoning identical to that of Sec. III, that $\mathbf{A}_1$, $\mathbf{A}_2$, and $\mathbf{A}_3$ form a complete set in the three-dimensional space and that $\mathbf{Z}$, Eq. (3.18), still determines what force $\mathbf{J}$ at the surface is needed to maintain a given amplitude $\mathbf{A}$. The integral expression (3.18) for the surface impedance is *generally* valid for $v < v_L$.

It is now also immediately clear that Eqs. (3.19)–(3.26) remain valid with nonsimple degeneracy.

V. SOME PROPERTIES OF THE IMPEDANCE AND SOME PROPERTIES OF THE LIMITING WAVE

We consider the velocity range $0 < v < v_L$ for which the theory in the foregoing applies. The appearance of the limiting wave at $v = v_L$ will also be discussed in more detail.

The impedance $\mathbf{Z}$, Eq. (3.18), is Hermitian. Thus it may be represented in the dyadic form

$$\mathbf{Z} = \sum_1^3 \lambda_i \mathbf{e}_i \cdot \mathbf{e}_i^{\dagger}, \quad \mathbf{e}_i^{\dagger}\mathbf{e}_j = \delta_{ij}, \tag{5.1}$$

where e_i are complex eigenvectors obeying orthogonality relations and λ_i are *real* eigenvalues.

The Lagrange function per unit length per unit depth for a surface disturbance in uniform motion is

$$L = \tfrac{1}{2}(\mathbf{J}^*\mathbf{A} + \mathbf{J}\mathbf{A}^*), \tag{5.2}$$

or by Eqs. (3.18) and (3.26),

$$-L = \tfrac{1}{4}\mathbf{A}^*\mathbf{Z}\mathbf{A}. \tag{5.3}$$

At $v = 0$, $-L$ is strain energy only and thus positive definite. Since $\mathbf{A}$ in (5.3) is arbitrary, it follows that

$$\lambda_i > 0, \quad i = 1,2,3 \text{ when } v = 0. \tag{5.4}$$

Keeping the amplitude $\mathbf{A}$ fixed but changing the velocity, the relation

$$2T = v\left(\frac{\partial L}{\partial v}\right)_{\mathbf{A}} \tag{5.5}$$

is valid, where T is kinetic energy per unit length per unit depth. Thus, by Eq. (5.3)

$$\frac{1}{4}\,v\mathbf{A}^*\left(\frac{\partial}{\partial v}\mathbf{Z}\right)\mathbf{A} = -2T. \tag{5.6}$$

Since T is positive definite, it follows that

$$\frac{\partial}{\partial v}\,\mathbf{Z} \text{ is negative definite} \tag{5.7}$$

and

$$\lambda_i, \quad i=1,2,3 \text{ decrease with increasing } v. \tag{5.8}$$

A similar conclusion based on the relation

$$E=v^2\frac{\partial}{\partial v}\left(\frac{1}{v}L\right),$$

where E is the total energy, was reached by Ingebrigtsen and Tonning.[3]

From Eqs. (3.18) and (3.23) it follows that

$$\mathbf{AZA}=-k\mathbf{AQ}^{-1}\mathbf{A}. \tag{5.9}$$

Since $\mathbf{Q}^{-1}$ is real and negative definite when $v<v_L$, it follows that

$$\mathbf{AZA}\geq 0 \quad \text{for real } \mathbf{A}, \tag{5.10}$$

the possible equality in (5.10) referring to $v=v_L$, which will be discussed later.

The power flux per unit area in the y direction, W_y, is

$$W_y=(\omega/4i)(\mathbf{J}^*\mathbf{A}-\mathbf{J}\mathbf{A}^*). \tag{5.11}$$

Of course, in a surface disturbance in uniform motion parallel with the surface

$$W_y=0. \tag{5.12}$$

The impedance (3.18) satisfies this requirement

$$W_y=-(\omega/4i)\{\mathbf{A}^*[(\mathbf{Z}^T)^*-\mathbf{Z}]\mathbf{A}\}=0. \tag{5.13}$$

As $v\to v_L$, $\mathbf{Q}$ diverges in the sense that one of its eigenvalues approaches infinity. $\mathbf{Q}^{-1}$ is convergent, and one of the eigenvalues approaches zero. $\mathbf{S}$ diverges, but $\mathbf{Q}^{-1}\mathbf{S}$ converges. This is ensured by the eigenvalue in $\mathbf{Q}^{-1}$ approaching zero. Thus as is well established and can be ascertained in the present formalism by the methods of Barnett and Lothe,[1] $\mathbf{Z}(v)$ approaches a finite limit as $v\to v_L$, and we define $\mathbf{Z}(v_L)$ through this limit

$$\mathbf{Z}(v_L)=\lim_{v\to v_L}\mathbf{Z}(v). \tag{5.14}$$

The limiting wave arises by coalescence of two partial waves ξ_α and ξ_α^* as $v\to v_L$. Since $Z(v)$ applies to one of the two coalescing waves (that for which $\mathrm{Im}\,p_\alpha>0$), we must expect $\mathbf{Z}(v_L)$ to apply to the limiting wave itself

$$\mathbf{J}_L=-\mathbf{Z}(v_L)\mathbf{A}_L. \tag{5.15}$$

Indeed, the validity of this relation can be proven.

$\mathbf{A}_L$ is the eigenvector of a real matrix, Eq. (2.15). Thus $\mathbf{A}_L$, the amplitude of the limiting wave, can be chosen as purely *real*. The limiting wave is linearly polarized. We will always choose

$$\mathbf{A}_L \text{ real}. \tag{5.16}$$

With $\mathbf{A}_L$ real and the fact that the limiting wave is a bulk wave, it follows that

$$\mathbf{J}_L \text{ purely imaginary}. \tag{5.17}$$

From the construction (see for example Ref. 1) of the limiting wave from the slowness surface, it follows that the group velocity is parallel with the surface so that $W_y=0$ also for the limiting wave. Alternatively, we may say that the limiting wave has inherited this property from ξ_α, $\mathrm{Im}\,p_\alpha>0$. Since $\mathbf{A}_L$ is real and $\mathbf{J}_L$ purely imaginary, it now follows from Eq. (5.11)

$$\mathbf{J}_L\mathbf{A}_L=0. \tag{5.18}$$

VI. EXISTENCE THEOREMS

Most of the facts listed in Sec. are well known and therefore detailed proofs have been omitted. The only property which appears not to be commonly realized is that of (5.10), which also will be of some importance in the considerations to follow.

However, what apparently has not been realized before is that the preceding list of facts provide sufficient basis for the construction of existence theorems.

If a velocity $v_R<v_L$ for which

$$\|\mathbf{Z}(v_R)\|=0 \tag{6.1}$$

can be found, then a surface wave satisfying the condition of free surface, i.e., a Rayleigh wave (RW), with phase velocity v_R, exists. Condition (6.1) is the condition that $\mathbf{J}=0$ in Eq. (3.17) be compatible with some nonzero $\mathbf{A}$. The amplitude of the surface wave satisfies

$$\mathbf{Z}(v_R)\mathbf{A}_R=0. \tag{6.2}$$

Condition (6.1) is equivalent with the condition that one of the eigenvalues λ_i in Eq. (5.1) be zero at $v=v_R$.

Comparing (5.10) and Eq. (6.2), it is immediately clear that the RW, if it exists, is elliptically polarized.

Now make the following supposition: The limiting wave does not satisfy the condition of free boundary

$$\mathbf{J}_L\neq 0 \tag{6.3}$$

and no RW exists for $v<v_L$. We shall see that a contradiction arises.

From Eq. (6.3)

$$\mathbf{J}_L^\dagger\mathbf{J}_L>0, \tag{6.4}$$

or, by Eq. (5.15), (5.16), and Eq. (3.26)

$$\mathbf{A}_L\mathbf{Z}^2(v_L)\mathbf{A}_L>0, \tag{6.5}$$

which by Eq. (5.1) takes the form

$$\sum_{i=1}^{3}\lambda_{i,L}^2|\mathbf{e}_{i,L}\mathbf{A}_L|^2>0, \tag{6.6}$$

where $\lambda_{i,L}$ is the value of λ_i at $v=v_L$, etc.

According, to Eq. (5.18)

$$\sum_{i=1}^{3}\lambda_{i,L}|\mathbf{e}_{i,L}\mathbf{A}_L|^2=0. \tag{6.7}$$

Let $\lambda_{p,L}$ be the largest eigenvalue. Multiply Eq. (6.7) by $\lambda_{p,L}$ and subtract it from inequality (6.6)

$$\sum_{i=1}^{3}\lambda_{i,L}(\lambda_{i,L}-\lambda_{p,L})|\mathbf{e}_i\mathbf{A}_L|^2>0. \tag{6.8}$$

With no RW for $v<v_L$, all $\lambda_{i,L}\geq 0$ according to Eqs. (5.4), (5.8), and (6.1). All terms $\lambda_{i,L}-\lambda_{p,L}$ are negative or zero according to the definition of $\lambda_{p,L}$. Inequality (6.8) is therefore incompatible with our assumption and we have arrived at the following theorem:

When the limiting wave does not satisfy the con-

dition of a free surface, it can be asserted that a Rayleigh-wave solution exists for some $v_R < v_L$. (6.9)

Suppose two RW solutions exist, for $v_{R_1} < v_L$ and $v_{R_2} < v_L$, respectively. Then two eigenvalues, say λ_1 and λ_2, must be negative at v_L,

$$\lambda_{1,L} < 0, \quad \lambda_{2,L} < 0. \tag{6.10}$$

We can always find a real vector **A** which is perpendicular to both the real and imaginary part of $e_{3,L}$. For this real vector **A**

$$\mathbf{A}Z\mathbf{A} = \lambda_{1,L}|e_{1,L}\mathbf{A}|^2 + \lambda_{2,L}|e_{2,L}\mathbf{A}|^2 < 0, \tag{6.11}$$

in violation of inequality (5.10).

Thus we also have the theorem:

There is at most one RW solution for $v < v_L$. (6.12)

VII. DISCUSSION

Some complications arise when more than one limiting wave exist at v_L. The various cases that may arise have previously been discussed quite exhaustively by the present authors. The general conclusion is a theorem actually somewhat less restrictive than theorem (6.9):

When one of the limiting waves at v_L does not satisfy the condition of a free surface, it can be asserted that a Rayleigh-wave solution exists for some $v_R < v_L$. (7.1)

When the limiting wave does satsify the condition of a free surface, a Rayleigh wave may or may not occur for some $v_R < v_L$. In this situation both cases occur. The previous considerations[1] by the present authors for transverse isotropy contained some algebraic errors and we will use this opportunity to present a corrected discussion.

We consider wave propagation in the x direction on the surface perpendicular to the y axis. The elastic coefficients C_{11}, C_{33}, C_{44}, C_{66}, C_{12}, and C_{13} describe the crystal. Isotropy about the z axis requires that

$$2C_{66} = C_{11} - C_{12}. \tag{7.2}$$

Lattice stability requires that C_{11}, C_{44}, and C_{66} be positive and that

$$C_{11}^2 - C_{12}^2 > 0. \tag{7.3}$$

Three bulk waves enter the problem. Their respective velocities are

$$V_1 = (C_{44}/\rho)^{1/2},$$

$$V_2 = (C_{66}/\rho)^{1/2}, \tag{7.4}$$

$$V_3 = (C_{11}/\rho)^{1/2},$$

where ρ is the density. Only the wave with velocity V_1 satisfies the condition of free surface. We are interested in the case when this wave defines the limiting velocity, thus

$$v_L = V_1 \begin{matrix} < V_2 \\ < V_3 \end{matrix}. \tag{7.5}$$

Since the only restriction on C_{44} is that C_{44} must be positive, this is a possible case.

From the isotropy condition (7.2) and the lattice stability requirement (7.3) it follows that

$$V_2 < V_3. \tag{7.6}$$

Thus we are discussing the case

$$V_1 < V_2 < V_3. \tag{7.7}$$

Explicit calculations show that v_R is a function of V_2 and V_3 only and because of inequality (7.6) v_R is smaller than V_2, so that

$$v_R = v_R(V_2, V_3) < V_2. \tag{7.8}$$

Now given V_2 and V_3 and thus also v_R, we may vary V_1 independently by changing C_{44} without violating lattice stability, to realize either one of the cases

$$v_R < v_L = V_1 < V_2 < V_3, \tag{7.9}$$

or

$$v_L = V_1 < v_R < V_2 < V_3. \tag{7.10}$$

In case (7.10) there is no RW for $v < v_L$. In this case the surface wave with velocity v_R belongs to a branch of leaky surface waves.[9]

The theoretical conclusions of this paper are in complete accord with and in fact rationalize the numerical work reported by Farnell.[9]

[1] D. M. Barnett and J. Lothe, J. Phys. F. 4, 671 (1974).
[2] A. N. Stroh, J. Math. Phys. 41, 77 (1962).
[3] K. A. Ingebrigtsen and A. Tonning, Phys. Rev. 184, 942 (1969).
[4] D. M. Barnett and J. Lothe, Phys. Norv. 7, 3 (1973).
[5] E. D. Nering, *Linear Algebra and Matrix Theory* (Wiley, London, 1963).
[6] M. C. Pease III, *Methods of Matrix Algebra* (Academic, New York, 1972).
[7] A. N. Stroh, Philos. Mag. 3, 625 (1958).
[8] K. Nishioka and J. Lothe, Phys. Status, Solidi B 51, 645 (1972).
[9] G. W. Farnell, in *Physical Acoustics VI*, edited by W. P. Mason (Academic, New York, 1970).